Environmental Management and Biodiversity Conservation of Forests, Woodlands, and Wetlands of the Rufiji Delta and Floodplain

Development of a Computerised Flood Warning Model and Study of Hydrological Characteristics of the Lower Rufiji Floodplain and Delta

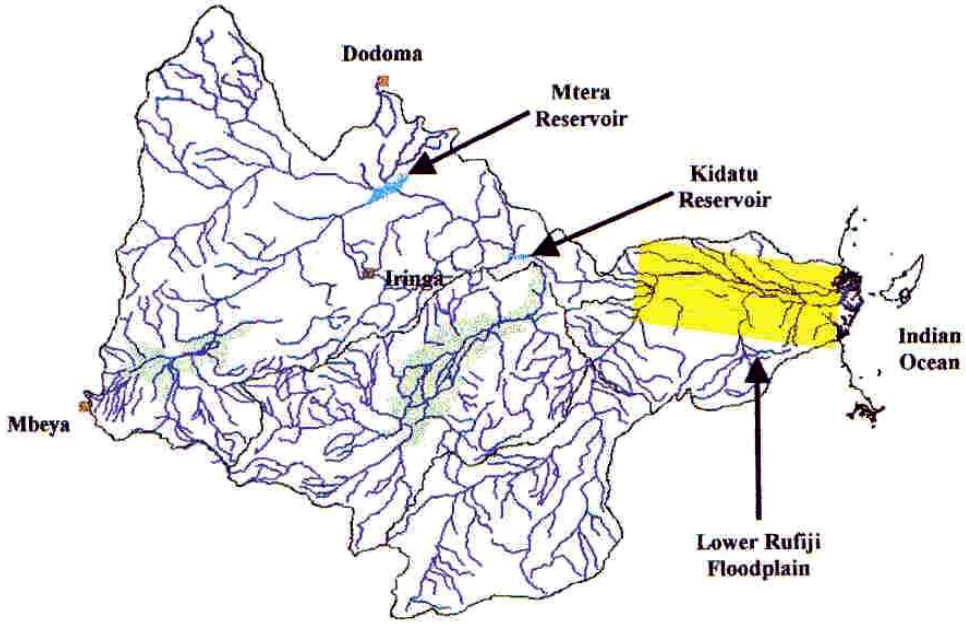

Technical Report No. 14 Vol. 1: Main Report

WREP
UDSM

March 2003

For more information please contact
Project Manager,
Rufiji Environment Management Project
P O Box 13513
Dar es Salaam, Tanzania.
Tel: 44 Utete Rufiji or 2666088 / 0741 322366 Dar es Salaam
Email: rempute1@bushmail.net or iucndar@epiq.or.tz

[1] The Rufiji District Council implements Rufiji Environment Management Project with technical assistance from IUCN – The World Conservation Union, and funding from the Royal Netherlands Embassy.

Rufiji Environment Management Project – REMP

Project Goal: To promote the long-term conservation through 'wise use' of the lower Rufiji forests, woodlands and wetlands, such that biodiversity is conserved, critical ecological functions are maintained, renewable natural resources are used sustainably and the livelihoods of the area's inhabitants are secured and enhanced**.**

Objectives

- To promote the integration of environmental conservation and sustainable development through environmental planning within the Rufiji Delta and Floodplain.

- To promote the sustainable use of natural resources and enhance the livelihoods of local communities by implementing sustainable pilot development activities based on wise use principles.

- To promote awareness of the values of forests, woodlands and wetlands and the importance of wise use at village, district, regional and central government levels, and to influence national policies on natural resource management.

Project Area

The project area is within Rufiji District in the ecosystems affected by the flooding of the river (floodplain and delta), downstream of the Selous Game Reserve and also including several upland forests of special importance.

Project Implementation

The project is run from the district Headquarters in Utete by the Rufiji District Administration through a district Environmental Management Team coordinated by the District Executive Director. The Project Manager is employed by the project and two Technical Advisers are employed by IUCN.

Project partners, particularly NEMC, the Coast Region, RUBADA, The Royal Netherlands Embassy and the Ministry of Natural Resources and Tourism, collaborate formally through their participation in the Project Steering Committee and also informally.

Project Outputs

At the end of the first five –year phase (1998-2003) of the project the expected outputs are:

An Environmental Management Plan: an integrated plan for the management of the ecosystems (forests, woodlands and wetlands) and natural resources of the project area that has been tested and revised so that it can be assured of success - especially through development hand-in-hand with the District council and the people of Rufiji.

Village (or community) Natural Resource Management Plans: These will be produced in pilot villages to facilitate village planning for natural resource management. The project will support the implementation of these plans by researching the legislation, providing training and some support for zoning, mapping and gazettement of reserves.

Established Wise Use Activities: These will consist of the successful sustainable development activities that are being tried and tested with pilot village and communities and are shown to be sustainable

Key forests will be conserved: Forests in Rufiji District that have shown high levels of plant biodiversity, endemism or other valuable biodiversity characteristics will be conserved by gazettement, forest management for conservation, and /or awareness-raising with their traditional owners.

Table of Contents

List of Figures

List of Tables

Chapter 1

1 Introduction

1.1 Background

Rufiji River Basin is the biggest river basin in Tanzania. It covers an area of approximately 180,000 km^2. It comprises four sub-basins, namely; the Great Ruaha, the Kilombero, the Luwegu and the Floodplain. The first three sub-basins drain into the fourth, i.e., the Floodplain. The drainage area of the Great Ruaha River at the Kidatu Reservoir is approximately 80,000 km^2. Luwegu sub-basin that is roughly of 26,000 km^2 is completely ungauged. The Kilombero sub-basin is of 33,000 km^2. The Lower Rufiji floodplain lies between longitudes of 37.0^0 and 39.5^0 East and latitude 7.0^0 and 9.0^0 South. It stretches some 130 km from West to East and ranges from 7 km to 35 km wide around the delta area.

The Rufiji River Basin varies greatly in the topographic, climatic and hydrological conditions. It has a humid and hot climate at the coast and in the Kilombero valley. The climate is hot and dry in the North-Western part of the Great Ruaha River Basin. In the mountainous regions it is cold. Rainfall is high along the mountain chain in the West of Kilombero valley with an annual average of around 1,600 mm. This decreases towards the middle of Great Ruaha with an annual average of less than 800 mm. High rainfall is also found around Mahenge Hills in Morogoro Region. Rainfall in the Luwegu sub-basin is estimated to be ranging between 850 mm and 1,700 mm per year. The Rufiji River has an average annual flow of about 800 Cumecs and carries an average of 16.5 million tons of sediments yearly, which it deposits on the floodplain and the delta.

About 100,000 to 150,000 people live on small scale farming and fishing along the Rufiji floodplain and its delta. About 20,000 ha of land are estimated to be cultivated in the floodplain, while the potential area for cultivation is estimated at 80,000 ha. The floodplain, which is about 150 km long, is generally flooded between January and May. The extent and duration of the flooding varies from year to year. Major floods that have occurred in the past have led to the destruction of crops, infrastructure and loss of human life in the floodplain. It is interesting to note that the economic activity in the floodplain is dependent on seasonal flooding of the plains.

An objective of this work was to develop a computerised flood warning model for the populations that are living and farming in the Rufiji floodplain. The model, of course, is only a part of the flood warning system. The entire system requires communication facilities to transmit water level data from a number of upstream locations into a central location where it is fed into a model. The development of the model, itself involves calibration, error updating and fine tuning of the parameters over a number of years.

The river is an important resource for the country. The Usangu Plains in the headwaters of the river are famous for cultivation of rice. Farming is done in the catchment of Little Ruaha, Kilombero and in the floodplains of Lower Rufiji Basin. The river and its tributaries generate more than 50% of Tanzania's hydropower requirements and there is a great potential for hydropower development at the Stiegler's Gorge. The famous Rufiji Delta is a unique ecosystem and an environmental treasure. It is a habitat of rare flora and fauna.

If a major Water Resources Development takes place upstream in the basin, for instance, impoundment of water at the Stiegler's Gorge for generation of Hydropower, then such a development is bound to have an adverse impact on the Delta. Unless, of course, the development is designed in such a way that it takes into consideration the conservation requirements of the Delta. While no such development is likely to happen in the near future, but it is important to initiate the process of understanding. It takes long time to collect the data that, upon analysis, will form the parameters of a conservation sensitive Water Resources Design. In the case of the Rufiji River Basin, a correct design of any Water Resources Development must ensure that the conservation area of the Delta is not destroyed.

Initially, the focus of this work was to develop a flood warning system to protect the populations that live in the floodplain. In the revised version the scope of this study was extended from being completely focussed on the flooding problems of the floodplain to better understanding of the hydrological characteristics of the basin. In this study an attempt was made to document the hydrological and climatic data that are available in the entire basin. These data were procured from various sources, processed and then used for the development of a quantitative hydrological model. Such a model can be used to simulate the effect of a major impoundment, like the proposed Stiegler's Gorge development, on flooding and silt deposition in the plains. Such a model can also be used to design and to develop rules for the operation of the proposed development, to minimise damage to the ecosystem of the Delta and to ensure minimum disruption to the traditional means of livelihood of the inhabitants of the floodplain.

The modelling work, presented in this report, is of elementary nature. Nevertheless, it forms an excellent basis for future work. Unfortunately, very little information and data are available on sediment transported by the river and the amount that is deposited in the floodplain and in the Delta. This information is of critical importance. But it is not readily available.

1.2 Summary and Layout of the Report

This report comprises three volumes. The first volume has ten chapters including this introductory chapter. The 2nd and the 3rd chapters, of this volume, deal with documentation and processing of the climatic data comprising the rainfall and the evaporation. Chapter 4 deals with the river flow data that has been collected over a number of years. Chapter 5 documents, what ever, little data are available on suspended sediment in the basin. Chapter 6 presents summary of the spatial data used in the study followed by chapter 7 on simulation modelling. Chapter 8 describes the models that were developed for use in a flood warning system. In chapter 9, estimates of area that are likely to get inundated by floods are generated for various magnitudes of flood. The last chapter focuses on some few vital suggestions of work that need to be done in the basin in the future.

A user friendly computer package was developed as a part of the flood warning system. This computer package uses the models that are described in Chapter 8. It also uses the flood inundation images that were created in Chapter 9. A detailed description of the computer package is presented in volume 3 of this report. Volume 2 contains various appendices.

In **Chapter 2** daily data of 166 daily recording rain gauges and annual records of 1,240 stations were analysed for estimation of Mean Annual Precipitation (MAP); estimation of Average Daily Rainfall (ADR); detection of trend, and for establishing dates of rainfall onset, cessation and the duration of the rainy season.

A suitable Kriging model was used for spatial interpolation of MAP. IDRISI and SURFER software were used to produce the MAP diagram for the entire Rufiji River Basin. The method of Simple Arithmetic Mean was used to estimate time series of Average Daily Rainfall (ADR) over a number of sub basins. Estimation of ADR by the method of Thiessen Polygon was carried out only for the sub-catchments of the Kilombero sub-basin. Luwegu sub-basin has no rain gauges. It is an area of about 26,000 square kilometres. A method was devised to estimate rainfall on this sub-basin. Standard methods of statistical trend analysis were applied to time series of Annual Rainfall (AR) data of twelve stations with long records, and the average time series of these twelve records. There was no evidence of any significant trend in any of the time series under consideration. The date of onset of rainfall, for 159 locations in the basin, was determined from analyses of time series of Expected Dekadal Rainfall (EDR). Generally, the onset of the rain starts from the South Western mountainous regions of the basin on the 30th dekad (i.e. 21st – 31st of October). The cessation of rains follows a similar, but opposite pattern, to that of the onset. The rains cease from the mountainous sections at the central part of the basin two dekads later than the rest of the basin. It normally ceases around the 14th dekad (i.e. 11th – 20th May). The average duration of rainfall is about 18 dekades in the mountainous regions and less than 16 dekads in other parts of the basin except for the floodplain area where it is beyond 18 dekads.

Chapter 3 deals with the analysis of a limited amount of climatic data for estimation of potential evapotranspiration in the Rufiji River Basin. Climatic data available for eight locations, namely, Dodoma, Iringa, Mbeya, Songea, Morogoro, Igawa, Madibira and Kilwa Kivinje were processed. Large chunks of these data are missing in all the locations. The quality of data is known to be poor except in the case of synoptic stations like Dodoma, Iringa and Mbeya.

Lumemo, Tenende and Malinyi climatic stations were chosen for estimation of Potential Evapotranspiration for the Kilombero sub-basin because of their proximity to the sub-basin. The Thornthwaite model was calibrated on Dodoma, Iringa and Mbeya and then used to fill in the missing data. The mean annual potential evaporation in Dodoma is estimated to be about 1,900 mm. In Iringa it is about 1,700 mm and in Mbeya it is 1,600 mm. The time series of Potential Evapotranspiration estimated for Dodoma was used for the Kilombero sub-basin. The mean annual Potential Evapotranspiration (MAPET) surface of the entire was constructed from spatial extrapolation of 12 MAPET values (from the 12 available climatic stations) using Surfer and a suitable Kriging model.

Chapter 4 describes the historical river flow data available within the basin. There are data for 50 flow gauging stations available in the basin but only 16 stations were used in this study. The remaining, that are upstream of the Mtera Reservoir, were not included in this study. Rating data, for construction of the rating curves for the 16 stations used in this study, were obtained, checked and analysed. Fairly good rating curves were obtained for most of the stations considered in this study. Only exception is that of 1kb15a. The curve established for this location is very poor. Special attention was given to the rating curve at the Stiegler's Gorge because this location is highly unstable. A few spot discharge measurements that were made, recently as part of this project, at Mloka, Utete and Ndundu are also listed in Chapter 4. The bank full discharge was established at flow of above 2,500 Cumecs.

Missing discharge data were reconstructed using simple techniques of linear interpolation and the use of mathematical models. The Linear Perturbation Model (LPM) in its Linear Transfer Function Form (LTF) was used to relate the catchment average rainfall with the observed discharge at the outlet station. The Multiple-Input Linear Perturbation Model (MILPM) was chosen to fill in the missing data at locations where upstream data were available. The models were applied to fill missing data at high flow and where long records of data of more than 3 months and above were missing.

Chapter 5 documents the limited amount of data that are available on the suspended sediment load of the river at Stiegler's Gorge station. The Sediment rating curve for the Stiegler's Gorge is of a very poor quality. An estimate of 16.6 million tons of sediment per year was arrived at the Stiegler's Gorge. The methodology used in past studies for estimation of bed load is also discussed in this chapter. The recent spot measurements of suspended sediment are also documented in this chapter.

Chapter 6 documents the river cross-section surveys that were done, as part of this study, at four different sites, namely; Mloka, Kipo, Utete and Ndundu in the Lower Rufiji River. The chapter also explains the methodology used in the delineation of 1 km x 1 km DEM of the Rufiji River Basin and its component sub-basins from the DEM of Africa.

Two-metre interval contours maps of a scale of 1:10,000 covering the Lower Rufiji floodplain area were acquired from Rufiji River Basin Development Authority (RUBADA) and then digitised at the Institute of Resource Assessment (IRA) of the University of Dar es Salaam (UDSM). The aerial photographs of these maps were taken in July of 1976 by GEOSURVEY International, while ground control and photogrammetric mapping was done by NORPLAN in 1976/77. The acquired digitised maps are all stored in a compact disc. The digitised maps including the reconstructed missing maps were put together into a single shape file. Using a 3-D Analyst of the ArcView GIS. The Triangular Irregular Network (TIN) of this shape file was created for use in the floodplain

modelling. All the details are presented in chapter 6. Manning's roughness coefficients were estimated for each grid in the floodplain by processing information from the digital land use and land cover map of the basin.

This work, presented in **Chapter 7,** is a first step towards the ultimate objective of having a single simulation model for the basin, which can be used for impact analysis and for choosing various management options. The sub-models tried in this chapter are:

(a) Inflow estimates into Mtera Reservoir.
(b) Inflow estimate into Kidatu Reservoir.
(c) Kidatu to Stiegler's Gorge Sub-Basin Model.
(d) Steigler's Gorge to Mloka Sub-Basin Model.
(e) Kilombero catchment Sub-Basin Model.

The models used were predominantly of the systems type but in the Kilombero sub-basin the simplest version of the Lumped Conceptual model (SMAR) and the simplest version of the Semi-Distributed Hydrological model (HEC) were also tried. Much work is required to bring the application of these models to fruitful levels of application. On the other hand, application of the systems type of models was conclusive. These models were used for developing real-time flood warning systems and for establishing the impact of the construction of Mtera/Kidatu Reservoir System on the annual maximum floods in the Rufiji River Basin.

Normally, one would have thought that an impoundment of the size of Mtera/Kidatu Reservoir System would reduce the annual maximum floods in the river. But it was interesting to note that since the impoundment the magnitude of the highest floods have actually increased rather than decreased due to releases of high floods from the Kidatu Reservoir. It seems that in the event of a very high floods a lot of water is released from the Kidatu Reservoir, which has the effect of creating an artificial flood wave.

Chapter 8 deals with the development of a Real-Time Flow Forecasting Model for the Lower Rufiji floodplain. It comprises two sub-models: The Kilombero-Kidatu-Stiegler's Gorge sub-model and The Stiegler's Gorge-Mloka sub-model. The purpose of the first sub-model is to forecast flows at Stiegler's Gorge (1k3) on daily basis, based on observed or forecasted flows at Kidatu (1ka3), Kilombero (1kb17) and the intervening catchment average rainfall. The second sub-model forecasts flows at Mloka (1k4) on daily basis, using observed or forecast flows at Stiegler's Gorge as input. The models used were of Linear Transfer Function type. The results of calibration and verification for both the sub-models were found to be satisfactory. One-day lead forecasts are naturally better than the four-day lead forecasts for both of the sub-models. For Stiegler's Gorge, the one-day lead model efficiency was 97%. This value reduced to 90% at four-day lead. Similarly, for Mloka the one-day lead efficiency was 96%. This value decreased to 86% at the four-day level.

A user-friendly computer package was developed in Visual Basic language to generate flood warnings within Lower Rufiji River. This stand-alone package is ready for installation in the basin. The description of the computer programme and its user manual is presented in volume 3 of this report.

Chapter 9 deals with the magnitude of flows that are in excess of 2,500 Cumecs. Flows of this magnitude are known to overflow the banks in the Lower Rufiji River and cause flooding in the floodplain. The model used was HEC-RAS and the HEC-GeoRAS. The computer program was operated to estimate the extent of inundation in the floodplain for an assumed flood peak at Mloka of 1,500 Cumecs, 2,000 Cumecs, 2,500 Cumecs and so on up to a flood magnitude of 7,000 Cumecs. The raster images of flood inundation were stored for use in the flood warning system.

Chapter 10 deals with some suggestions for future work. Clearly, much work is needed in data collection and in its processing. There are hardly any data on sediment transported by the river. This is very serious. There are no records of rainfall or river flow in the Luwegu sub-basin. This needs to be rectified along with general upgrading of data collection facilities. The rating curves at

many locations are 20 years old. Most of them need to be updated. Climatic data are sparse and inaccurate. Information on irrigation abstractions are not accurate.

It is necessary to develop a single simulation model of the entire Rufiji basin. This model must be custom built for assessing the impact of upstream Water Resources Development on the Delta. This model must also serve as a basic instrument of a management Decision Support System and provide parameters for the design of an ecologically friendly water resources development.

Development of such models requires spatial data like accurate DEMs. This, in turn, requires aerial surveys of the floodplain and that of the Delta.

Information on the ecology of the Mangrove Delta is of vital importance. One has to know as to what is required in terms of Silt and Water to sustain a mangrove forest. This information must be available before any sensible model can be built for any impact analysis.

Chapter 2

2 Rainfall Analysis

2.1 Introduction

Daily data of 166 daily recording rain gauging stations that are located within and just outside the Rufiji River Basin and annual records of 1,240 rain gauging stations, located in a rectangular window around the basin, were analysed for

(a) Estimation of Mean Annual Precipitation (MAP),
(b) Estimation of Average Daily Rainfall (ADR),
(c) Detection of any Trend, and for
(d) Establishment of dates of rainfall onset and cessation and the duration of the raining season.

Locations of the daily rain gauges used in the analysis are presented in Figure F2.1. Of the 166 stations roughly 63% or 106 stations lie within the basin. The remaining stations lie outside the basin boundary. Many are located along the mountainous regions of Kilombero and Great Ruaha sub-basins. The density of stations is very low in the rest of the basin. There are no stations in Luwegu sub-basin, which is at the southeastern part of the basin. Unfortunately, the river flow is also not gauged in the basin.

The details, associated with each rain gauging station, like; station number, location co-ordinates, length of the available record, etc., are presented in Appendix A2.1 and the distribution of the record length is presented in Figure F2.2. The average length is 35 years with an average missing data of about 17 percent. At least 30 stations have data up to 1998. The longest record is of 78 years at station number 09933002 (Tukuyu Agriculture). This record is up to 1998 and has surprisingly very low number of missing values comprising only 1.64 percent of the total available length of the data. This station and other stations with long records are highlighted in Figure F2.1.

2.2 Rainfall Averaging

2.2.1 Mean Annual Precipitation (MAP)

Mean Annual Precipitation is defined as the mean rainfall that a basin receives in a year. It was estimated using the methods of:

(i) Arithmetic mean, and
(ii) Spatial interpolation using a suitable Kriging model.

The method of Arithmetic Mean calculates the sum of all daily observations divided by the total number of observations. This figure multiplied by 365 is the MAP. Observations are summed for all stations with records within or just outside the basin.

The method of spatial interpolation uses a suitable Kriging model for spatial interpolation of MAP of each gauging station. This results in a value of MAP for each grid cell over the basin. The average of estimated MAP for each grid cell is the MAP for the basin. The grid based spatial interpolation using a kriging model and superposition of the catchment boundary involves application of GIS software. In this work, IDRISI and SURFER software were used. Figure F2.3 shows the location of rain gauging stations with annual rainfall data that were used to produce the MAP diagram for the Rufiji River Basin. Spatially interpolated surface for 1 sq. km grid surface is presented as Figure F2.4. Annual data of 1,240 rain gauges were used in this exercise as opposed to the 166 stations with daily data. The stations with annual rainfall data are located evenly distributed compared to the ones with daily records.

Table T2.1 and Figure F2.5 present a comparison of the two methods of estimation of MAP for a number of sub-catchments. The chosen sub-catchments are the ones whose digitised catchment boundaries were readily available. It seems that with the exception of the sub-catchment of 1kb8,

which is within the Kilombero sub-basin, the estimates of MAP by Arithmetic mean and by the method of spatial interpolation compare reasonably well. The deviation between the two methods, in the case of 1kb8, is about 26%. The arithmetic mean estimates the average in the range of 1,800 mm compared to the Krigging estimate of about 1,400 mm. It is very likely that the latter is more accurate estimate. The Kilombero sub-basin receives a higher amount of rainfall than the rest of the Rufiji basin. The average precipitation in the Kilombero sub-basin seems to be in the range of 1,400 mm per year.

Table T2.1: Comparison of Mean Annual Precipitation (MAP) estimated by Arithmetic Mean and Kriging for Digitised Catchments within the Rufiji River Basin

Catchment Name		MAP Arithmetic mean (Millimetres)	MAP Kriging (Millimetres)
Kilombero Sub-Basin	Mpanga at Mpanga (1kb8)	1,747	1,385
	Ruhudji at Mkasu (1kb10)	1,460	1,414
	Kilombero at Ifwema (1kb4)	1,568	1,449
	Lumemo at Kibaoni (1kb14)	1,440	1,486
	Mngeta at Mngeta Mission (1kb15a)	1,476	1,415
	Mngeta at Mchombe downstream (1kb15)	1,476	1,425
Great Ruaha Sub-Basin	Chimala at Chitekelo (1ka7a)	1,481	1,427
	Great Ruaha at Salimwani (1ka8a)	1,412	1,327
	Kimani at Gt. North Rd. (1ka9)	1,004	1,100
	Mbarali at Igawa (1ka11a)	1,170	1,114
	Mloboji and Mbarali to the Road	929	844
	Halali at Iyayi, Kioga (1ka12 including 1ka23a)	817	765
	Kioga to the North of Mbeya Road	719	678
	Ndembera at Ilonga upstream (1ka15a)	971	1,047
	Ndembera at Madibira (1ka33b)	945	972
	Umrobo at downstream Gt. North Rd. (1ka51a)	1,312	1,227
	High catchment areas of the Usangu Basin	1,520	1,101
	Usangu Plains	738	635
	Great Ruaha at Hausmann's Bridge (1ka27)	1,268	825
	Mlowo	1,425	1,252

2.2.2 Calculation of Average Daily Rainfall (ADR)

The method of Simple Arithmetic Mean was used to estimate time series of Average Daily Rainfall (ADR) over a catchment.

The method calculates ADR as sum of rainfall observations made on day *d* divided by the number of observations made on the day. For 166 rain gauges, it is not always necessary that on each day all 166 observations were made. If only 80 observations were made on day *d*, then the sum of observations made on that day was divided by 80 to give ADR for that day.

The method of kriging is not suitable for this purpose because of frequent records of zero daily rainfall values. This gives rise to numerical instability in the solution of kriging models. Hence the method was not used for the calculation of ADR. To allow for high variability in rainfall over the basin ADR was calculated for major sub-catchments and the intervening catchments within the Rufiji River Basin.

Estimation of ADR by the method of Thiessen Polygon was carried out only for the sub-catchments of the Kilombero sub-basin. The details are presented latter in a separate sub-section.

2.2.3 Estimation of ADR for Selected Catchments

Six gauged catchments within the Kilombero sub-basin (namely; 1kb8, 1kb10, 1kb4, 1kb14 and 1kb15 and 1kb15a), the complete sub-basin at 1kb17 and the intervening catchments within the sub-basin were identified for the estimation of ADR. Three catchments in the Great Ruaha River

sub-basin downstream of Mtera Reservoir and upstream of the Kidatu Reservoir (1kb37a, 1kb38 and 1kb61) including the intervening catchment were also identified for ADR estimation.

ADR estimates of catchments upstream of Mtera Reservoir (i.e. up to 1ka59) were already prepared in a previous study entitled Sustainable Management of the Usangu Wetland and its Catchment (SMUWC). Hence, it was not repeated in this study.

Figure F2.6 shows the location of the daily rainfall gauging stations that were used for the intervening catchments. ADR over the selected gauged catchments and the intervening catchments were calculated using the Arithmetic mean procedure. List of the stations that were used in the estimation of ADR for each sub-catchment is presented in Table T2.2.

Table T2.2: List of Rainfall Stations Used in creating the Average Daily Rainfall for each catchment or intervening catchment

Mpanga at Mpanga, Iringa (1kb8) 13 Stations	Ruhudji at Mkasu, Morogoro (1kb10) 30 Stations	Kilombero at Ifwema, Morogoro (1kb4) 43 Stations		Mngeta at Mngeta Mission, Morogoro (1kb15a) 17 Stations	Lumemo at Kibaoni, Morogoro (1kb14) 17 Stations	Kilombero at Swero, Morogoro (1kb17) 58 Stations	
09835007	09834001	09834001	09935006	09735007	09735007	09736004	09934022
09835009	09834005	09834005	09935007	09835005	09835005	09736016	09934023
09835019	09834011	09834011	09935009	09835009	09835009	09834001	09934024
09835021	09834016	09834016	09935012	09835015	09835015	09834005	09934025
09835022	09934001	09835007	09935014	09835019	09835019	09834011	09934026
09835023	09934013	09835009		09835022	09835022	09834016	09934027
09835024	09934015	09835019		09835023	09835023	09835005	09934029
09835025	09934018	09835021		09835026	09835026	09835007	09934032
09835026	09934019	09835022		09835027	09835027	09835009	09934034
09835030	09934020	09835023		09835030	09835030	09835019	09934038
09835034	09934021	09835024		09835034	09835034	09835021	09934039
09835036	09934022	09835025		09835041	09835041	09835022	09935002
09935007	09934023	09835026		09835043	09835043	09835023	09935003
	09934024	09835030		09835044	09835044	09835024	09935004
	09934025	09835034		09835047	09835047	09835025	09935005
	09934026	09835036		09835050	09835050	09835026	09935006
	09934027	09934001		09835053	09835053	09835030	09935007
	09934029	09934013				09835034	09935009
	09934032	09934015				09835036	09935012
	09934034	09934018				09835041	09935014
	09934038	09934019				09835043	
	09934039	09934020				09835044	
	09935002	09934021				09835047	
	09935003	09934022				09835050	
	09935004	09934023				09836000	
	09935005	09934024				09836001	
	09935006	09934025				09836002	
	09935009	09934026				09836003	
	09935012	09934027				09836004	
	09935014	09934029				09836006	
		09934032				09836011	
		09934034				09934001	
		09934038				09934013	
		09934039				09934015	
		09935002				09934018	
		09935003				09934019	
		09935004				09934020	
		09935005				09934021	

Table T2.2 Continued: List of Rainfall Stations Used in creating the Average Daily Rainfall for each catchment or intervening catchment

Int-1kb17 ------ 9 Stations	Lukosi at Mtandika, Iringa (1ka37a) 12 Stations	Yovi at Great Ruaha Confluence, Iringa (1ka38) 11 Stations	Great Ruaha at Gorge, Iringa (1ka61) 22 Stations	Int-Kid ------ 12 Stations	Int-1k3 ------ 16 Stations
09736004	09735002	09636000	09636000	09636027	09736004
09736016	09735003	09636006	09636006	09735002	09736016
09836000	09735007	09636008	09636008	09735007	09737000
09836001	09735013	09636011	09636011	09736003	09737005
09836002	09735014	09636018	09636018	09736004	09737006
09836003	09735015	09636027	09636027	09736006	09737008
09836004	09736003	09736006	09735002	09736007	09737011
09836006	09736012	09736007	09735003	09736008	09737013
09836011	09835002	09736008	09735007	09736012	09737014
	09835015	09736012	09735013	09736016	09836000
	09835027	09736017	09735014	09736017	09836001
	09835053		09735015	09835027	09836002
			09736003		09836003
			09736006		09836004
			09736007		09836006
			09736008		09836011
			09736012		
			09736017		
			09835002		
			09835015		
			09835027		
			09835053		

where

Int-1kb17* is the intervening catchment between the outlet of Kilombero sub-basin and the upstream catchments of 1kb4, 1kb15a and 1kb14.

Int-Kid* is the intervening catchment between the Kidatu Reservoir and Mtera Reservoir.

Int-1k3* is the intervening catchment between Stiegler's Gorge and upstream sub-basins of Kidatu, Kilombero and Luwego.

* Refer to Figure F2.6 for the actual location of the rainfall stations that were considered for these intervening catchments.

If one estimates the Mean Annual Rainfall (MAP) for a sub-catchment, by arithmetic averaging, from the same number of stations that were used in the estimation of ADR for these catchments, the estimated MAP is close to the MAP of these sub-basins estimated by the method of Kriging described earlier. This comparison presented in Figure F2.5, subjectively, indicates that the choice of stations for estimation of ADR for each sub-basin is correct.

2.2.4 Estimation of ADR for Ungauged Luwegu Sub-Basin

Luwegu sub-basin has no rain gauges. It is an area of about 26,000 square kilometres. The stream flow in the sub-basin is also ungauged. This section describes the methodology that was used to estimate a time series of average daily rainfall for later use in modelling exercises.

From the MAP surface of the Rufiji River Basin, created from 1,240 annual values, it can be seen that the Luwegu sub-basin comprises predominantly of three different annual rainfall regimes. These are marked in Figure F2.7. One band ranges from 1,200 to 1,400 mm. The second one ranges from 1,000 to 1,200 mm and the third one ranges from 800 to 1000 mm. The daily rain gauging stations that were found to lie within these three bands from the neighbouring areas were also identified. The stations that fall within Band-1 are coloured as white circles in the figure. Those that fall in Band-2 are presented as blue circles and those that fall in band-3 are denoted as black circles. Twenty stations were identified for band-1, 18 stations were identified for band-2 and 11 stations were chosen in band-3. Table T2.3 presents the list of all these stations.

Table T2.3: List of Rainfall Stations Used in creating the Areal Rainfall for Ungauged Luwegu Sub-Basin

Luwegu Sub-Basin		
Band-1 (20 Stations) Weight=0.5	**Band-2 (18 Stations) Weight=0.3**	**Band-3 (11 Stations) Weight=0.2**
09737005	09737000	09738000
09737011	09737008	09738017
09737014	09738004	09738018
09835009	09738014	09834001
09835019	09739022	09834005
09835026	09835005	09834011
09835030	09835036	09834016
09835034	09835041	09838002
09835047	09835043	09839001
09835050	09835044	09839004
09836000	09839003	09934034
09836004	09934018	
09836006	09934019	
09836011	09934020	
09934001	09934021	
09934015	09934022	
09934032	09934038	
09935006	09934039	
09935012		
09935014		

Note: Refer to Figure F2.7 for spatial location of these stations (Band-1 stations are represented as white circles, Band-2 as blue circles and Band-3 as black circles).

Band-1 constitutes about half of the total area of the Luwegu sub-basin. Band-2 is about 30% of the total area and the remaining 20% of the area is contributed by Band-3. The average daily rainfall for the sub-basin was, therefore, estimated from the average of the chosen rainfall stations for each band but the total average for the sub-basin was calculated by weighted averaging of the average of the three bands. The weight assigned to the 1st band was 0.5; to the 2nd band was 0.3 and to the third band was 0.2.

Annual values computed from the estimated ADR of the Luwegu sub-basin were correlated with annual values correlated from the estimated ADRs of the neighbouring areas. The Coefficients of Determination are presented in table T2.4. The same data length from 1950 to 1990 was used for each sub-basin to make the results comparable. The analysis shows that the Luwegu basin rainfall

is highly correlated with that of the Kilombero sub-basin. It is hardly surprising because most of the rainfall stations used in the estimation of ADR for the Luwegu sub-basin are the same as those of the Kilombero sub-basin.

Table T2.4: Comparison of Estimated Annual Rainfall Values for Luwegu Sub-Basin with other neighbouring sub-basins and catchments

No.	Sub-Basin or Catchment	Coefficient, α	Efficiency, R^2 (%)
1	Kilombero sub-basin	0.7810	85.31
2	Intervening catchment of Kilombero	0.7282	30.16
3	Intervening catchment of Stiegler's Gorge	0.7131	19.07
4	Rufiji floodplain	0.8416	-55.33
5	Intervening catchment of Mtera-Kidatu	1.3571	-30.82
6	1kb10 catchment	0.8427	73.53

Note: AR of Luwegu sub-basin = α * AR of sub-basin or catchment, where AR is the annual rainfall value

2.2.5 Estimation of Average Daily Rainfall (ADR) using Thiessen Polygon Method

An attempt was made to estimate the daily average rainfall (ADR) time series for various catchments within the Kilombero sub-basin using the Thiessen Polygon method. The exercise was not extended to all the catchments in the Rufiji River Basin because of complications and the time it takes to delineate such a large basin, like the Rufiji River Basin, into Thiessen Polygons. For the Kilombero sub-basin this work was done by the use of GIS ARC-VIEW Software. The basin was delineated from 1 sq. km grid DEM of Africa.

The list of the stations and their associated Thiessen Polygon weights are presented in Appendix A2.2 of this report. Figure F2.8 presents the Thiesen Polygon network for the delineated Kilombero sub-basin and how each rainfall station contributes spatially to each sub-catchment.

The procedure for dealing with the missing data of various stations that needed to be filled before the Thiessen Polygon method could be applied is as follows:

1. Monthly correlation analysis was performed among the rainfall stations for each catchment. Appendix A2.3 shows the results of this monthly correlation among stations for the four catchments considered for comparative analysis.

2. If for a particular day, there was a missing rainfall value, the value was to be filled with the data from another station that correlated highly with this station. In a situation where the highest correlated station was also having missing data for that day, the next station in rank of strongest correlation was used to do the filling.

The catchments considered for the analyses were 1kb8, 1kb10, the intervening catchment of 1kb4, and the intervening catchment of 1kb17. Catchments of station 1kb14 and 1kb15a were excluded from the analysis because the method of Thiessen Polygon could only use 3 stations and 1 station, respectively, for 1kb14 and 1kb15a. In estimation by Simple Arithmetic mean 17 stations were used. Under the circumstances the comparison seemed a bit superfluous. More over these two stations were found to have large chunks of missing daily data.

The Comparison of ADR estimated by the method of simple Arithmetic averaging and by averaging with the Thiessen weights is presented in Tables T2.5 and T2.6. The comparison was made on daily, monthly and annual basis. Figure F2.9 illustrates the comparison between the two methods of estimation for Catchment 1kb10. It is difficult to make any comments on these results

except that they are as one would have expected them to be. The Thiessen polygon estimates are likely to be more accurate, simply, from a theoretical point of view.

Table T2.5: Results of the Thiessen Polygon Method compared with the Arithmetic Mean Method on Daily Basis

Catchment	Period	Mean Value (mm)		Coefficient of Correlation	Efficiency, R^2 (%)
		Thiessen	Arithmetic		
1kb8	1938-1999	4.59	4.50	0.7844	68.97
1kb10	1926-1998	3.69	3.44	0.7310	66.37
Intervening of 1kb4	1921-1998	4.09	3.77	0.7425	68.73
Intervening of 1kb17	1921-1995	4.52	4.37	0.9693	91.23

Table T2.6: Results of the Thiessen Polygon Method compared with the Arithmetic Mean Method on Monthly Basis

Catchment	Period	Mean Value (mm)		Coefficient of Correlation	Efficiency, R^2 (%)
		Thiessen	Arithmetic		
1kb8	1938-1999	137.63	137.58	0.9244	84.76
1kb10	1926-1998	112.46	106.62	0.9097	90.63
Intervening of 1kb4	1921-1998	119.93	113.98	0.8875	87.90
Intervening of 1kb17	1921-1995	132.92	131.58	0.9763	94.40

2.3 Trend Analysis

Standard methods of statistical trend analysis were applied to time series of Annual Rainfall (AR) data of :

(a) twelve stations with long records, and
(b) the average time series of these twelve records.

The time series of Daily Rainfall (DR) for the selected long records were converted into a time series of Annual Rainfall by summing up the daily data from the 1st of August up to 31st of July of the following year. If a substantial number of daily values in a year, for instance 50% or above, were found to be missing then the full year was considered as missing.

A simple linear trend model for AR series y_i, recorded at years u_i can be written as:

$$y_i = y_0 + \beta u_i + \varepsilon_i \qquad i=1,2,.....,n \tag{2.1}$$

where

n is the number of years in the record,
$\mathbf{y_0}$ is the intercept,
β is the slope of the trend line and
$\boldsymbol{\varepsilon_i}$ are the residuals.
β can be estimated by seeking the ordinary least squares solution of equation 2.1.

The hypothesis that the estimated value of β is not equal to zero was tested by the use the t-statistics. The null hypothesis of no linear trend (β=0) was rejected at 95% level of significance if

the absolute value of the t-statistic was found to be greater than the critical value of the student t-distribution.

The linear trend model was applied to the selected time series of which twelve are the time series of long records and the thirteenth is the time series of the average of the twelve series. The location of these stations is shown in Figure F2.1. Results of the trend analysis are presented in Table T2.7. Only one time series plot is presented in the report and that is of the average time series. It is presented in Figure F2.10.

Table T2.7: Result of Trend analysis to Selected long Record Stations

THE SELECTED LONG RECORD STATIONS											
No.	Station Code	Long.	Lat.	Available record		No. of Years	Used Record	Trendline Slope	Estimated t-statistic	Critical t-value at 95% Confidence	Trendline Remarks
				Start Year	End Year						
1	09635001	35.767	-6.167	1932	1995	64	56	-0.564	-0.891	2.00630	No Sig. Trend
2	09737005	37.717	-7.250	1935	1995	61	56	-1.570	-0.789	2.00630	No Sig. Trend
3	09833001	33.467	-8.933	1937	1998	62	56	-0.159	-0.236	2.00630	No Sig. Trend
4	09833002	33.417	-8.533	1934	1998	65	57	0.437	0.491	2.00525	No Sig. Trend
5	09834000	34.817	-8.233	1923	1995	73	36	-0.504	-0.319	2.03360	No Sig. Trend
6	09834001	34.917	-8.567	1921	1991	71	47	1.191	1.327	2.03150	No Sig. Trend
7	09835009	35.333	-8.583	1938	1998	61	53	-1.432	-0.911	2.00945	No Sig. Trend
8	09836001	36.717	-8.683	1921	1995	75	56	2.114	1.081	2.00630	No Sig. Trend
9	09838002	37.750	-8.017	1922	1998	77	66	1.085	1.558	1.99868	No Sig. Trend
10	09933002	33.633	-9.250	1921	1998	78	71	0.324	0.223	1.99703	No Sig. Trend
11	09934001	34.767	-9.333	1926	1991	66	57	0.410	0.492	2.00525	No Sig. Trend
12	09935006	35.367	-9.917	1934	1994	61	58	0.158	-0.108	2.00420	No Sig. Trend
13	Average of the above 12 Stations			1922	1998	77	76	0.184	0.347	1.99439	No Sig.Trend

The conclusion, based purely on the statistical analysis, is that there is no evidence of any significant trend in any of the time series under consideration. This may be observed from the trend line in Figure F2.10 and the time series graph of AR, which fluctuates between 850 mm and 1,650 mm.

2.4 Rainfall Onset, Cessation and Duration analysis

The date of onset of rainfall, for 159 locations in the basin, was determined from analyses of time series of Expected Dekadal Rainfall (EDR). The remaining 7 stations out of the total 166 daily rainfall stations were not included in this analysis because their records are of very short duration. The time series of EDR is of 36 values. The first value represents the expected rainfall during the first ten days of a year. Such a time series is presented, for purposes of illustration, in Figure F2.11 for rain gauge number 09838002. Each point on this graph is average rainfall recorded at the station for each dekad. Average was calculated for all those years for which records were available.

The analysis comprised calculation of the following:

(a) The time of onset of rainfall was defined as the time that corresponds to the point of maximum positive curvature of the graph of EDR.
(b) The time of cessation of the rainfall was defined as the point of maximum negative curvature on the graph of EDR.
(c) Average Rainfall Season was calculated as the difference in time between the time of onset and the cessation of the rainfall.
(d) Mean Magnitude is the magnitude of rainfall that was recorded over an Average Rainfall Season.

The results for the 12 stations with long record (same stations that were used in the trend analysis) are presented in Table T2.8. The results for the full set of 159 rain gauging stations are presented in Appendix A2.4. The results are illustrated in Figures F2.12 through to F2.14. These figures show, respectively, the spatial distribution of the date of onset, the time of cessation and the average duration of the rainfall season. The mean magnitude of rainfall during the rainy season is presented in Figure F2.15.

Table T2.8: Time of the Onset and Cessation; Average Duration and Magnitude of rainfall of the 12 Selected Long Record Rain Gauge Stations

No.	Station	Onset	Cessation	Duration	Long Rains (mm)	Mean Annual Rainfall (mm)
1	09635001	33	11	15	526.14	566.35
2	09737005	33	15	19	1340.36	1608.87
3	09833001	32	12	17	871.76	938.72
4	09833002	33	10	14	781.45	866.68
5	09834000	33	12	16	648.79	724.81
6	09834001	32	10	15	733.98	805.31
7	09835009	33	14	18	1254.68	1421.49
8	09836001	33	13	17	1695.33	1960.22
9	09838002	31	14	20	779.14	875.93
10	09933002	32	15	20	2025.98	2432.94
11	09934001	33	12	16	980.84	1078.92
12	09935006	32	13	18	1220.54	1294.30

Generally, the onset of the rain starts from the South Western mountainous regions of the basin on the 30th dekad (i.e. 21st – 31st of October). The cessation of rains follows a similar, but opposite pattern, to that of the onset. The rains cease from the mountainous sections at the central part of the basin two dekads later than the rest of the basin. It normally ceases around the 14th dekad (i.e. 11th – 20th May). Naturally, these areas have an advantage of having a bit longer duration of rainfall. The average duration of rainfall is about 18 dekades in the mountainous regions and less than 16 dekads in other parts of the basin except for the floodplain area where it is beyond 18 dekads.

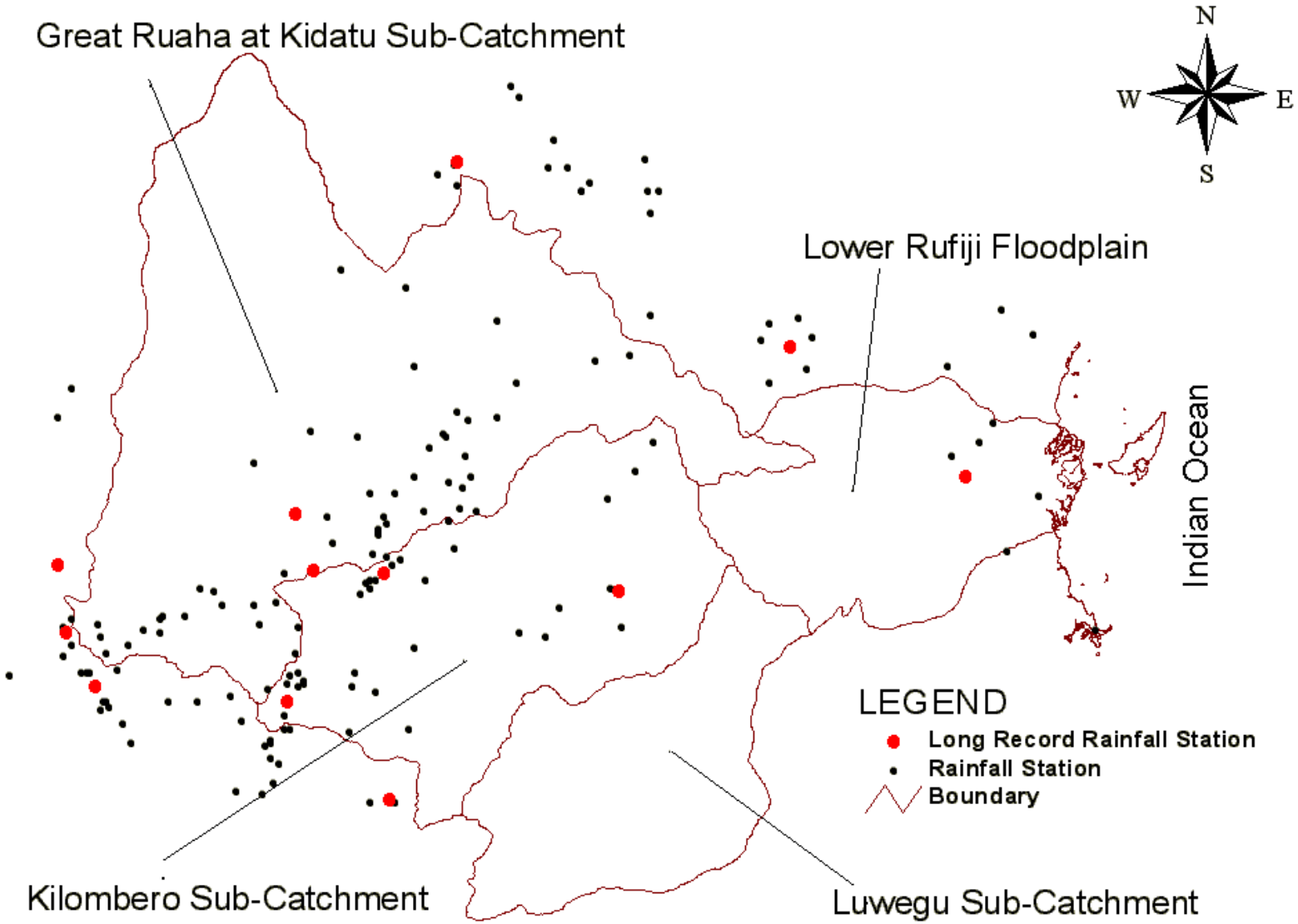

Figure F2.1: Map showing Rainfall Stations, with Daily Data, in and just outside of the Rufiji River Basin used in this work

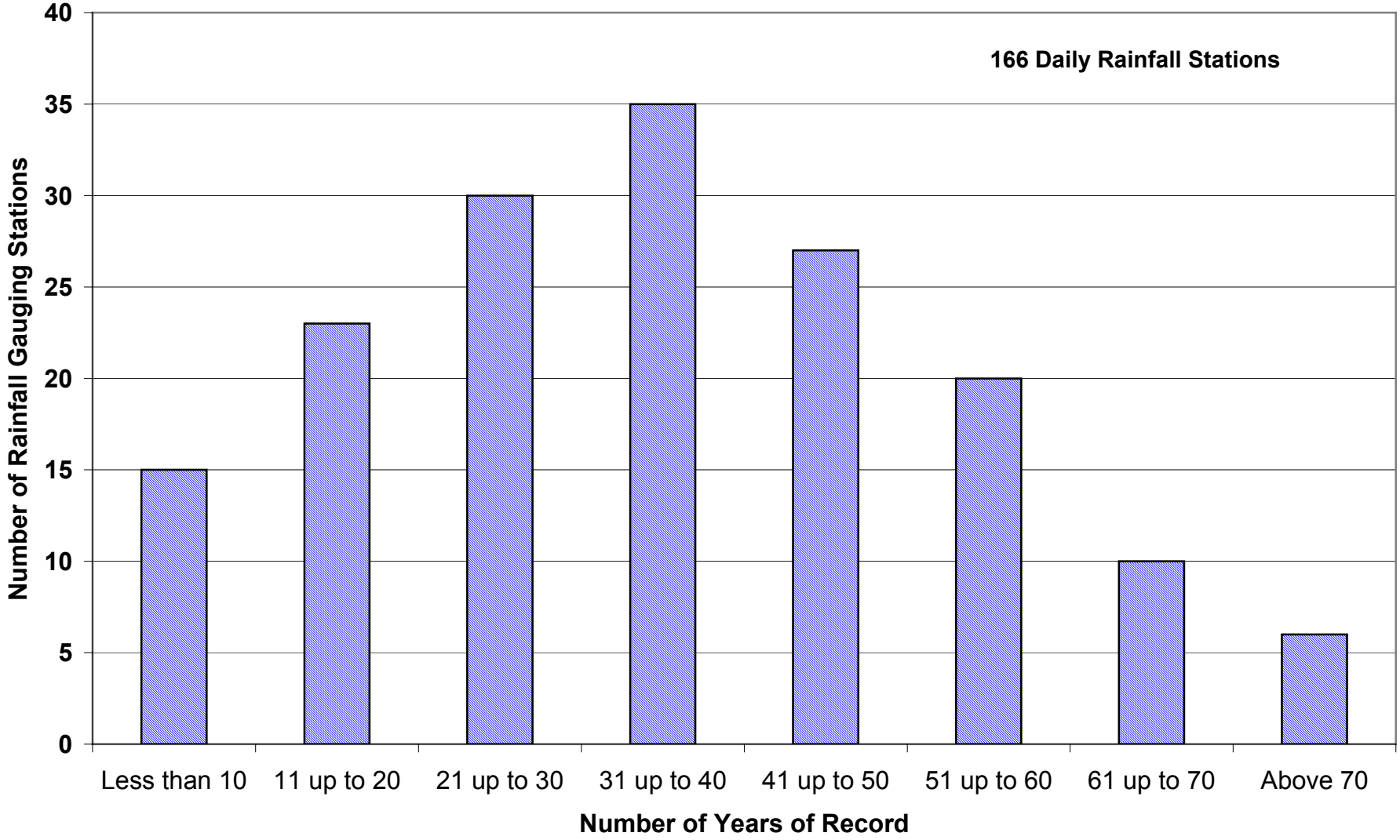

Figure F2.2: Distribution of the Record Length of Daily Rainfall Stations of the Rufiji River Basin as used in this Analysis

Figure F2.3: Map of Rufiji Basin showing location of 1,240 rain gauging stations with annual rainfall records.

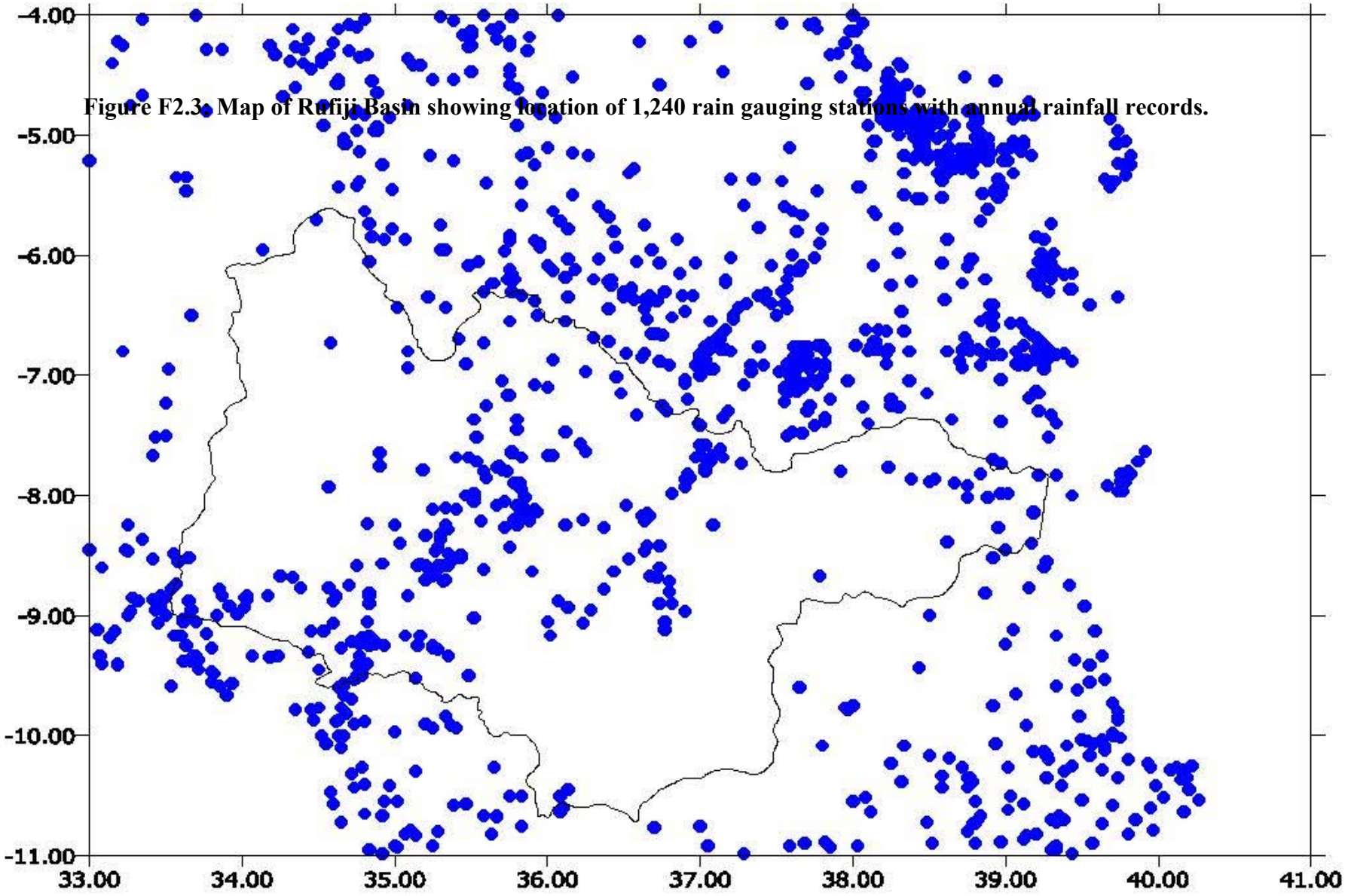

Figure F2.3: Map of Rufiji Basin showing location of 1,240 rain gauging stations with annual rainfall records. These data were used to produce MAP map for the basin, using a suitable Kriging model.

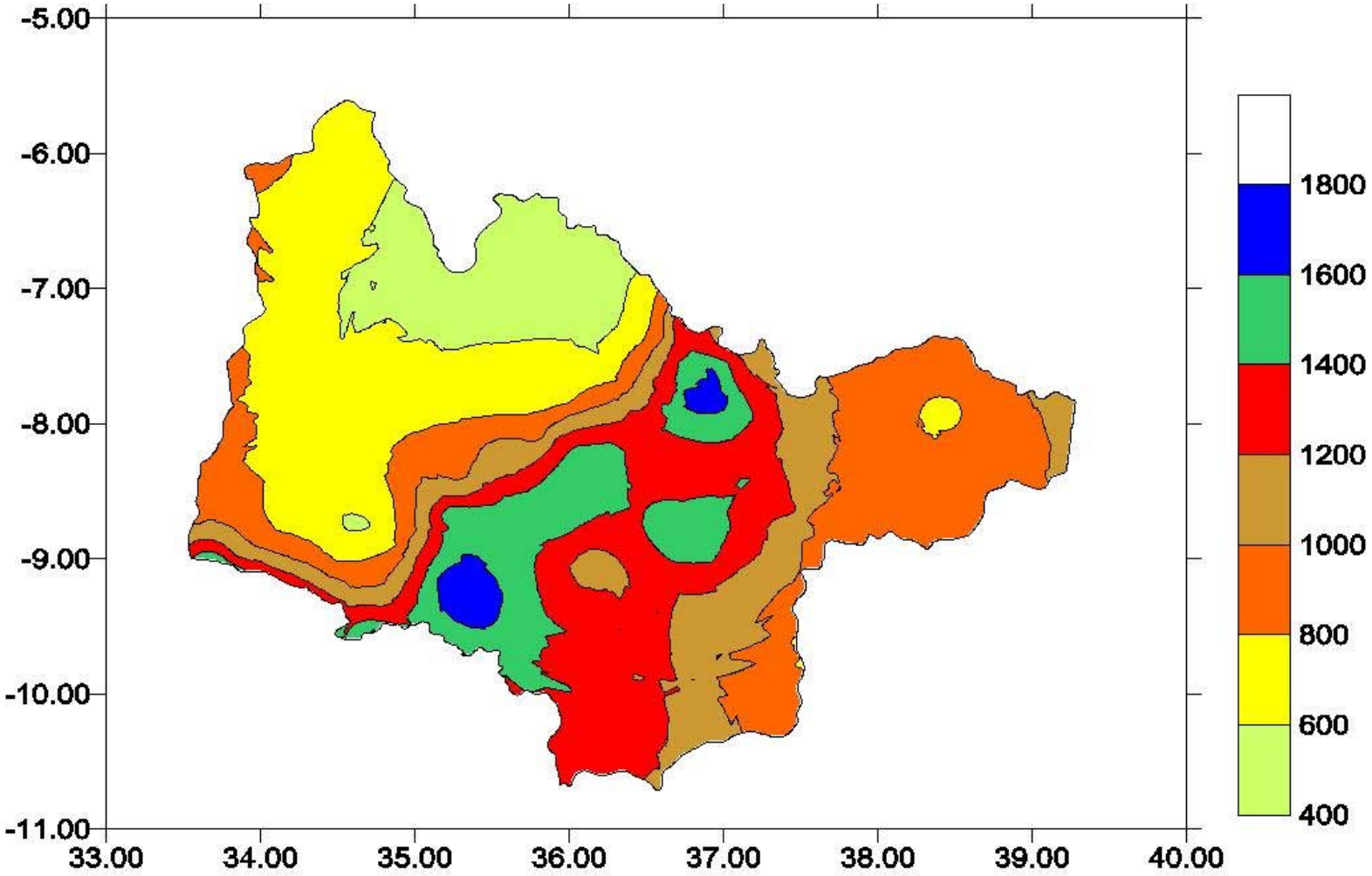

Figure F2.4: Spatial Distribution of the Mean Annual Precipitation of the Rufiji Basin.

It is based on 1 sq. km Grid Interpolation using Ordinary Kriging Model

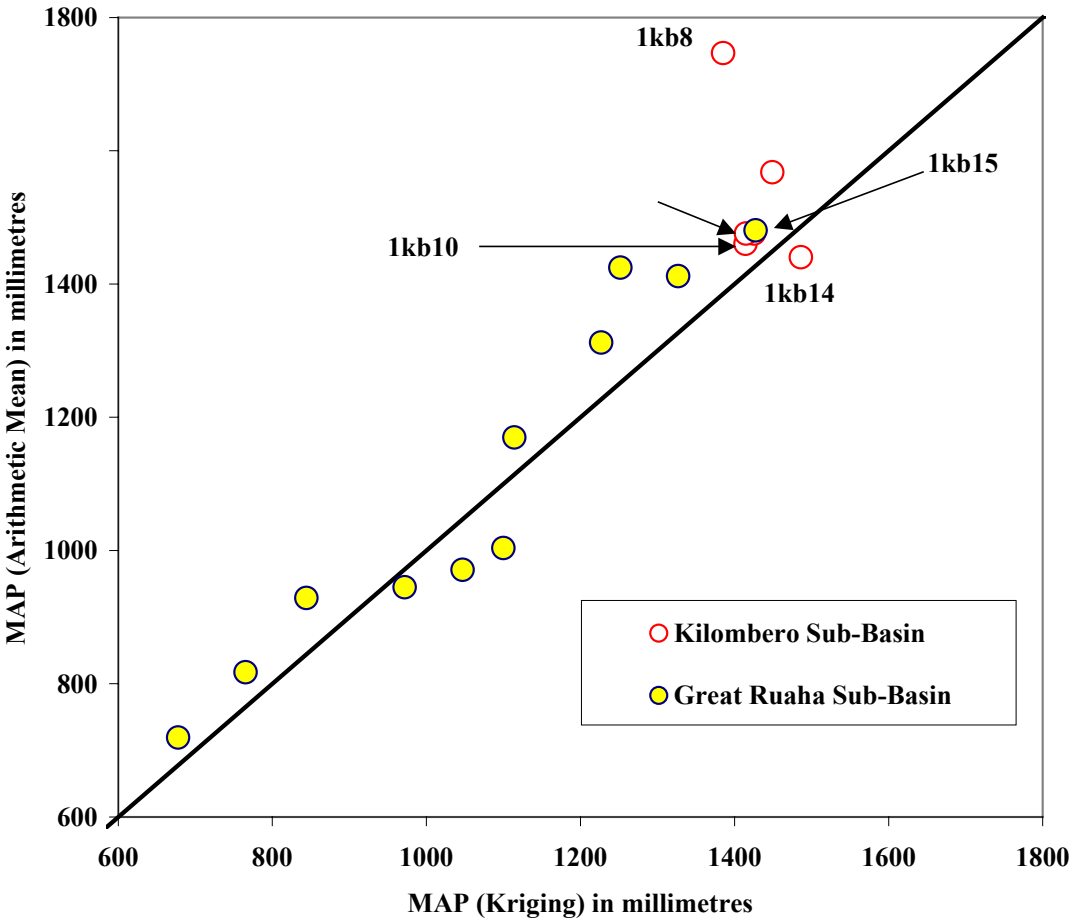

Figure 2.5: Comparison of Estimated MAP by Kriging and Arithmetic Mean for Some Catchments of the Rufiji River Basin (the Catchments within Kilombero Sub-Basin are labelled)

Figure F2.6: Location of Rainfall Stations selected for the Intervening Catchments of Stiegler's Gorge (Int-1k3), Kilombero (Int-1kb17) and Mtera-Kidatu (Int-Kid)

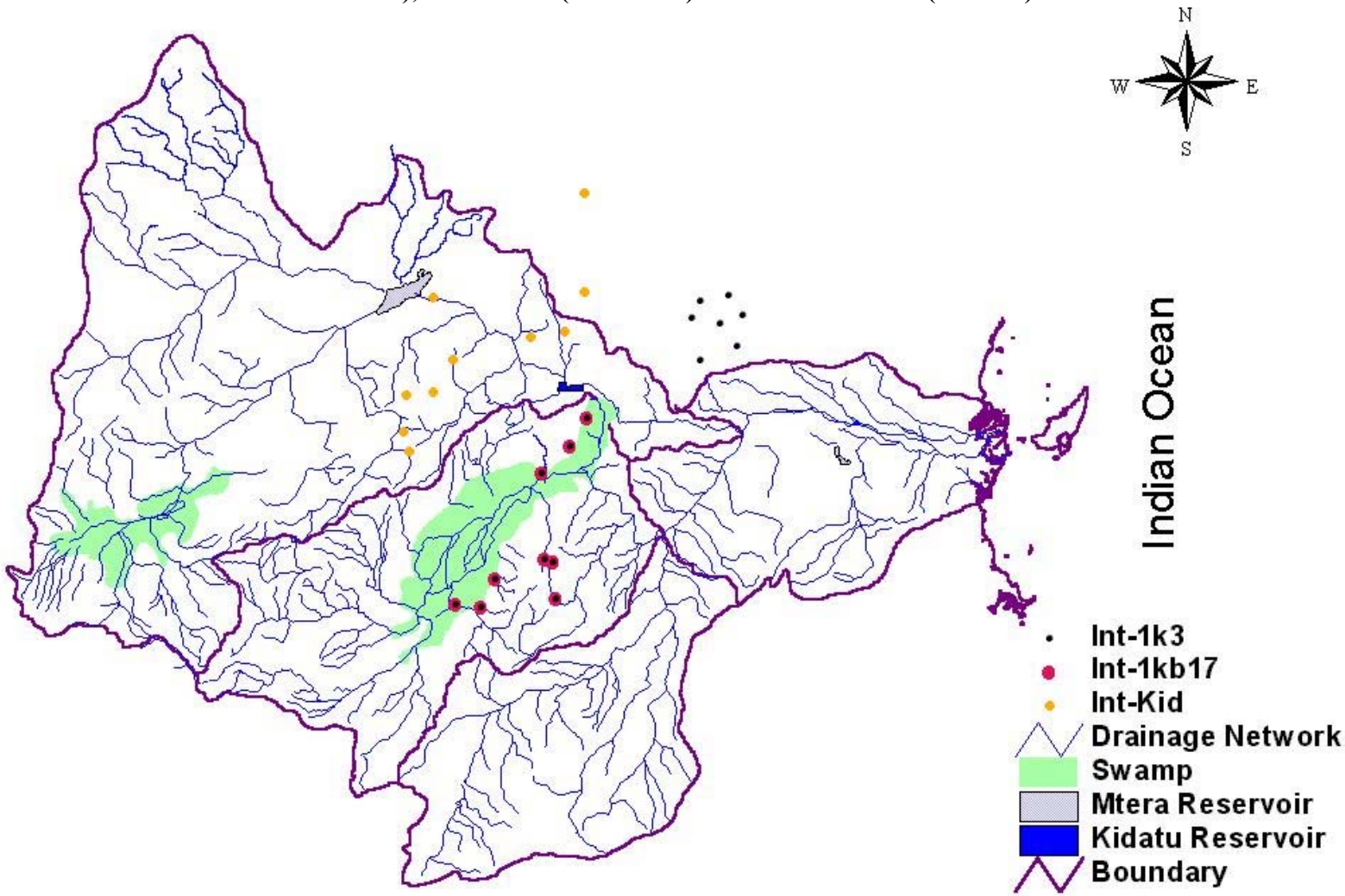

Figure F2.6: Location of Rainfall Stations selected for the Intervening Catchments of Stiegler's Gorge (Int-1k3), Kilombero (Int-1kb17) and Mtera-Kidatu (Int-Kid)

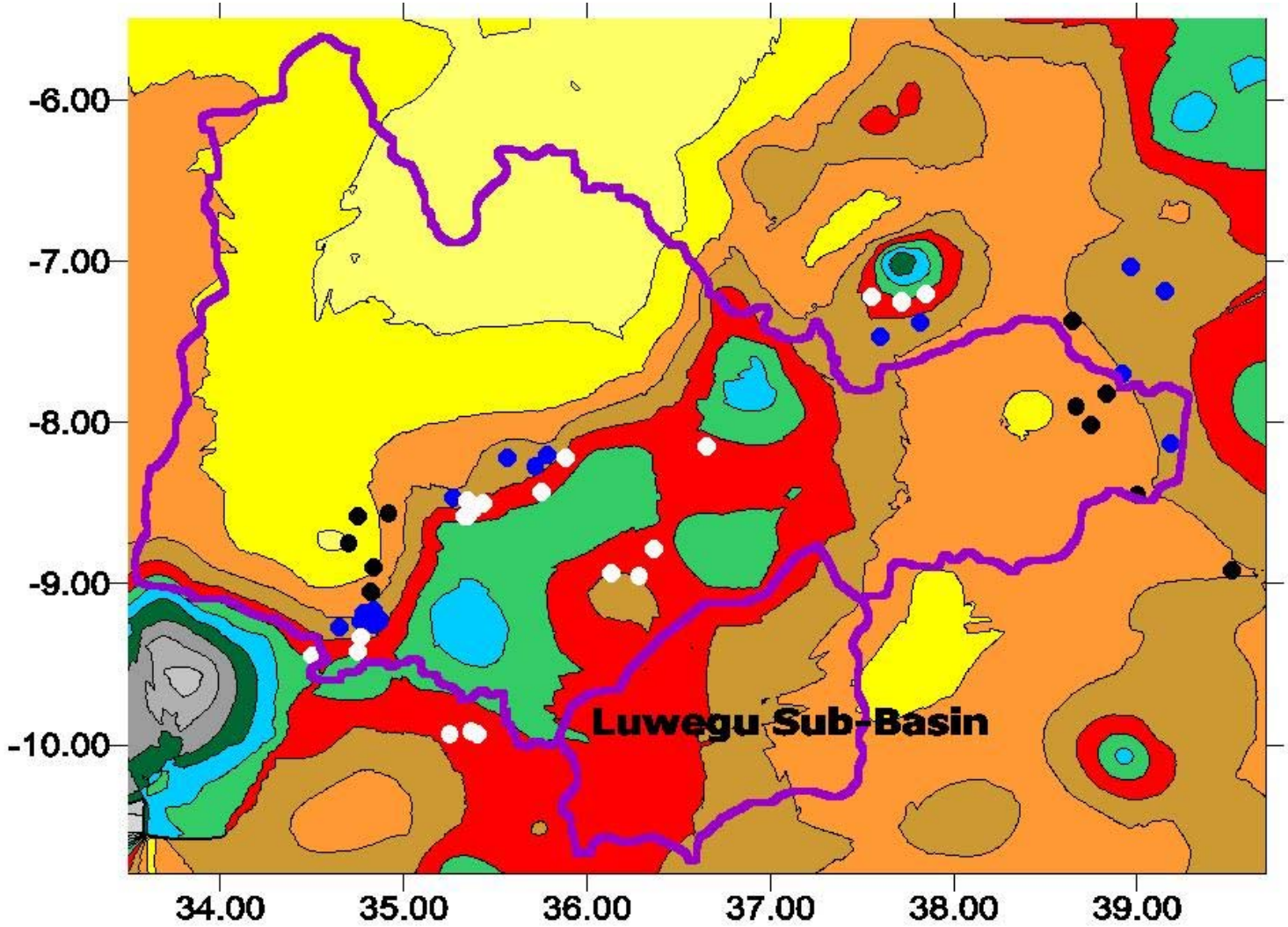

Figure F2.7: Location of Daily Rainfall Stations, superimpose on MAP diagram, that were used to create average rainfall over Ungauged Luwegu Sub-Basin

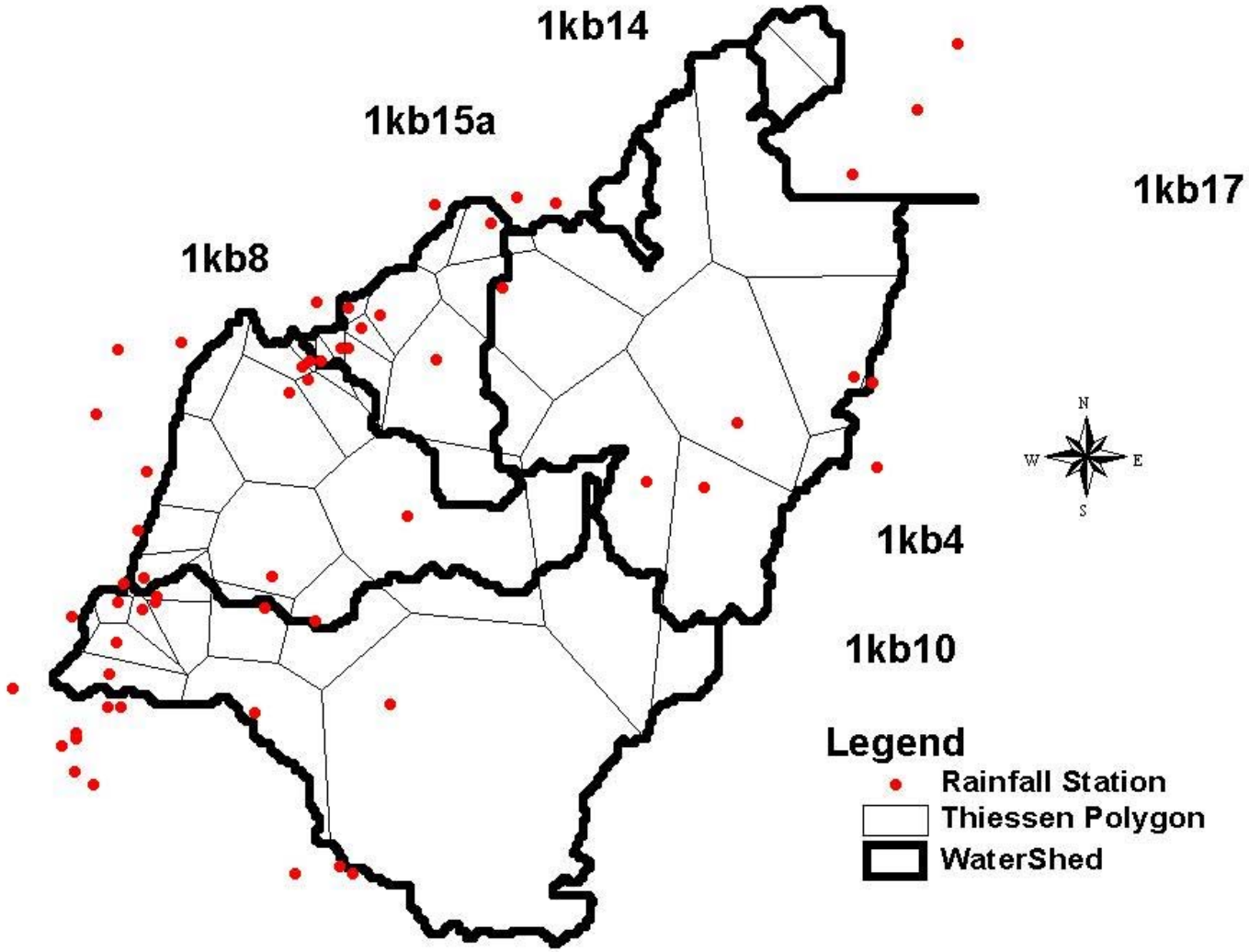

Figure F2.8: Map of Kilombero Sub-Basin delineated from DEM showing the Thiessen Polygon Network created from the Available Daily Rainfall Stations

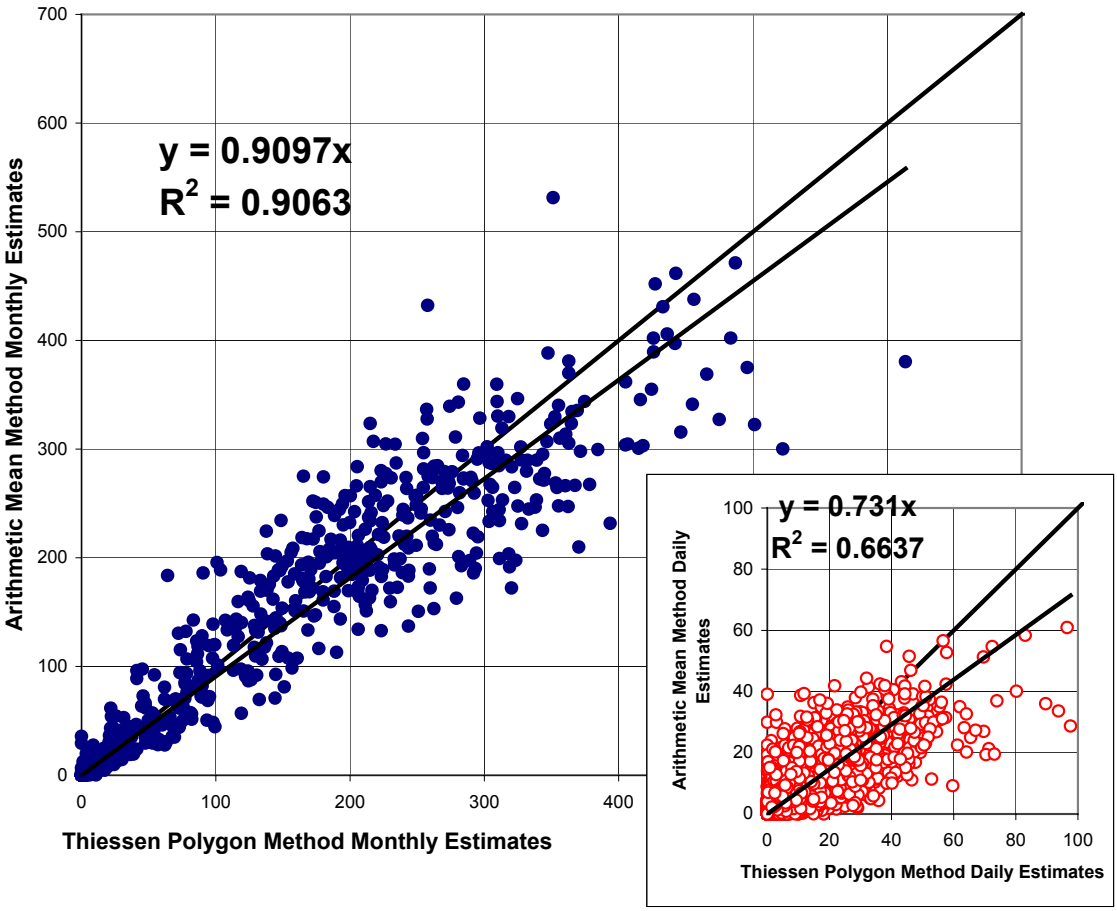

Figure F2.9: Comparison of ADR Estimates for Catchment 1kb10 by Thiessen Polygon and Arithmetic Mean Methods on Daily and Monthly Basis

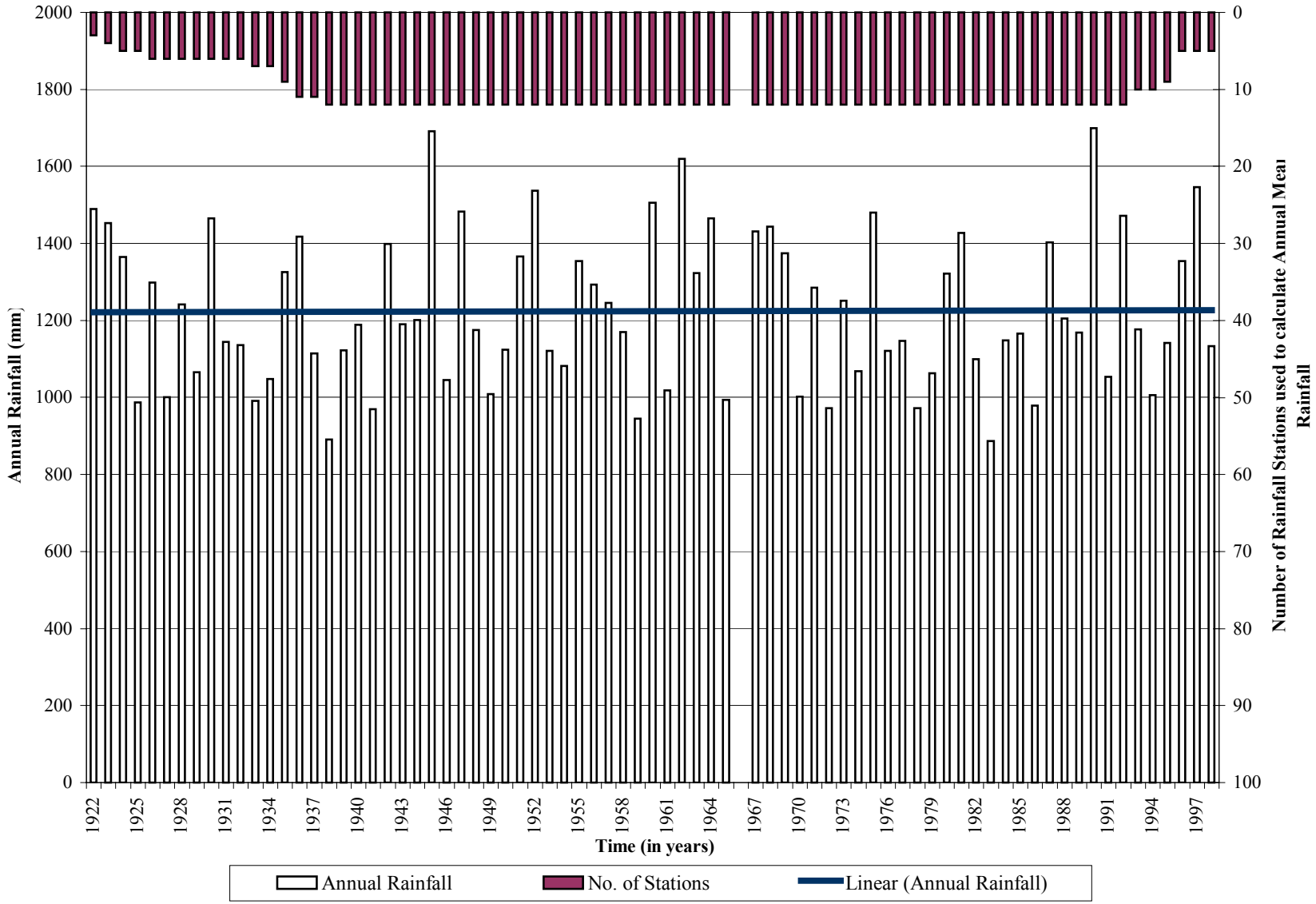

Figure F2.10: Annual Mean Rainfall of the Average of the 12 Selected Long Record Stations Fitted with Linear Trend Line

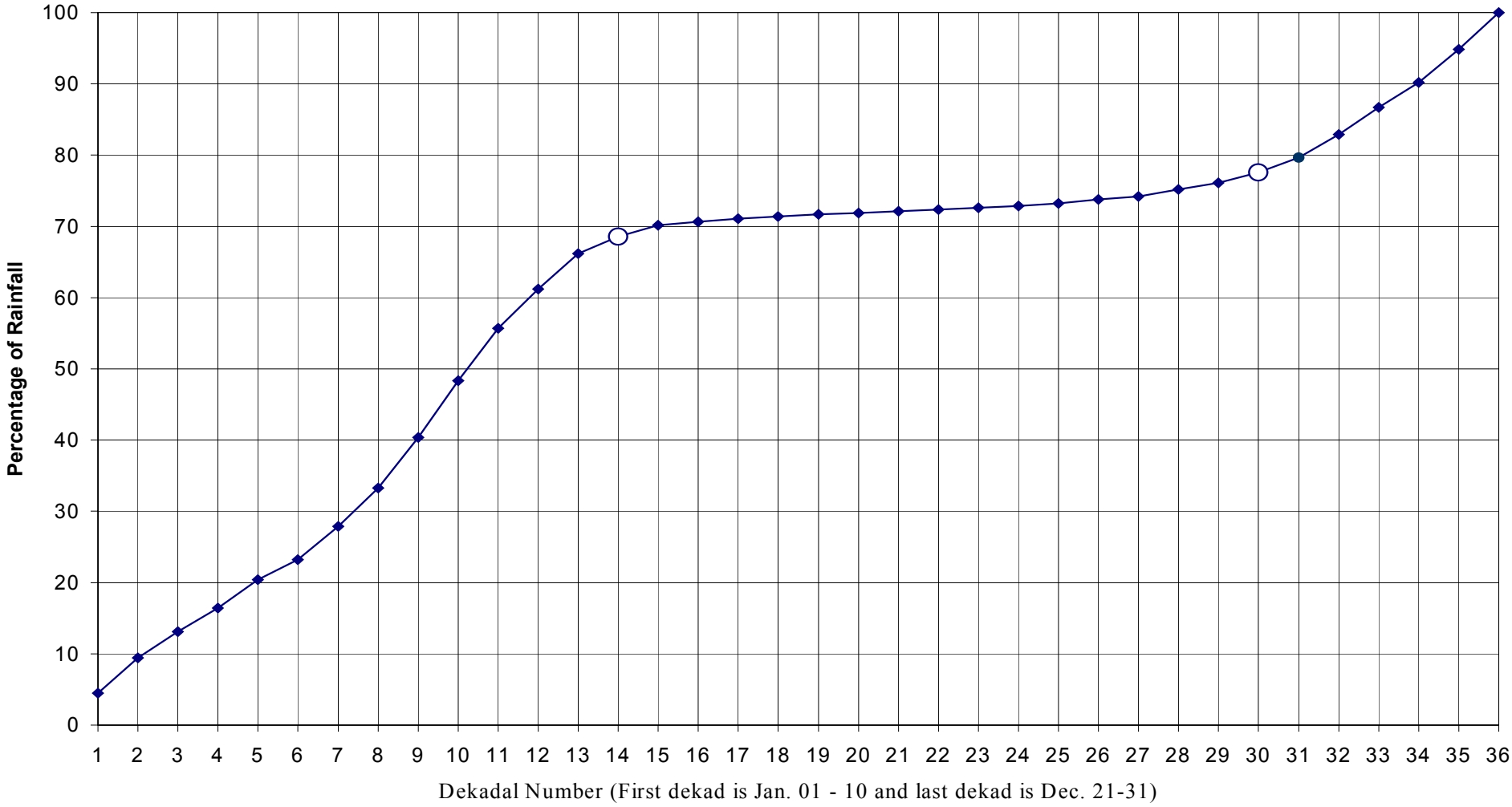

Figure F2.11: Plot of the Cummulated Seasonal Rainfall for Station 09838002

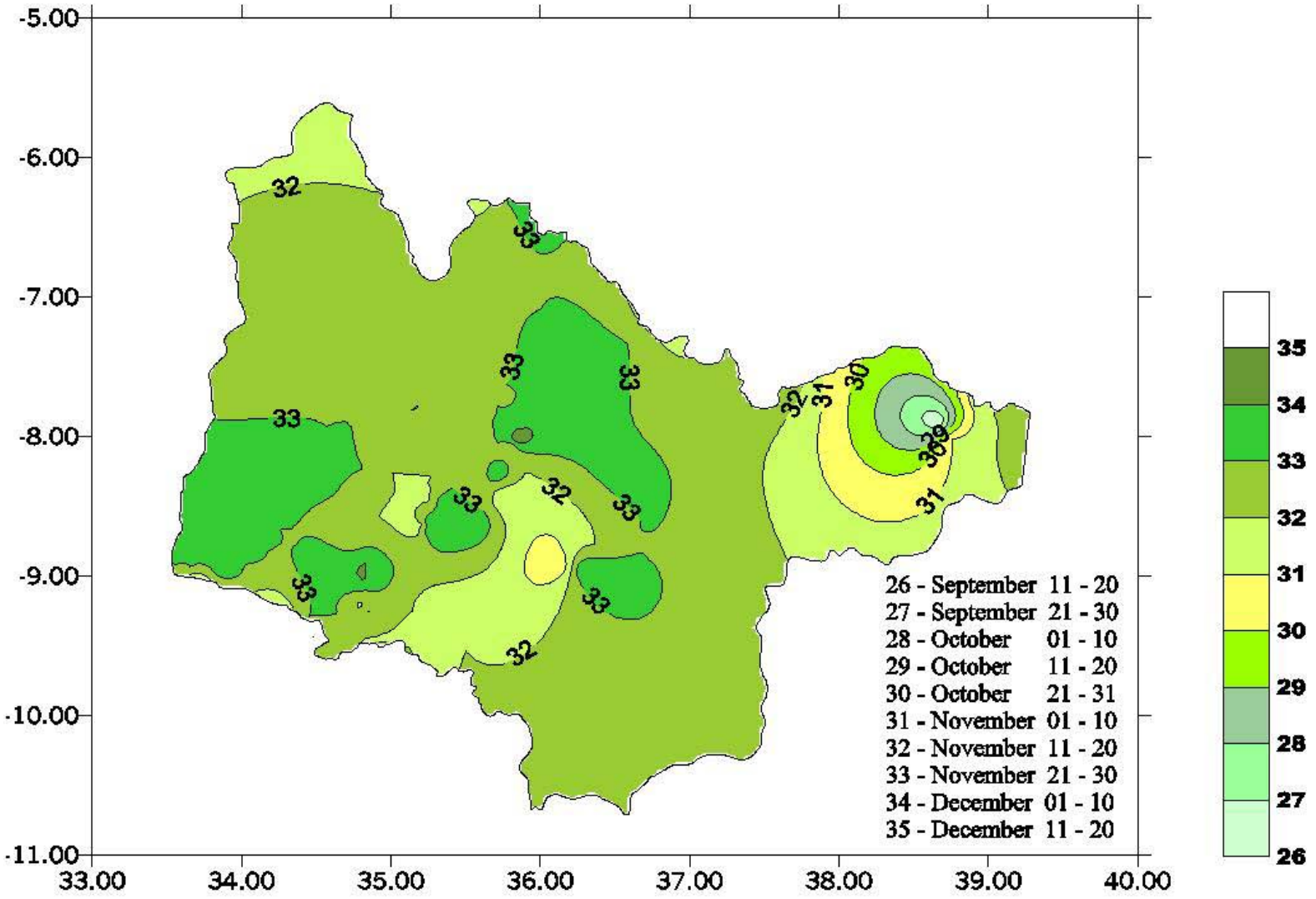

Figure F2.12: Spatial Distribution of the Onset of the Rainfall

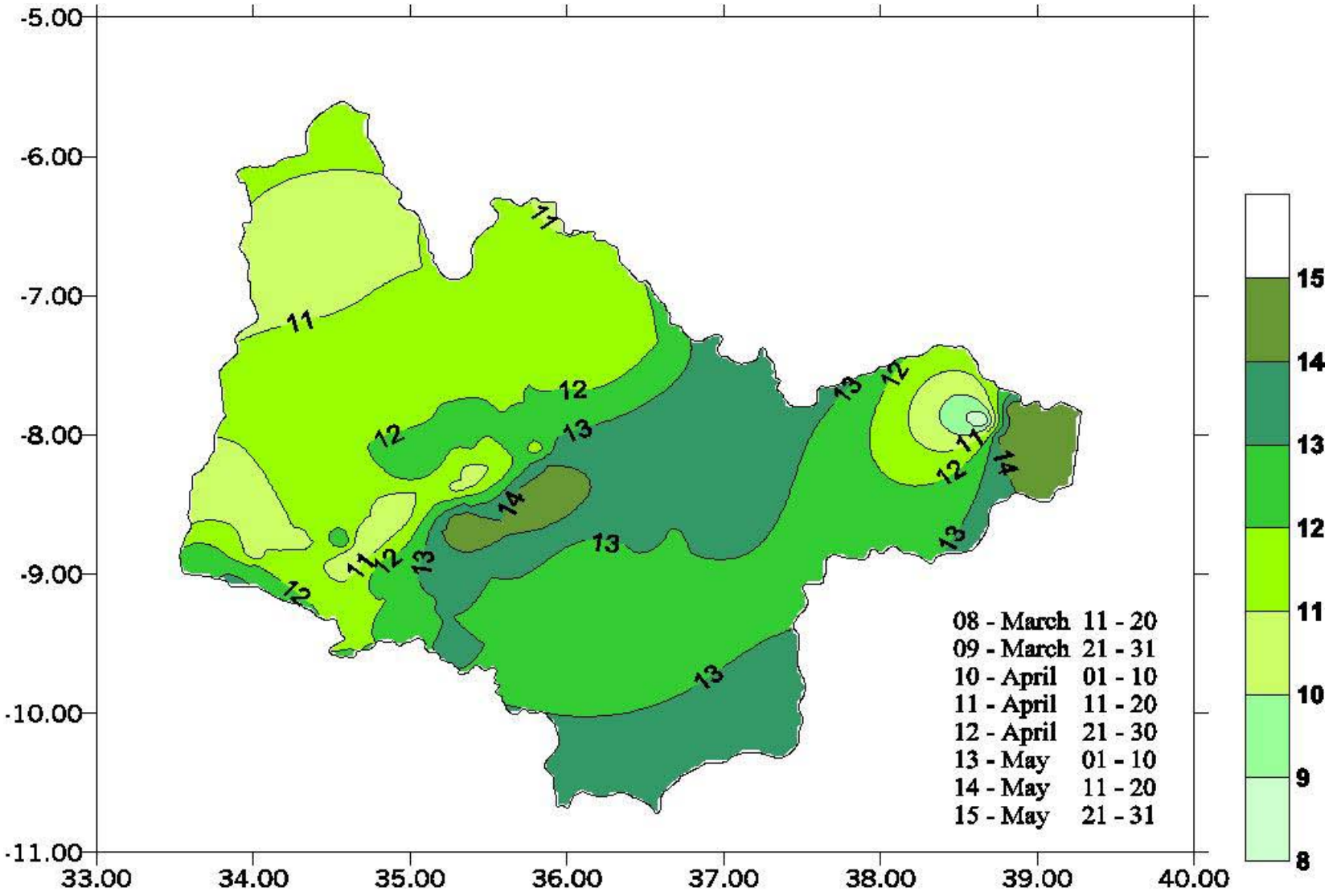

Figure F2.13: Spatial Distribution of the Cessation of the Rainfall

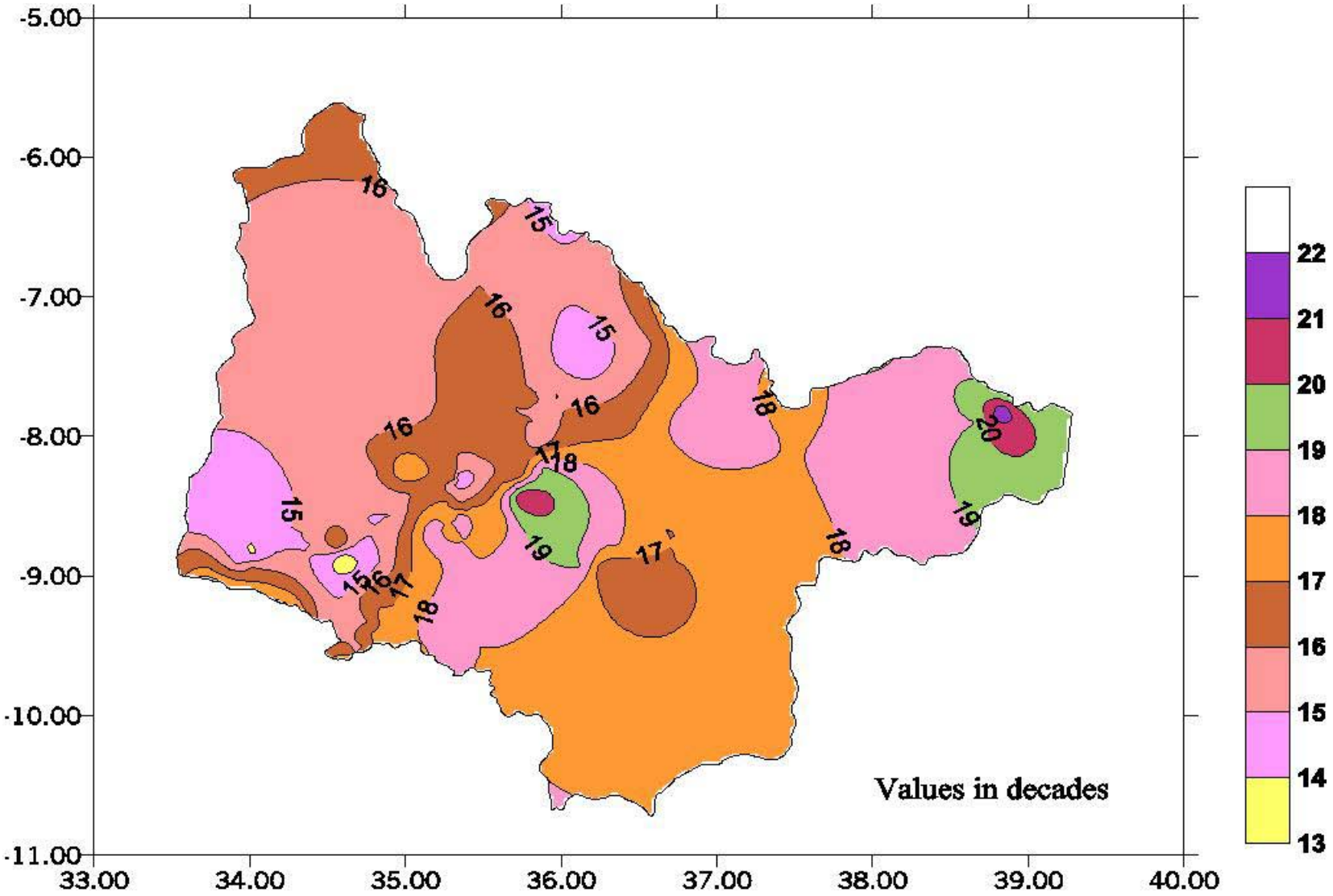

Figure F2.14: Spatial Distribution of the Duration of the Rainfall

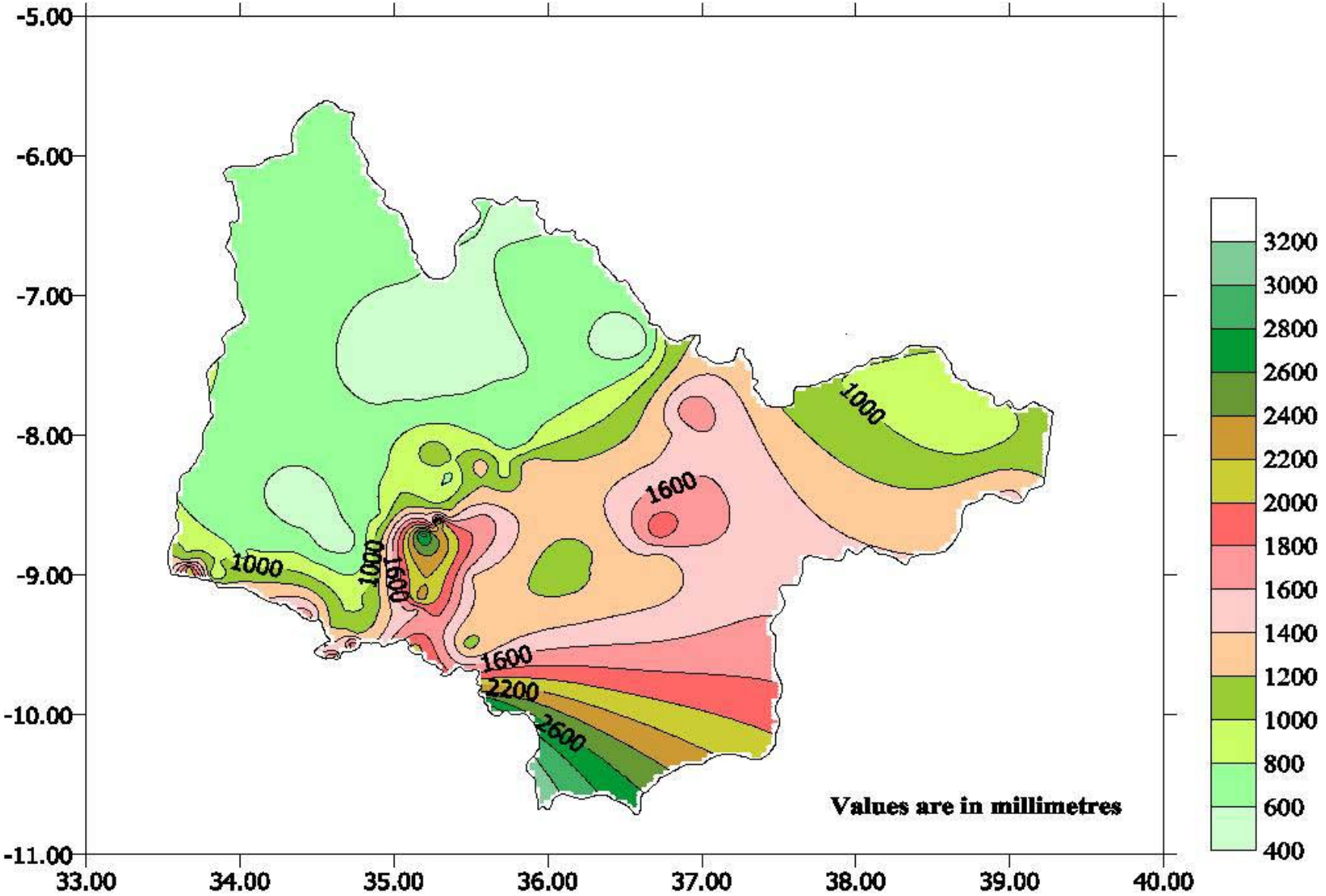

Figure F2.15: Spatial Distribution of the Magnitudes of the Rains from Onset to Cessation

Chapter 3

3 Evaporation Calculations

3.1 The Data

There are limited amounts of climatic data that are available for estimation of potential evapotranspiration in the Rufiji River Basin. Limited data of minimum and maximum daily temperatures or daily mean temperature, wind speed, sunshine hours and the relative humidity are available for eight locations, namely, Dodoma, Iringa, Mbeya, Songea, Morogoro, Igawa, Madibira and Kilwa Kivinje. All these locations are marked in Figure F3.11. Five of these stations (Dodoma, Mbeya, Songea, Morogoro and Kilwa Kivinje) are not within the basin but they are located slightly outside of the basin. The other climatic stations like Stiegler's Gorge, Lumemo, Tenende, and Malinyi, which are within the basin, do not have any records of sunshine hours that are required for Potential Evapotranspiration calculations.

The details of the available climatic data are presented in Table T3.1. Madibira has the shortest length of data of about 8 years and Mbeya has the longest length of data of about 46 years but large chunks of data are missing in at all the locations. The quality of data is known to be very low except in the case of synoptic stations Dodoma, Iringa and Mbeya.

Lumemo, Tenende and Malinyi climatic stations were chosen for estimation of Potential Evapotranspiration for the Kilombero sub-basin because of their proximity to the sub-basin. But because there was not sufficient data for all Penman parameters to estimate the Penman Potential rates it was decided to estimate the Potential Evapotranspiration rate based only on the temperature data.

3.2 Penman-Monteith Calculations

The Penman-Monteith method, recommended by FAO was used to estimate daily potential evapotranspiration (ET_0) at climatic stations, for which the data were available. (*The text and the work, presented in this sub-section, was done by WREP as part of SMUWC Project*).

The Potential evapotranspiration, ET_0, is defined as the rate of evapotranspiration from a hypothetical reference crop with an assumed crop height 0.12 m, a fixed crop surface resistance of 70 and an albedo of 0.23, closely resembling the evapotranspiration from an extensive surface of green grass cover of uniform height completely shading the ground and with adequate water. It is given by:

$$ET_0 = \frac{1}{\lambda}\frac{\Delta R_n + \rho_a \dfrac{c_p}{r_a}\left(e_a - e_d\right)}{\Delta + \gamma\left(1 + \dfrac{r_c}{r_a}\right)} \tag{3.1}$$

where

$\mathbf{R_n}$	the net radiation at the crop surface [$MJm^{-2}d^{-1}$].
$\mathbf{e_a - e_d}$	vapour pressure deficit [kPa].
Δ	slope of vapour pressure curve [-].
γ	Psychrometric constant [-].
$\boldsymbol{\rho_a}$	air density.
$\mathbf{c_p}$	is the specific heat of the air.
$\mathbf{r_c}$	net resistance to diffusion through the surfaces of the leaves and soil.
$\mathbf{r_a}$	net resistance to diffusion through the air from the surfaces to height of measuring instrument.
$\boldsymbol{\lambda}$	the latent heat of vaporization of water.

To calculate ET_0, therefore, mean temperature, wind speed, sunshine hours and relative humidity are needed. The estimates using this method were carried out in detailed for the three synoptic stations of Dodoma, Iringa and Mbeya because there are sufficient data at these locations for the Penman calculations.

3.3 Thornthwaite Calculations

Data on all parameters that are necessary for calculation of Penman-Monteith Potential Evapotranspiration (PET) have large chunks of data missing. The details, in terms of percentages of missing data, are presented in Table T3.1. Among all the parameters it is the temperature data that covers the longest time span with minimum missing data. In this regard, the calculation of potential evaporation in the region was based on temperature records. The Thornthwaite model for estimating potential evaporation, which requires only the mean monthly temperature and the number of days in a month as inputs, was used to estimate the potential evaporation.

The model was applied to Lumemo, Tenende and Malinyi climatic stations (the selected climatic stations that are presumed representative of the Kilombero sub-basin) as well as Dodoma, Iringa and Mbeya climatic stations.

Thornthwaite model is given as:

$$\begin{aligned} T_i' &= \left(\frac{T_i}{5}\right)^{1.514} \\ E_i &= 16 * a * \left(\frac{10 * T_i}{I}\right)^b \\ I &= \sum_{i=1}^{12} T_i' \\ b &= 6.75 * 10^{-7} * I^3 - 7.71 * 10^{-5} * I^2 + 1.792 * 10^{-2} * I + 0.4924 \end{aligned} \tag{3.2}$$

where

T_i is the monthly mean temperature in degrees centigrade,
E_i is the monthly evaporation in mm for month i, and
a is a correction factor to account for the day length.

3.4 Data Reconstruction

Data reconstruction was done for those stations that have data on all the parameters that are necessary for the calculation of Penman-Monteith Potential Evapotranspiration (PET) but there are chunks of missing data.

The reconstruction procedure followed the following steps.

Step 1:

Thornthwaite model, described by a set of equations 3.2, was used as a starting point to create a suitable temperature based model. The model was applied to the stations of Dodoma, Iringa and Mbeya, because these stations had a long length of temperature data of above 35 years and data of all other parameters to estimate PET using Penman-Monteith method.

Step 2:

The results of the application of the model are presented in Figure F3.1 for the climatic station of Dodoma. In this diagram the estimated PET by the Thornthwaite model (equation 3.2) is plotted against the observed temperature at Dodoma and has been presented by hollow circles. In the same diagram PET values, calculated by the application of Penman-Monteith model, are plotted against the observed temperature values and these are denoted by full black circles. Figures F3.2 and F3.3 are figures similar to that of Figure F3.1 but for the stations of Iringa and Mbeya, respectively.

Step 3:

From Figure F3.1 one can clearly see that the Thornthwaite model under estimates the PET. The same observations can be made for the case of Iringa and for Mbeya from Figures F3.2 and F3.3, respectively. To correct this under estimation by the Thornthwaite model (equation 3.2) it was decided to modify the coefficients of the model to arrive at a suitable estimation model. The modified models for the three stations under consideration are presented by equation 3.3 and the results are presented by hollow triangles on Figure F3.1 for Dodoma; on Figure F3.2 for Iringa and on Figure F3.3 for Mbeya.

The recommended models of equation 3.3 were arrived at, by changing the parameters of the Thornthwaite model, systematically, until the estimated values of PET matched reasonably well with the values that were calculated by the application of the Penman–Monteith model.

The modified models are as follows:

$$
\begin{aligned}
&\textit{for Dodoma}\\
E_i \;=\; &\begin{cases} 0.126 * T_i + 2.274 & \textit{for } T_i \le 23 \\ 16 * a * \left(\dfrac{10 * T_i}{I}\right)^b & \textit{for } T_i > 23 \end{cases}\\
&\textit{for Iringa}\\
E_i \;=\; &\begin{cases} 36 * a * \left(\dfrac{10 * T_i}{I}\right)^b & \textit{for } T_i \le 19.6 \\ 30 * a * \left(\dfrac{10 * T_i}{I}\right)^b & \textit{for } 19.6 < T_i \le 21 \\ 16 * a * \left(\dfrac{10 * T_i}{I}\right)^b & \textit{for } T_i > 21 \end{cases}\\
&\textit{for Mbeya}\\
E_i \;=\; &\begin{cases} 0.059 * T_i + 3.395 & \textit{for } T_i \le 18 \\ 16 * a * \left(\dfrac{10 * T_i}{I}\right)^b & \textit{for } T_i > 18 \end{cases}
\end{aligned}
\qquad (3.3)
$$

where the terms have the same meaning as in equation (3.2).

The mean annual potential evaporation in Dodoma is about 1,900 mm. In Iringa it is about 1,700 mm and in Mbeya it is 1,600 mm.

3.5 PET estimate of the Kilombero Sub-Basin

The estimation of Potential Evapotranspiration (PET) for the Kilombero sub-basin involved much subjective judgement because the climatic stations, that are considered to be representative of the sub-basin, namely Lumemo, Tenende and Malinyi, have hardly any data required for Penman calculations. These stations have only the temperature data that covers a long span. The quality of the Pan Evaporation data is questionable at all the stations. There is unrealistic variation of Pan evaporation values within a given month. This can, of course, be attributed to poor recording.

The estimation of potential Evapotranspiration for Kilombero sub-basin, was, therefore, based only on temperature records using Standard Thornthwaite model. The set of equations for Standard Thornthwaite model as described by equation 3.2 were applied.

The computed PET values using the Thornthwaite model were compared with the recorded Pan evaporation values. This was done at all climatic stations within the Kilombero sub-basin, that is, Lumemo, Malinyi and Tenende as shown in Figures F3.4 to F3.6. The comparison indicates that there is no clear relationship between the PET estimates using the Thornthwaite model and the Pan Evaporation estimates. This comparison clearly indicates that the Pan Evaporation data are poor.

The average Kilombero temperature was calculated by averaging the recorded temperature values of the three stations; Malinyi, Tenende and Lumemo. The resulting temperature data were correlated with the temperature records of Dodoma, Iringa and Mbeya as shown in Figures F3.7 to F3.9. A good relationship was observed between the average Kilombero temperature and that of Dodoma. It has a Coefficient of Determination of 72%. The average temperature of other stations, Iringa and Mbeya, did not match the Average temperature of the Kilombero basin. The temperatures at these stations are lower than the Kilombero temperature.

A plot of Monthly Thornthwaite Evaporation for the Dodoma station and that estimated for the Kilombero sub-basin based on average Monthly Thornthwaite Evaporation is shown in Figure F3.10. It also indicates a good relationship of about 71% coefficient of determination.

Based on these comparisons, it was concluded that the time series of PET estimated for Dodoma could be used for modelling the Kilombero sub-basin.

3.6 Mean Annual Potential Evapotranspiration (MAPET)

The mean annual Potential Evapotranspiration (MAPET) surface of the entire basin is presented in Figure F3.11. This was constructed from spatial extrapolation of 12 MAPET values (from the 12 available climatic stations) using Surfer and a suitable Krigging model. Three of the 12 stations are synoptic stations. They are presented as squares in the figure. Three other stations that are regarded as representative for the Kilombero sub-basin are presented as triangles. The rest of the stations are presented as circles in the same figure.

Given that the MAPET surface, Figure F3.11, has been created from only 12 values, that too sparsely distributed in the basin, therefore one cannot rely on the accuracy of the final result. Nevertheless, the overall picture is clear. The rate of MAPET is high, of the order of about 1,300 mm at the southern part of the basin. It goes up to 1,900 mm in the north of the basin.

Table T3.1: Statistics of climatic data for stations in and around the study area (the Rufiji River Basin)

	Station	Maximum Temperature			Minimum Temperature			Mean Temperature			Sunshine Hours			Relative Humidity			Wind Speed			Pan Evaporation		
		Start year	No. of yrs	% mis-sing	Start year	No. of yrs	% mis-sing	Start year	No. of yrs	% mis-sing	Start year	No. of yrs	% mis-sing	Start year	No. of yrs	% mis-sing	Start year	No. of yrs	% mis-sing	Start year	No. of yrs	% mis-sing
1	Dodoma	1958	40	3.2	1958	40	3.5	-	-	-	1973	18	23.3	1972	23	2.9	1973	22	21.9	1973	22	35.3
2	Iringa	1960	39	8.6	1960	39	2.6	-	-	-	1973	26	42.3	1972	27	0.7	1973	26	25.1	1973	26	56.4
3	Mbeya	1953	46	5.4	1953	46	2.9	-	-	-	1967	32	44.6	1972	27	10.8	1971	28	18.0	1971	28	48.7
4	Songea	1960	34	5.6	1960	34	3.2	-	-	-	1970	24	24.2	1973	22	5.7	1971	24	15.1	1976	19	62.2
5	Morogoro	1970	24	3.0	1970	24	5.2	-	-	-	1970	24	17.1	1973	19	3.1	1971	23	1.6	1970	24	10.6
6	Igawa	-	-	-	-	-	-	1974	23	45.1	1974	23	62.6	1974	23	76.5	1974	23	18.9	1974	23	64.2
7	Madibira	-	-	-	-	-	-	1975	8	31.0	1975	8	28.7	1975	8	36.1	1975	8	30.1	1975	8	29.3
8	Kilwa Kivinje	-	-	-	-	-	-	1964	31	30.8	1964	31	80.7	1964	31	33.8	1964	31	32.1	1964	31	63.7
9	Stiegler's Gorge	-	-	-	-	-	-	1975	15	3.7	-	-	-	1975	15	9.3	1975	15	11.9	1975	15	48.6
10	Lumemo	-	-	-	-	-	-	1960	36	48.8	-	-	-	-	-	-	-	-	-	1960	36	66.5
11	Tenende	-	-	-	-	-	-	1967	29	68.0	-	-	-	-	-	-	-	-	-	1967	29	76.4
12	Malinyi	-	-	-	-	-	-	1963	19	13.8	-	-	-	-	-	-	-	-	-	1963	19	72.7

Locations of the climatic stations

z	Station	Eastern	Northern
1	Dodoma	806244.9	9317540.0
2	Iringa	797905.1	9155341.0
3	Mbeya	551339.6	9012523.0
4	Songea	782578.7	8819660.0
5	Morogoro	1014330.4	9242225.0
6	Igawa	652121.1	9030628.0
7	Madibira	700149.2	9089489.0

	Station	Longitude	Latitude
8	Kilwa Kivinje	39° 25'	8° 35'
9	Stiegler's Gorge	38° 55'	7° 48'
10	Lumemo	36° 37'	8° 10'
11	Tenende	34° 59'	9° 33'
12	Malinyi	36° 05'	8° 56'

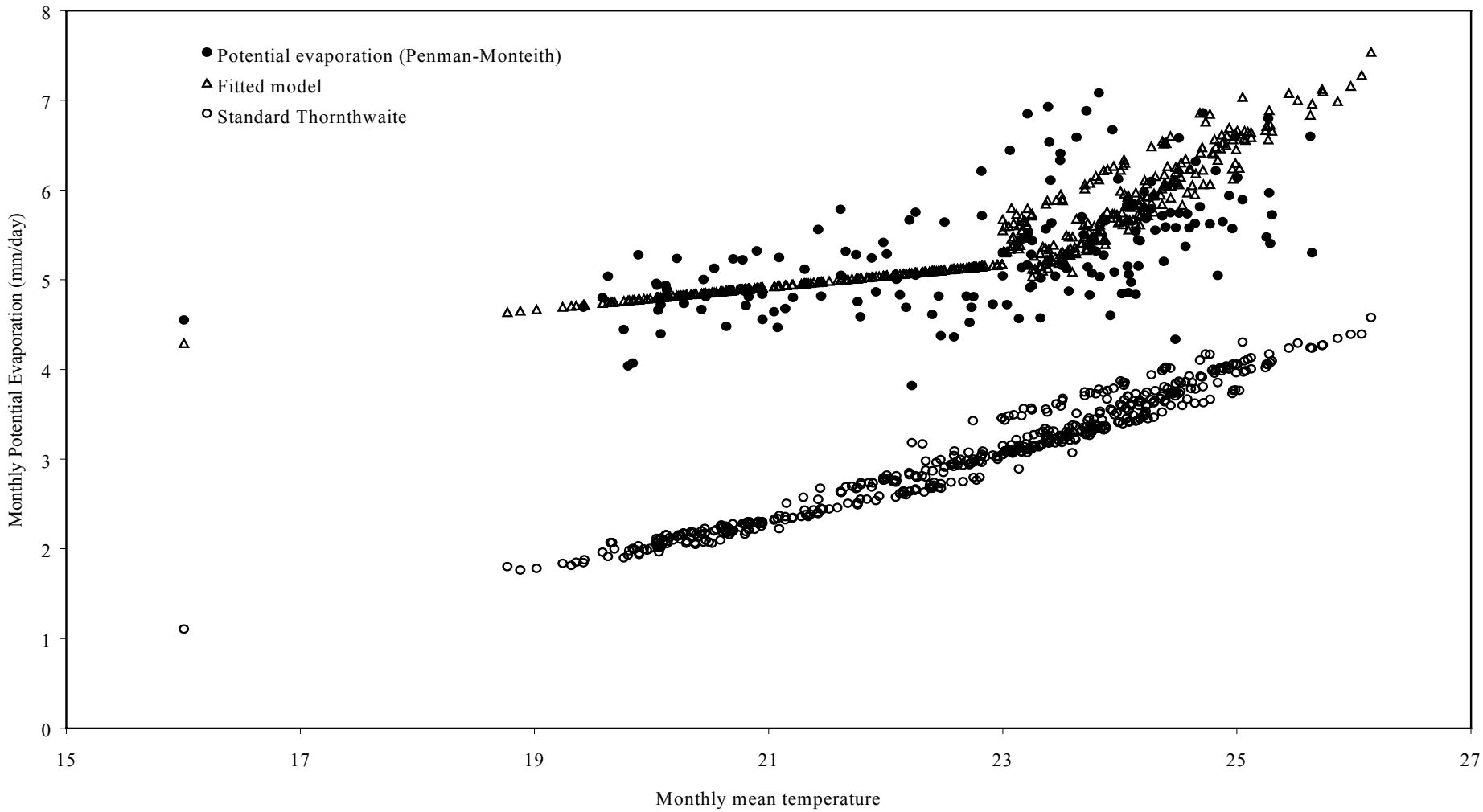

Figure F3.1 Dodoma mean Monthly Penman-Monteith Potential Evaporation versus mean monthly temperature

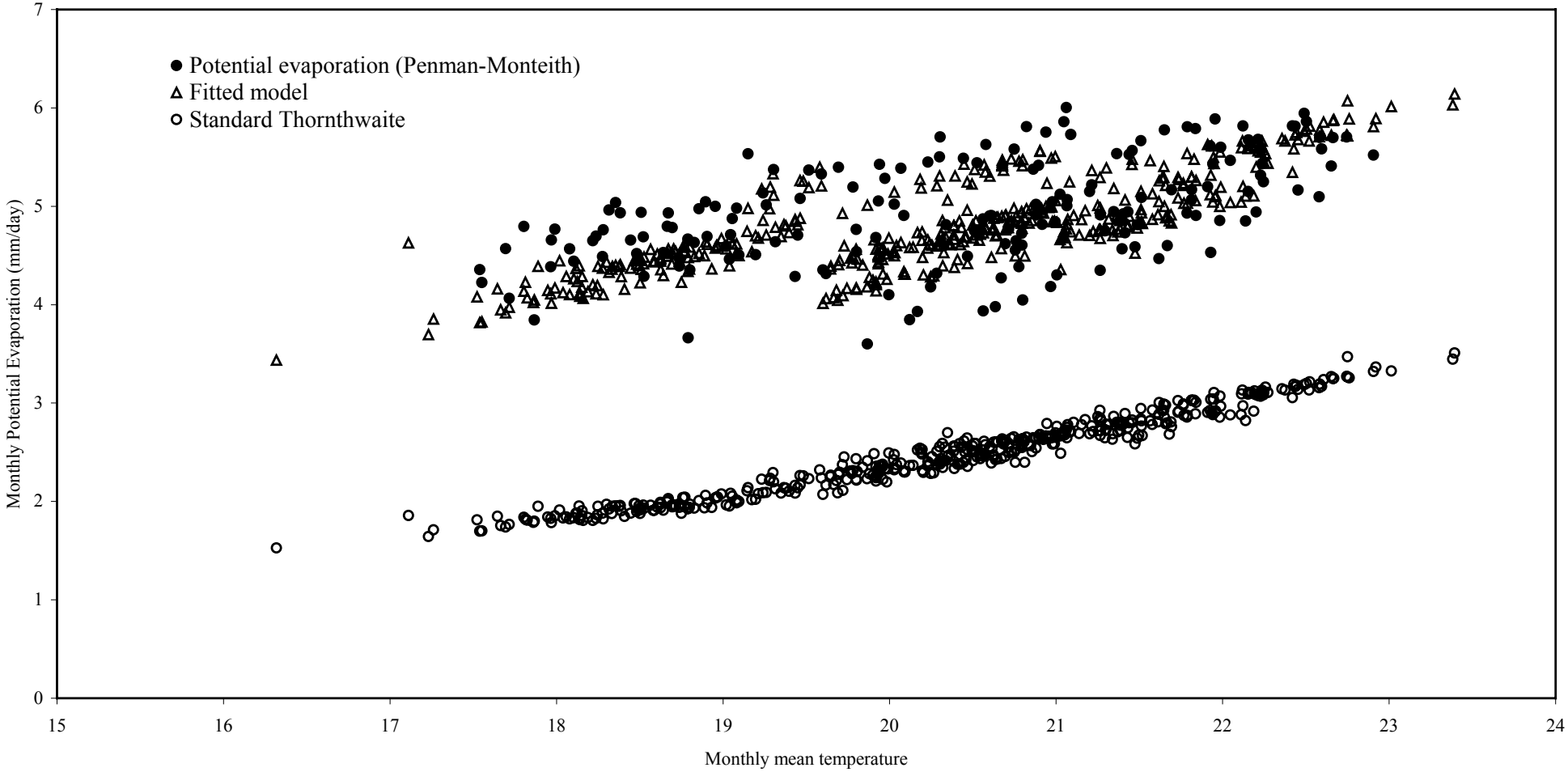

Figure F3.2: Iringa mean monthly Penman-Montieth Potetnial Evaporation versus mean monthly temperature

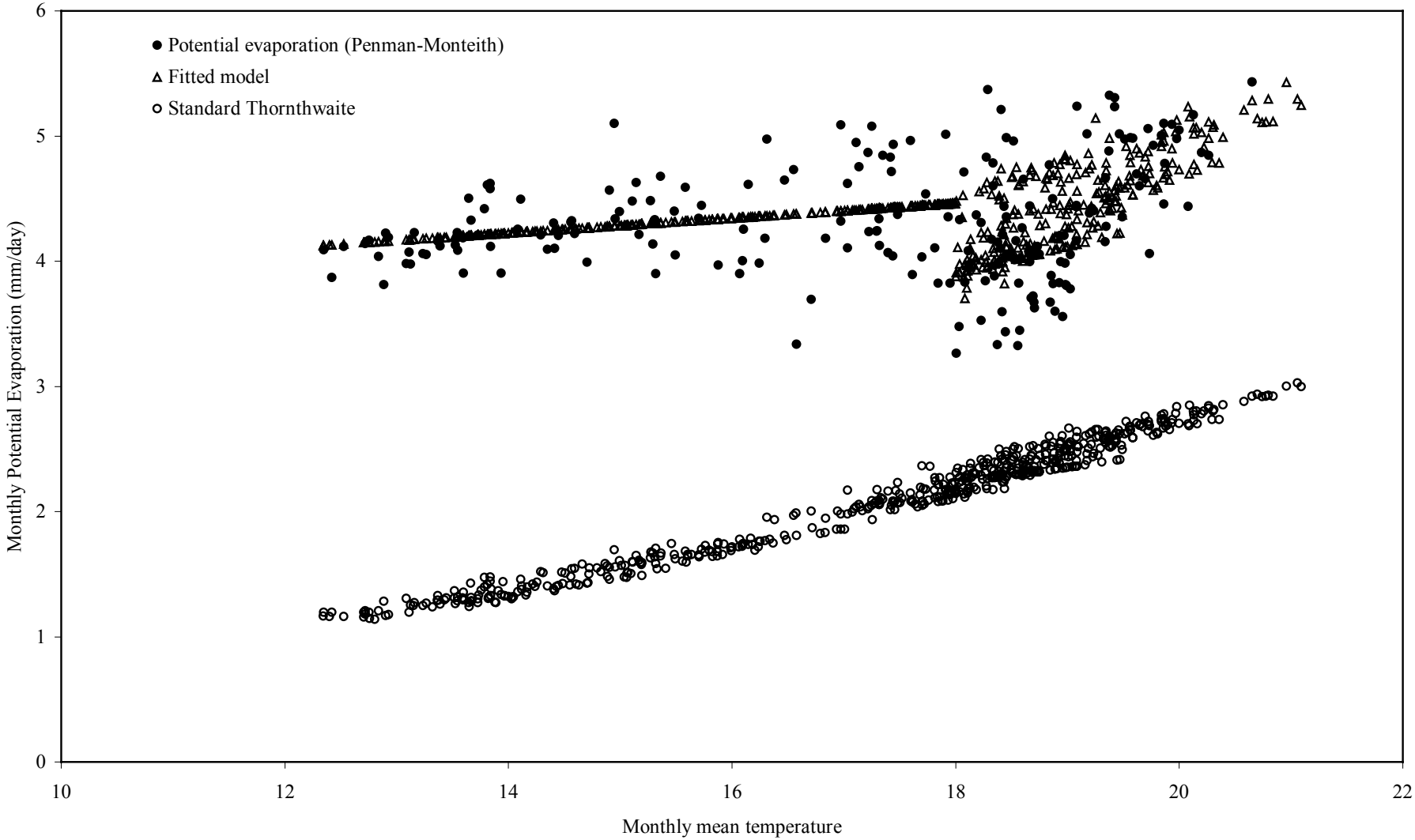

Figure F3.3 Mbeya mean monthly Penman-Montieth Potetnial Evaporation versus mean monthly temperature

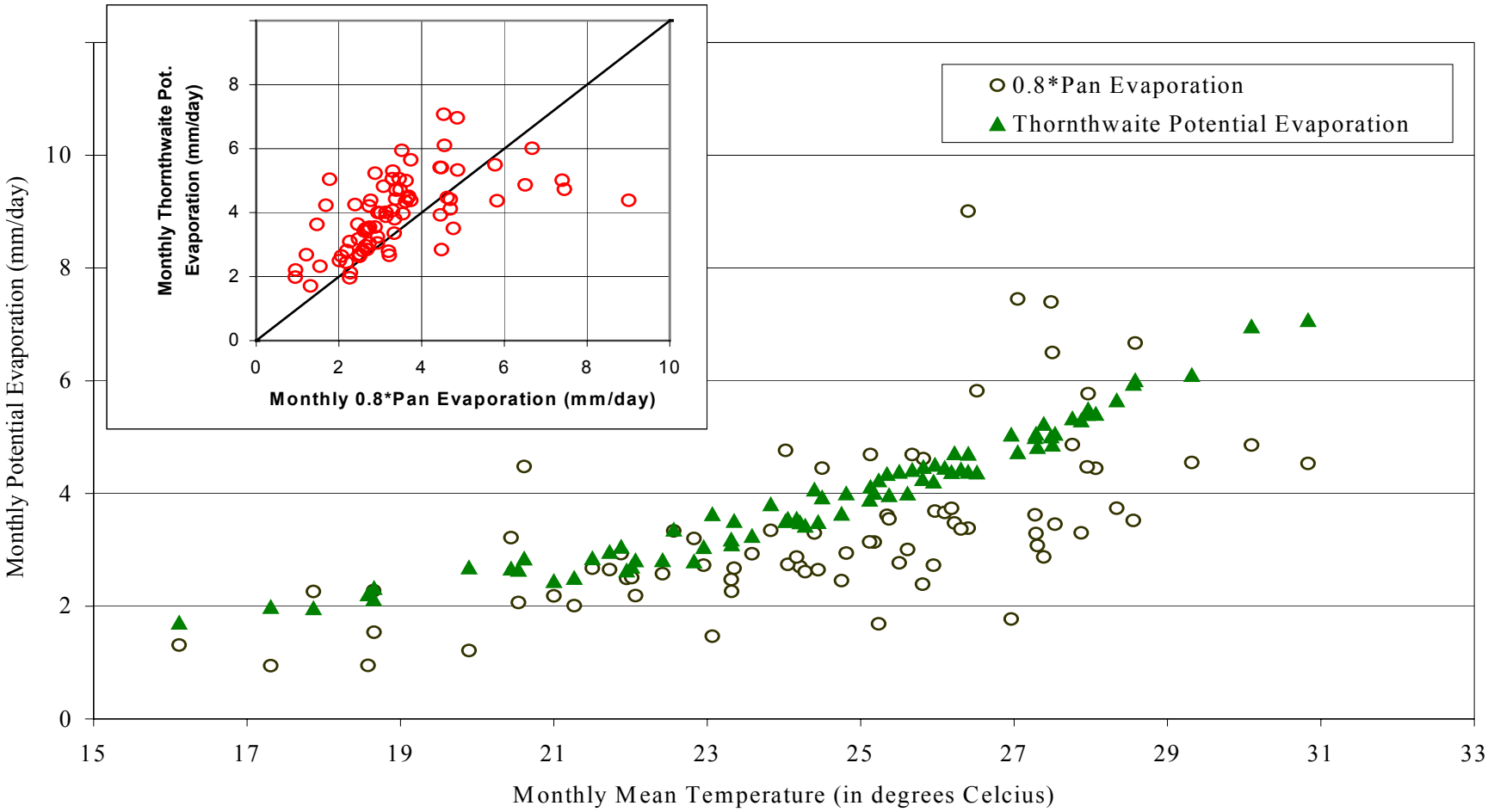

Figure F3.4: Comparison between Pan Evaporation and Estimated Potential Evaporation using Thornthwaite Method against Temperature at Malinyi Climatic Station

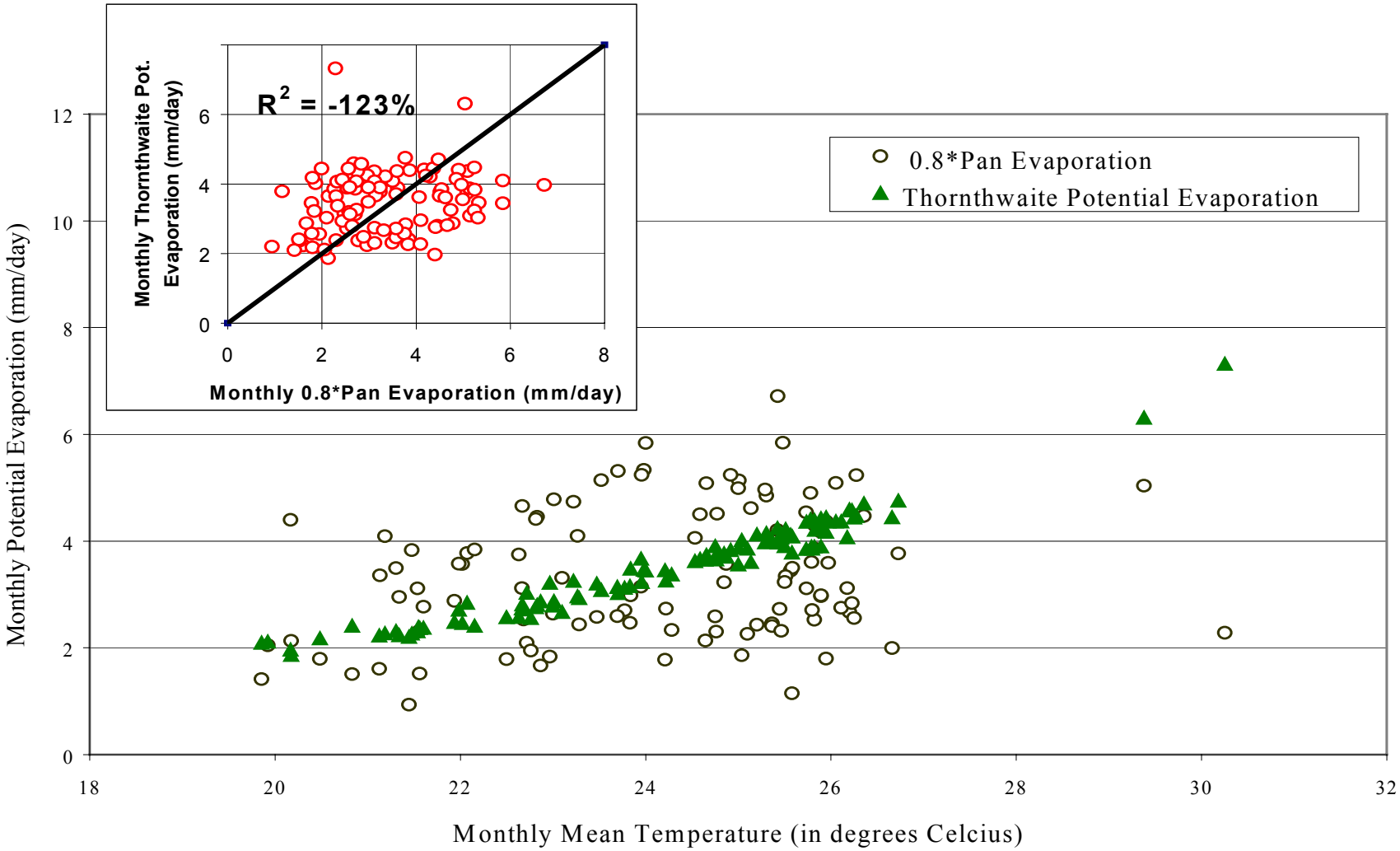

Figure F3.5: Comparison between Pan Evaporation and Estimated Potential Evaporation using Thornthwaite method against Temperature at Tenende Climatic Station

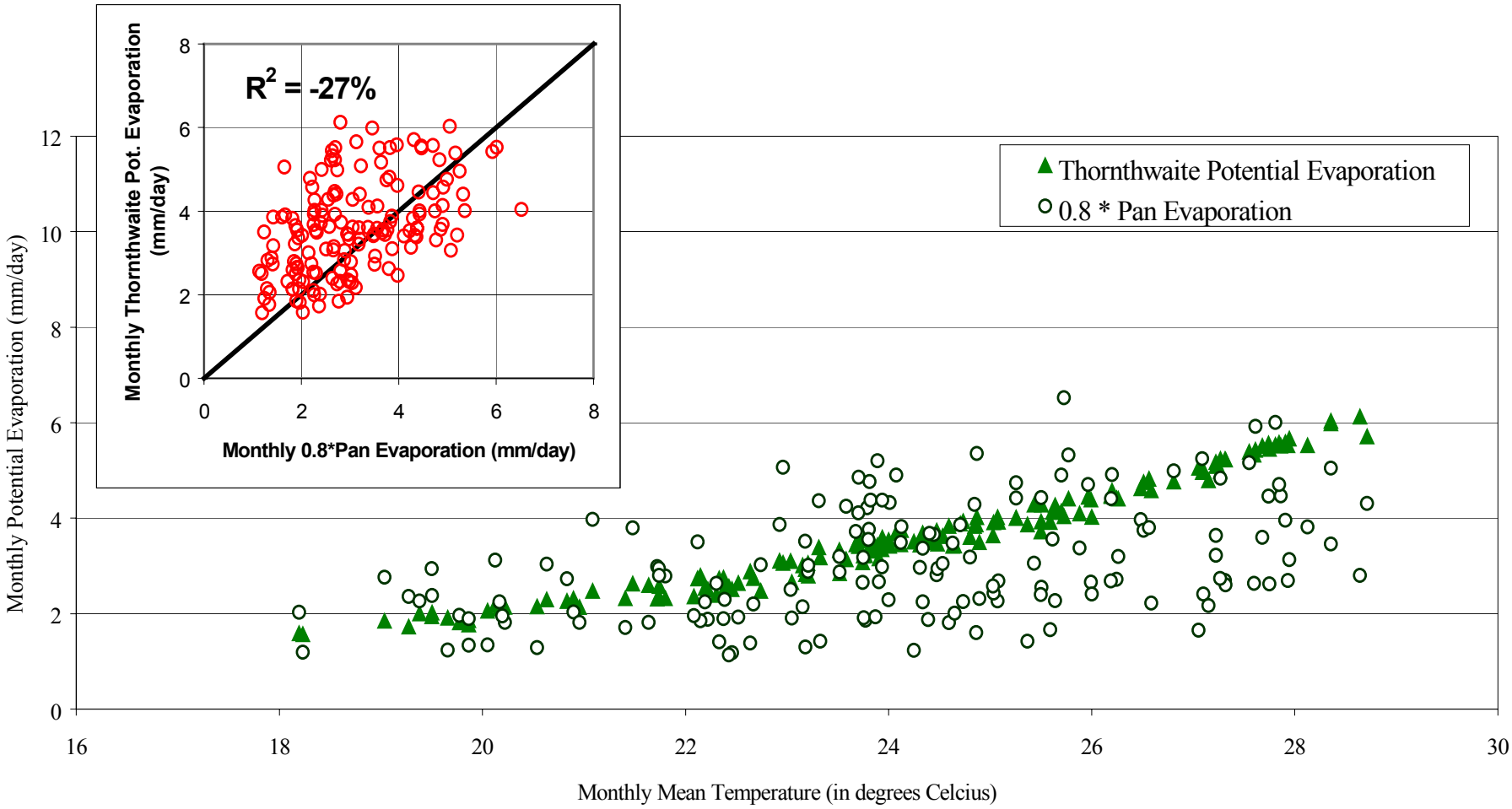

Figure F3.6: Comparison between Pan Evaporation and Estimated Potential Evaporation using Thornthwaite Method against Temperature at Lumemo Climatic Station

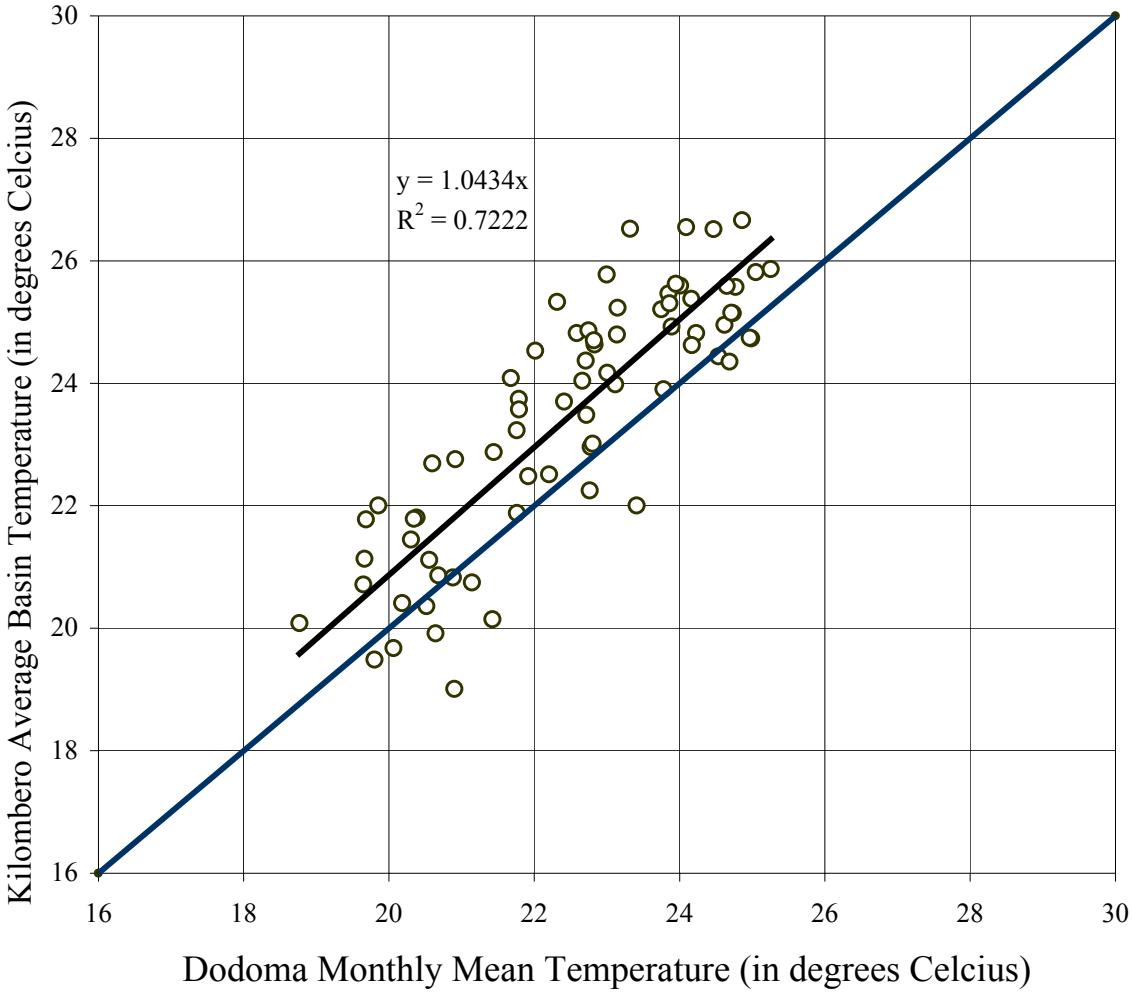

Figure F3.7: Comparison between Monthly Mean Temperature at Dodoma station and Kilombero, average Basin Temperature estimated from Malinyi, Lumemo and Tenende Climatic Stations

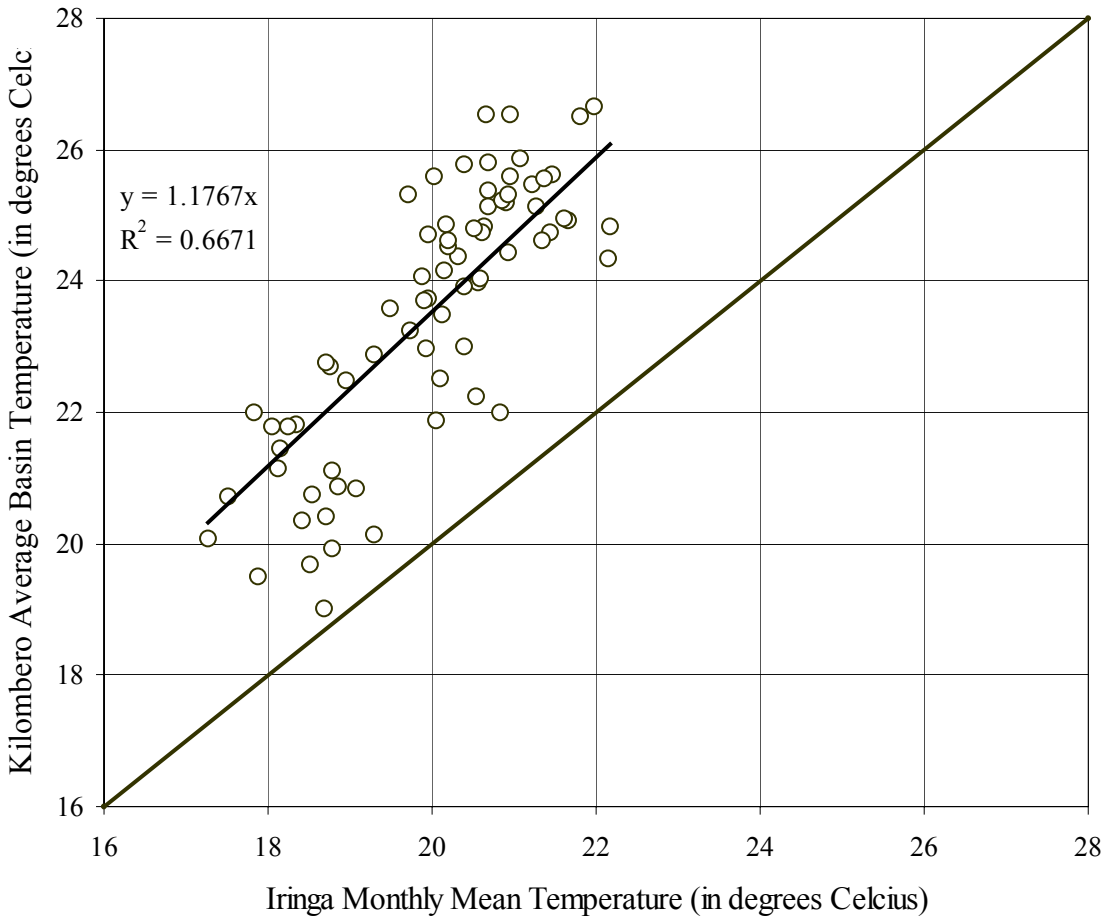

Figure F3.8: Comparison between Monthly Mean Temperature at Iringa station and Kilombero, average Basin Temperature estimated from Malinyi, Lumemo and Tenende Climatic Stations

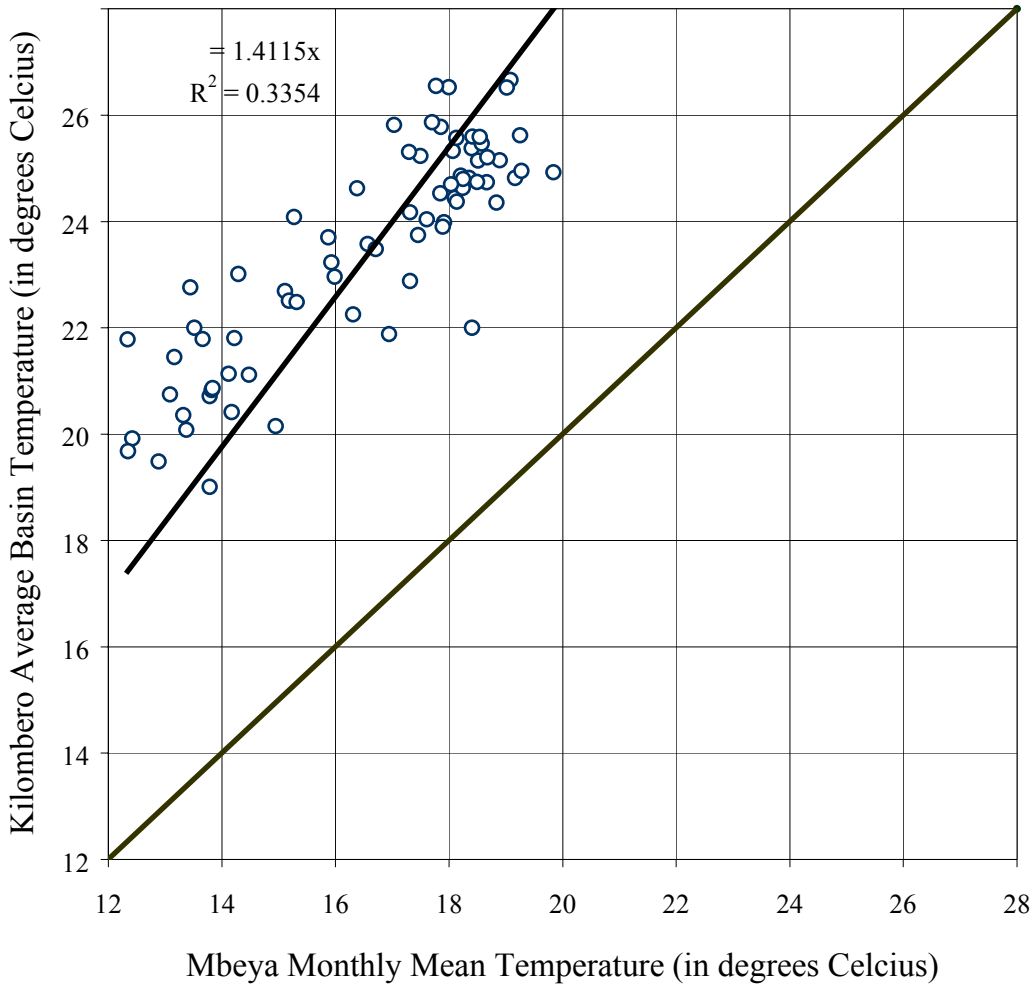

Figure F3.9: Comparison between Monthly Mean Temperature at Mbeya station and Kilombero Average Basin Temperature estimated from Malinyi, Lumemo and TenendeClimatic Stations

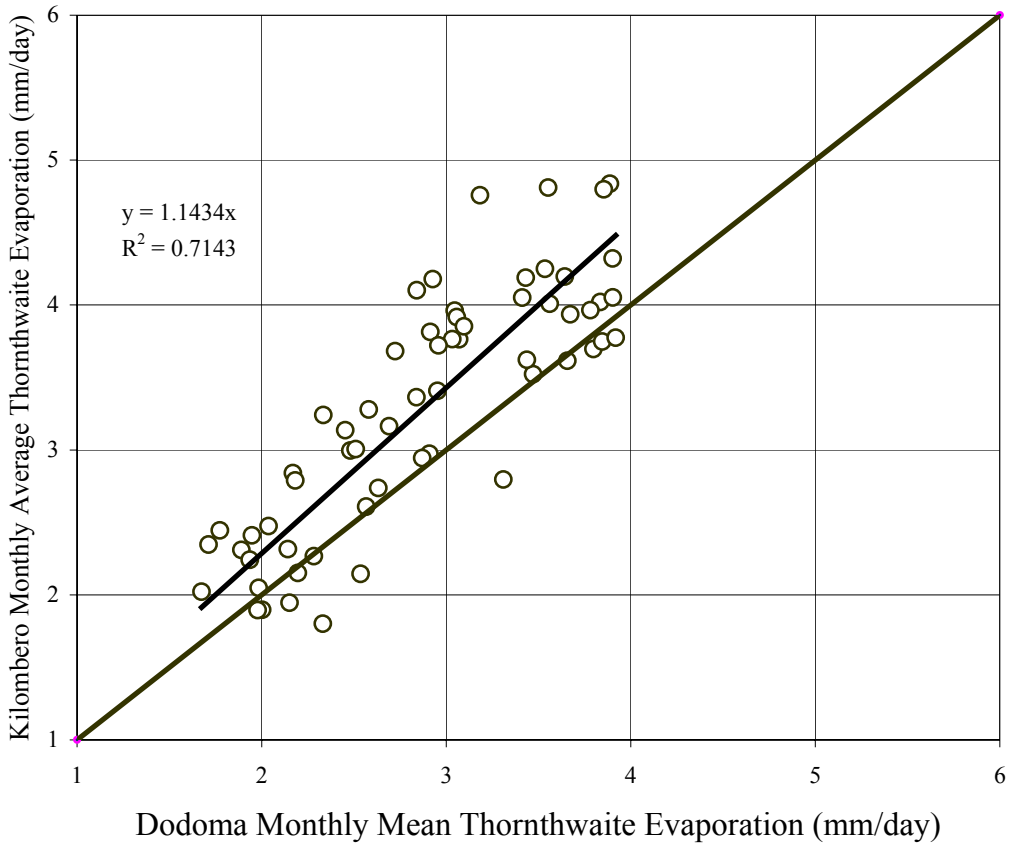

Figure F3.10: Comparison between Estimated Kilombero Monthly Average Basin Thornwaite Potential Eavporation and Monthly Mean Thormwaite Potential Evaporation at Dodoma Climatic Station

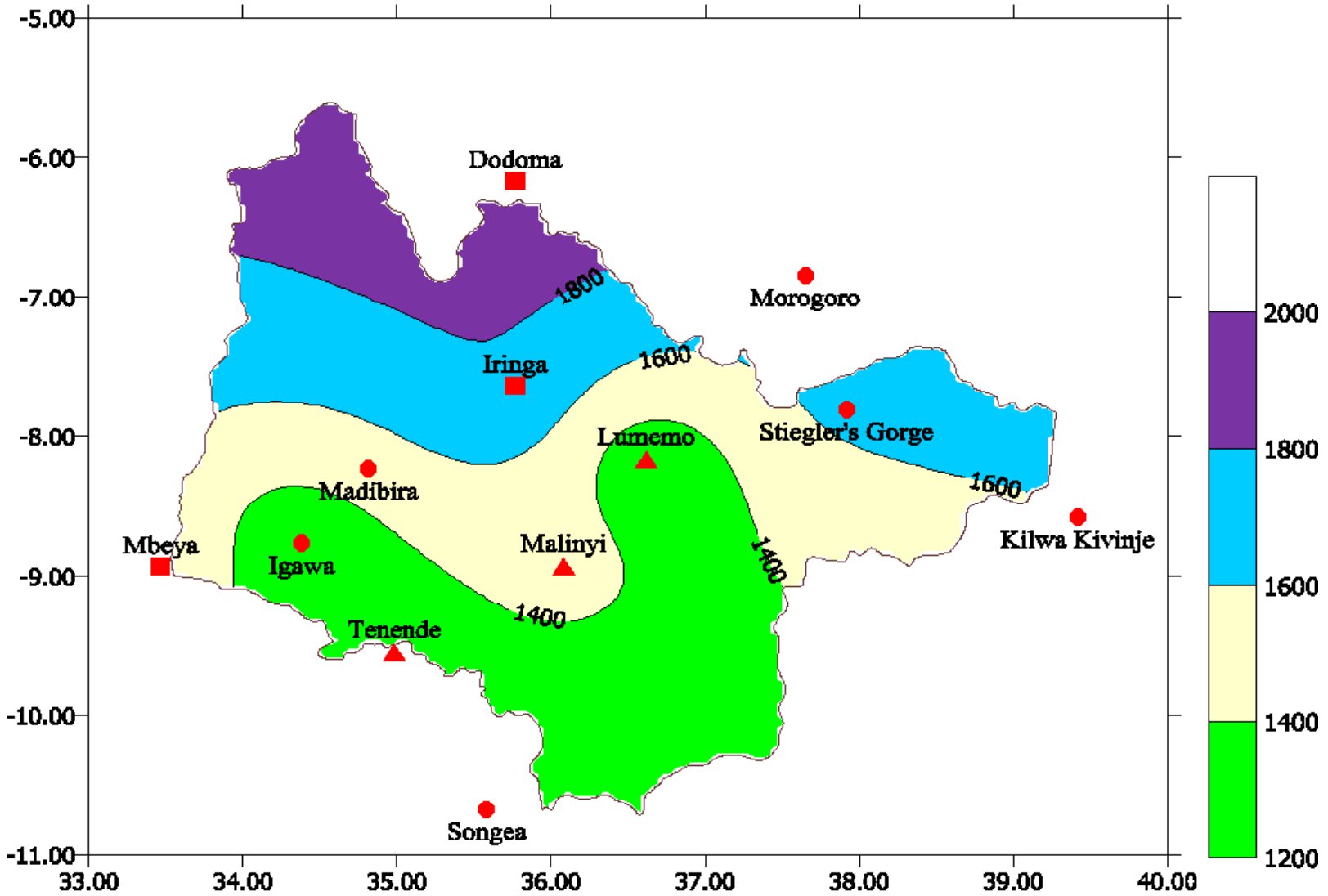

Figure F3.11: Spatial Variation of the Mean Annual Potential Evaporation in the Rufiji River Basin

Chapter 4

4 The Flow Data

4.1 Introduction

River flow data from 50 discharge stations in the Rufiji River Basin were made available for use in this study. The source of these data was the Ministry of Water (MoW), with the exception of data at Mtera (1ka5) and Kidatu (1ka3) from 1983 to 1997. These data were obtained from Tanzania National Electricity Supply Company (TANESCO).

Out the 50 stations only 16 were used in this study. They were chosen due to their strategic position in the river network especially in Kilombero sub-basin and also for their better quality of data. Table T4.1 gives the name and location of each of the 16 stations. Appendix A4.1 presents a summary of the status of data for all the 50 stations of the Rufiji River Basin. A map indicating the location of these stations is given in Figure F4.1. A schematic diagram showing the layout of the key stations is given in Figure F4.2

4.2 Rating Curves of the Stations used in the Study

Rating data, for construction of the rating curves for the 16 stations used in this study, were obtained, checked and analysed.

Table T4.2 presents the mathematical equations that describe the rating curves. It may be observed that, several stations have more than one rating curve; each valid for specific period of time and occasionally for a specific range of flows. This is because the river cross-section at these locations is not stable. The instability is caused by sedimentation or erosion. The later being the predominant cause. Most of the curves are valid for an average maximum gauge height of 10 metres, with the minimum being -4.97 metres. Fairly good rating curves were obtained for most of the stations considered in this study. Only exception is that of 1kb15a. The curve established for this location is very poor.

Graphs of all the rating curves are presented in Appendix A4.2 of this report.

4.2.1 Rating Curves at the Stiegler's Gorge

The river cross-section at Stiegler's Gorge (1k3) is highly unstable due to scouring of the river channel by floods and then subsequent deposition during the recession of floods. The Ministry of Water (MoW), i.e., the agency responsible for collecting the rating data and for recommending the appropriate rating curves, has recommended six rating curves for the station. Each of them covers a few years each. In this work, all the six rating curves were reviewed. All the six, recommended curves, are plotted in Figure F4.3

Five rating curves that seemed to produce a similar range of high flows were grouped together to produce a single curve, except for one, which was uniquely defined for low flows and is visibly different from the other five. This led to development of two rating curves at Stiegler's Gorge. These are shown in Figure F4.4.

The first curve is valid from 05/09/1959 to 18/06/83 except for the period between 17/02/1962 to 15/02/1963, which is covered by the second rating curve. The first rating curve is defined by the following equation:

$$Q = 1.64548 * \left(H + 4.97\right)^{3.0036} \qquad (4.1)$$

The second curve is defined by the following equation:

$$Q = 211.6122 * (H + 1.82)^{1.3982} \quad (4.2)$$

where

Q is the discharge (m^3/s)

H is the gauge height (m)

A comparison was made between the two sets of rating curves at Stiegler's Gorge, i.e., 6 curves and 2 curves. Each set of curves was used to estimate flows for the Gauge height records. Discharges, estimated using the two sets of rating curves, are plotted against each other in Figure F4.5. The comparison seems to indicate that it was a good decision to combine five recommended curves into a single curve. In any case, the standard error of estimate, in both the situations is likely to be very high. Under the circumstances it is, probably, better to choose a robust solution.

There are 9 recorded gauge heights that produced discharge estimates that deviate significantly when the two set of rating curves were used, as can be seen in the figure. These values are high recorded gauge heights. Obviously, they correspond to very high floods and it is always of interest to make an attempt to estimate these floods as accurately as is possible. Therefore, statistical analysis was carried out to ascertain which of the two sets of rating curves is suitable in estimating high flows at Stiegler's Gorge.

The applied statistical procedure involved assuming that the 9 points had a normal distribution, and hence the standard error of each flow estimate from the two sets of curves on a concurrent point was determined, using a confidence interval of 90% (at $\alpha = 0.05$). The standard error of a flow estimate is given by equation 4.3 as:

$$S_e = \left(\frac{2 + Z^2}{n} \right)^{1/2} \quad (4.3)$$

where

$\mathbf{S_e}$ = the standard error of a flow estimate

Z = the standardised variable

n = the number of variables (data points)

The standard error for each flow estimate was then used to determine the respective expected lower and upper flow estimate limits for use as criteria to judge the authentic of each flow estimate. Any flow estimate which was out of its lower and upper limit range indicated that, the respective rating curve had an error greater than the maximum allowable limit in producing such an estimate hence not suitable. Tables T4.3 and T4.4 shows details of the 9 high flow estimates from the two sets of rating curves and results obtained from the statistical analysis. Two flow estimates from the 6 rating curves set failed the statistical test as opposed to only one estimate in the case of the 2 rating curves. This implied that the 2 curves performed better than the 6 curves developed by MoW. Surprisingly, where the set of 2 rating curves failed, that of 6 rating curves was successful. However, the two rating curves had more or less the same ability to produce high flow estimates and could be used to estimate high flows at Stieger's Gorge. The conclusion drawn from this analysis is quite vague owing to the fact that 9 data points are statistically not good enough. Hence, for the case of this study, the set of 6 rating curves developed and recommended by MoW was adopted to generate flows at Stiegler's Gorge (1k3).

4.2.2 Rating Curves at Mloka and Utete

Previous study by VHL in 1978, developed a rating curve at Mloka (1k4) by relating flows at Stiegler's Gorge (1k3) with the concurrent gauge heights at Mloka (1k4). This is based on the assumption that, flow at time **t** at Mloka (1k4) is the same as that of flows at Stiegler's Gorge (1k3) at time **t**. This is a reasonable assumption for high flows in the range of 1,500 Cumecs to 2,000 Cumecs. It was necessary for VHL to make such an assumption because there were no discharge measurements available at Mloka to develop a rating curve at this location.

Recently in the year 2000 and 2001, as part of this project, a few spot discharge measurements were made at Mloka, Utete and Ndundu. These data are presented in Table T4.5. It was unfortunate that, the data used by VHL in their 1978 study could not be traced for verification and subsequent use. In this study, the approach used by VHL was repeated using the historical measured Gauge heights at the Stigler's Gorge. The estimated Steigler's Gorge discharge values were related with the concurrent Gauge heights at Mloka to arrive at the following rating equation for Mloka:

$$Q = 395.6486 * (H - 0.1)^{1.207} \qquad (4.4)$$

Table T4.6 presents the data that were used to develop the above-described equation. The rating curve was developed for Gauge heights, recorded at Mloka, 22nd February 1978 and 25th May 1979.

A second stage-discharge relationship at Mloka was developed by assuming that the flow at the steigler's Gorge at time **t** will be the same at Mloka but at time **t + 1** day. The resulting equation developed for the same set of gauged data observations as before is as follows:

$$Q = 357.3171 * (H - 0.1)^{1.298} \qquad (4.5)$$

Plots of the two rating curves at Mloka (1k4) together with the respective error diagrams are as shown in Appendix A4.3.

A critical analysis on suitability of either of the two curves could not be carried out due to lack of enough measured flow data at Mloka. From the plots, it can be seen that the two curves are more or less the same. The recent spot measurements of discharge at Mloka (1k4) were included in plots of the two curves as seen in Appendix A4.4 for verification. It can be seen that, the two rating curves produced higher flow estimates than the measured flows, though the measured flows at Mloka were within the same scatter range as the measured flows at Stiegler's Gorge except for 1 point.

For this study, the second rating curve was used to generate flows at Mloka (1k4).

A rating curve at Utete was developed by Rufiji River Basin Development Authority (RUBADA) and published in the year book of 1993 on Rufiji project stations. The rating equation is as follows:

$$Q = 277.68 * (H - 0.86)^{1.565} \qquad (4.6)$$

The validity of this curve is supposed to be from 01/01/1978 to 30/06/1991.

Recently measured discharge data at Utete was used to verify this rating curve as shown in Figure F4.6. It was observed that, the rating curve at Utete underestimated the recent measured flows, though within an acceptable range. This curve was used to generate flows at Utete from observed gauge heights.

4.3 Bank-full Discharge

This discharge marks the condition of incipient flooding. Flow higher than the bank-full discharge will flow over the banks and cause flooding. From previous studies by VHL in 1978 and AHT in 1980, the bank-full capacities of six river cross-sections in the floodplains of Lower Rufiji River (downstream of Stiegler's Gorge) were determined by comparing the rating curve of a station with a theoretical curve of the type:

$$Q = K * (Y - Y_0)^{5/3} \qquad (4.7)$$

where

Y is the river stage, and

K and Y_o are constants

The point where these two curves departed was defined as the bank-full discharge for that river cross-section. These cross-sections were taken along a channel reach of the length of about 135 kilometres downstream of Mloka (1k4). The bank-full capacities at these cross-sections as referenced from these two studies (VHL, 1978 and AHT, 1980) are presented in Table T4.7 together with their locations. It was unfortunate that the location of these cross-sections could not be verified when a team of WREP technicians visited the sites in the year 2000. The benchmarks, that were placed in 1978, had been washed away by floods. From the two studies and by referring to Table T4.7, it can be seen that a flow of above 2,500 Cumecs can readily cause flooding in the Lower Rufiji floodplain.

4.4 Quality Assessment of Flow Data

A bar diagram, presented in Figure F4.7, was drawn for the 16 flow gauging stations used in this study. This diagram shows the length of data that is available for each gauging station and the extent of its missing data.

This figure makes it possible to view stations with availability of concurrent data. This information is of vital information in river flow modelling. From the plot, it can be observed that, every station has at least some data that are missing. Stations 1ka5, 1ka37a 1kb15a and 1kb14 have very little missing data. The 16 stations used in the study have data between 1966 and 1980.

The missing data were reconstructed as described in the following sub- sections. Obviously, records with larger amounts of missing data are less reliable than those records that have less missing data but the biggest source of error in the flow estimates comes from inaccuracies in the rating curves. The reliability of rating curves was discussed earlier in section 4.2

4.5 Recent Discharge Measurements

In the years 2000 and 2001, spot measurements of discharge were taken in the Lower Rufiji River at three stations namely; Utete, Mloka and Ndundu. Sediment concentration measurements were also taken at the same time. Those details are discussed in chapter 5 of this report. Results of discharge measurements are presented in Table T4.5. From this table it can be observed that, in all the three stations, the measured flow was in the range of 1,200 Cumecs to 2,000 Cumecs, which is below the bank-full capacity of most sections in the Lower Rufiji River. The bank full discharge is in excess of 2,500 Cumecs. Magnitudes of flows that are above 2,000 Cumecs could not be captured because the measurements were done during dry season when the Lower Rufiji River was accessible. It is very difficult and dangerous to access the river during floods.

4.6 Data Reconstruction

Missing discharge data were reconstructed using one or more of the 4 methods described underneath. The choice of using any one method was reached upon by plotting the hydrograph of each station on yearly basis. Although it might seem like a lot of plotting but it was found

necessary to do so because the choice of models for data reconstruction depends on the characteristics of the missing flows. For instance, it would be better to interpolate a few of flow in a recession rather than try to estimate them by a mathematical model and so on. The 4 methods used in the study are described as follows:

Method 1:

If the missing data event was of a short duration of up to 5 days, then the missing data points were estimated by linear interpolation between the data point observed just before and after the missing spell. This method was applied only where a linear trend of flow was established before and after the missing data points.

Method 2:

The missing data during low flow recessions were filled by date averaged mean flows. This method was applied to missing spells of data of more than 5 days but not exceeding 3 months and restricted to low flow periods.

Method 3:

For flow stations on the high-lying catchments of the Rufiji River Basin, rainfall-runoff modelling was used to estimate the missing data. This was applied to fill missing data points at high flows and where long records of data of more than 3 months and above were missing. Linear Perturbation Model (LPM) in its Linear Transfer Function Form (LTF) was used to relate the catchment average rainfall with the observed discharge at the outlet station. The model, which is a Seasonal Systems type of a model, was calibrated over the period for which observed flow and rainfall records were available. The calibrated model was then used to estimate the missing data.

The structure of LPM is outlined in chapter 7 of this report that deals with the development of a Simulation model of the Basin. The methods of parameter estimation used for the LPM and the measure of accuracy of forecasts, denoted by the model efficiency (R^2), together with the calibrated model coefficients, etc., are all described in this same chapter.

Method 4:

A hydrological or a systems type of a routing model was used to estimate missing data at stations where the main contributor of flow at the station with the missing data was one or more upstream river flow station(s). Multiple-Input Linear Perturbation Model (MILPM) was the chosen model. The details of this model are also presented in Chapter 7 of this report.

This method was applied to fill missing data at high flow and where long records of data of more than 3 months and above was missing.

Table T4.8 shows the efficiency (R^2) of MILPM together with the optimised Least Squares Coefficients for a number of stations in the Rufiji River Basin where the missing flow data were reconstructed.

4.7 Kilombero Sub-Basin

Only 6 of the 11 stations in the Kilombero Basin, that are marked on Figure F4.2, were used in this study. These stations are 1kb8, 1kb10, 1kb4, 1kb14, 1kb15a and 1kb17. Both 1kb8 and 1kb10 flow into 1kb4, and then 1kb4 together with 1kb14 and 1kb15a drain into 1kb17. The data on these stations may be considered of good quality.

A schematic diagram showing the layout of these six flow gauging stations and their flow connectivity as used in the semi-distributed hydrological modelling is as shown in Figure F4.8, whilst Figure F4.9 shows the map of the Basin with locations of the six gauging stations as derived by the HEC-HMS software from 1 km X 1 km DEM.

Table T4.1: Name and location of the 16 flow gauging stations in the Rufiji River Basin which were used in the study

No.	Station code	Station name	Location			Period	No. of data points	% of missing data	Daily mean flow (m^3/s)
			Region	Lat.	Long.				
1	1kb8	Mpanga at Mpanga	Iringa	-8.93	35.82	1956-1990	13,057	23.20	39.91
2	1kb10	Ruhudji at Mkasu	Morogoro	-8.57	36.59	1960-1987	10,318	23.20	221.87
3	1kb4	Kilombero at Ifwema	Morogoro	-8.92	35.93	1955-1982	10,347	38.90	205.23
4	1kb15a	Mngeta at Mngeta Mission	Morogoro	-8.33	36.08	1960-1989	11,139	3.50	22.22
5	1kb14	Lumemo at Kibaoni	Morogoro	-8.05	36.41	1958-1988	11,566	0.60	5.60
6	1kb17	Kilombero at Swero	Morogoro	-8.20	37.00	1957-1984	10,227	25.80	519.44
7	1ka31	Little Ruaha at Mawande	Iringa	-7.30	35.30	1956-1993	13,880	8.70	50.97
8	1ka59	Great Ruaha at Msembe	Iringa	-7.75	34.90	1963-1998	13,149	22.12	72.93
9	1ka42	Kisigo at Kinunguru	Dodoma	-6.08	35.03	1957-1995	14,244	57.30	50.65
10	1ka5	Great Ruaha at Mtera	Iringa/Dodoma	-7.08	35.98	1954-1979	9,770	7.50	117.79
11	1ka37a	Lukosi at Mtandika	Iringa	-7.57	36.43	1957-1994	13,879	4.40	25.60
12	1ka61	Great Ruaha at Gorge	Iringa	-7.58	36.78	1965-1988	8,125	14.30	139.95
13	1ka38	Yovi at Great Ruaha Confluence	Iringa	-7.57	36.78	1958-1986	10,773	17.70	3.72
14	1ka3	Great Ruaha at Kidatu	Iringa	-7.18	37.02	1954-1985	11,869	36.40	160.28
15	1k3	Rufiji at Stiegler's Gorge	Pwani	-7.80	37.92	1954-1989	12,935	17.11	808.28
16	1k4	Rufiji at Mloka	Pwani	-7.78	38.17	1978-1991	5,113	57.66	1,361.84

Table T4.2: Details of the rating curves for the 16 flow gauging stations used in this study

No.	Station	Rating curve(s)	Validity of the rating curve	Comments
1	1kb8	$Q=18.0447(H+0.35)^{1.423}$ $-0.35<H<10.0$	06/04/61 - 01/11/78	-Good rating
2	1kb10	$Q=24.6067(H-1.00)^{1.778}$ $1.0<H<10.0$	02/02/60 - 08/05/76	-Fairly good
3	1kb4	$Q=108.692(H-2.1)^{1.091}$ $-2.1<H<10.0$	16/02/60 - 24/08/76	-Good rating
4	1kb15a	$Q=26.378(H-0.21)^{1.009}$ $-10.0<H<30.0$	09/02/60 - 11/10/83	-Not very good rating
5	1kb14	$Q=9.091(H+0.50)^{2.623}$ $-0.50<H<10.0$	17/01/66 - 19/09/90	-Good rating
6	1kb17	$Q=171.0442(H-0.24)^{1.5246}$ $2.4<H<10.0$	20/11/59 - 05/09/76	-Fairly good
7	1ka31	$Q=3.3489(H-0.0)^{2.493}$ $0.0<H<6.0$	20/08/64 - 23/10/95	-Fairly good
8	1ka59	$Q=20.50186(H-0.39)^{3.2995}$ $0.39<H<10.0$ $Q=87.73802(H-0.71)^{2.0606}$ $0.71<H<10.0$	13/12/63 - 08/05/79 09/05/79 - 20/05/85	-Reliable for all flows -Reliable for high flows
9	1ka42	$Q=12.3031(H-0.0)^{2.504}$ $0.0<H<10.0$	24/03/61 - 02/03/82	-Not reliable for high flows
10	1ka5	$Q=29.607(H-0.63)^{2.057}$ $0.63<H<4.0$ $Q=31.871(H-0.00)^{1.705}$ $4.0<H<10.0$	03/02/60 - 13/05/80	-Fairly good
11	1ka37a	$Q=45.472(H-0.22)^{1.498}$ $0.22<H<10.0$ $Q=9.2125(H+0.36)^{2.695}$ $-0.36<H<10$	18/11/64 - 29/08/71 21/04/71 - 27/03/87	-Not reliable for high flows -Good rating for all flows
12	1ka61	$Q=233.293(H-1.21)^{1.574}$ $1.21<H<10.0$	20/04/67 - 08/03/73	-Good rating
13	1ka38	$Q=20.5872(H-0.1)^{1.9545}$ $1.0<H<10.0$ $Q=12.5067(H+2.0)^{2.3606}$ $-2.0<H<10.0$	14/08/59 - 07/01/68 08/01/68 - 17/11/84	-Reliable for high flows -Reliable for low flows
14	1ka3	$Q=15.8887(H+0.6)^{2.535}$ $-0.6<H<10$	04/09/59 - 14/10/69	-Fairly good
15	1k3	$Q=1.6548(H+4.97)^{3.0036}$ $-4.97<H<10.0$ $Q=211.6122(H+1.82)^{1.3982}$ $-1.82<H<10.0$	05/09/59 - 18/06/83 except 17/02/62 - 15/02/63	-Good rating -Good rating
16	1k4	$Q=357.3171(H-0.1)^{1.298}$ $-0.1<H<10.0$	23/02/78 - 26/05/79	-Poor rating

Table T4.3: Statistical Analysis of the Suitability of using the set of 6 Rating Curves for estimating flows at Stiegler's Gorge

Date	Value* (Cumecs)	Standard Error (Cumecs)	90% Confidence Interval		Does value lie within the limits?
			Lower Limit (Cumecs)	Upper Limit (Cumecs)	
24-04-1956	6,308.2	445.9650	6,245.144	7,712.368	Yes
01-05-1974	6,705.9	396.4800	6,326.546	7,630.966	Yes
03-05-1974	7,388.5	409.3637	6,305.353	7,652.159	Yes
04-05-1974	6,331.4	442.1396	6,251.436	7,706.076	Yes
16-04-1979	6,536.1	413.1534	6,299.119	7,658.393	Yes
17-04-1979	7,566.2	432.7442	6,266.892	7,690.620	Yes
18-04-1979	8,661.8	680.9270	5,858.631	8,098.881	No
24-04-1979	7,233.0	395.1030	6,328.812	7,628.700	Yes
20-03-1987	6,077.7	489.0148	6,174.327	7,783.185	No

* Mean of **6,978.756** Cumecs and standard deviation of **818.6322** Cumecs.

Table T4.4: Statistical Analysis of the Suitability of using the set of 2 Rating Curves for estimating flows at Stiegler's Gorge

Date	Value** (Cumecs)	Standard Error (Cumecs)	90% Confidence Interval		Does value lie within the limits?
			Lower Limit (Cumecs)	Upper Limit (Cumecs)	
24-04-1956	5,370.8	445.9650	4,519.903	6,692.809	Yes
01-05-1974	5,974.3	396.4800	4,765.911	6,446.801	Yes
03-05-1974	6,559.5	409.3637	4,931.195	6,281.517	No
04-05-1974	5,659.1	442.1396	4,643.752	6,568.960	Yes
16-04-1979	5,036.5	413.1534	4,366.507	6,846.205	Yes
17-04-1979	5,569.6	432.7442	4,606.337	6,606.375	Yes
18-04-1979	6,099.4	680.9270	4,809.180	6,403.532	Yes
24-04-1979	5,399.0	395.1030	4,532.414	6,680.298	Yes
20-03-1987	4,789.0	489.0148	4,248.154	6,964.558	Yes

** Mean of **5,606.356** Cumecs and standard deviation of **545.7084** Cumecs.

Table T4.5: Results of Recent Spot Measurement in Lower Rufiji River

Station	Date	Stage	Discharge	Cross section Area (m^2)	Velocity (m^3/s)	Width (m)
Utete	4/5/2000	-	1,443.47	1,183.35	1.22	450.0
	5/5/2000	-	1,357.01	1,151.93	1.18	535.0
	26/1/2001	4.42	1,699.08	-	-	-
	27/1/2001	4.58	1,732.17	-	-	-
	28/1/2001	4.56	1,787.44	-	-	-
	25/4/2001	4.39	1,623.37	-	-	-
	26/4/2001	4.49	1,615.90	-	-	-
Mloka	8/5/2000	-	1,596.56	1,039.10	1.54	309.0
	31/1/2001	3.17	2,072.60	-	-	-
	1/2/2001	2.95	1,950.70	-	-	-
Ndundu	11/5/2000	-	1,219.20	979.63	1.25	255.0
	12/5/2000	-	1,402.28	965.70	1.45	255.0
	4/2/2001	2.94	1,404.02	-	-	-
	5/2/2001	2.85	1,364.90	-	-	-

Table T4.6: Details of the Measured Flow Data at Stiegler's Gorge (1k3) together with the Concurrent Gauge Heights used to develop the Rating Curves at Mloka (1k4)

No.	Zero-day lag for flows at Stiegler's Gorge					One-Day lag for flows at Stiegler's Gorge				
	Day	Month	Year	Mloka Water levels (m)	Discharge (Cumecs)	Day	Month	Year	Mloka Water levels (m)	Discharge (Cumecs)
1	22	2	78	1.91	720.427	23	2	78	1.93	720.427
2	23	2	78	1.93	788.849	24	2	78	2.02	788.849
3	24	2	78	2.02	932.837	25	2	78	2.02	932.837
4	25	2	78	2.02	727.182	26	2	78	2.36	727.182
5	27	2	78	2.6	1594.645	28	2	78	2.57	1594.645
6	28	2	78	2.57	1168.291	1	3	78	2.46	1168.291
7	1	3	78	2.46	1137.13	2	3	78	2.39	1137.13
8	2	3	78	2.39	897.784	3	3	78	2.19	897.784
9	4	3	78	2.01	852.376	5	3	78	1.98	852.376
10	6	3	78	2.15	1134.292	7	3	78	2.25	1134.292
11	8	3	78	2.2	869.059	9	3	78	2.11	869.059
12	9	3	78	2.11	898.813	10	3	78	2.12	898.813
13	10	3	78	2.12	1243.001	11	3	78	2.63	1243.001
14	11	3	78	2.63	1302.012	12	3	78	2.87	1302.012
15	13	3	78	2.72	1371.03	14	3	78	2.77	1371.03
16	14	3	78	2.77	1878.457	15	3	78	2.95	1878.457
17	15	3	78	2.95	1553.793	16	3	78	2.92	1553.793
18	17	3	78	2.95	1653.142	18	3	78	3.13	1653.142
19	5	4	78	4.01	2581.969	6	4	78	3.86	2581.969
20	6	4	78	3.86	2277.411	7	4	78	3.7	2277.411
21	10	4	78	3.59	2248.107	11	4	78	3.56	2248.107
22	11	4	78	3.56	2465.344	12	4	78	3.49	2465.344
23	12	4	78	3.49	2313.407	13	4	78	3.4	2313.407
24	13	4	78	3.4	1757.702	14	4	78	3.33	1757.702
25	17	4	78	3.8	2086.395	18	4	78	3.7	2086.395
26	18	4	78	3.7	2197.876	19	4	78	3.9	2197.876
27	20	4	78	3.62	2177.573	21	4	78	3.48	2177.573
28	25	4	78	3.41	2024.888	26	4	78	3.32	2024.888
29	5	4	79	4.44	2060.336	6	4	79	4.38	2060.336
30	6	4	79	4.38	2095.795	7	4	79	4.41	2095.795
31	25	4	79	5.38	4335	26	4	79	5.06	4335
32	10	5	79	4.27	2209.439	11	5	79	4.17	2209.439
33	11	5	79	4.17	1936.99	12	5	79	4.08	1936.99
34	12	5	79	4.08	1869.805	13	5	79	4.02	1869.805
35	14	5	79	3.94	1102.042	14	5	79	3.94	1102.042
36	21	5	79	3.42	735.772	22	5	79	3.34	735.772
37	23	5	79	3.28	686.169	24	5	79	3.23	686.169
38	25	5	79	3.18	847.71	26	5	79	3.12	847.71

No.	Section Number	Site Name	Longitude	Latitude	Bank-full discharge (By VHL) (m^3/s)	Bank-full discharge (By AHT) (m^3/s)
1	4	Mloka	38.172	-7.778	2,500	2,500
2	6	Mtanza	38.357	-7.839	2,600	2,500
3	7	Kipo	38.501	-7.867	2,600	2,500
4	11	Utete	38.758	-7.969	2,900	2,500
5	14	Ndundu	39.011	-8.021	2,200	2,500
6	17	Msomeni	39.260	-8.036	2,500	2,500

Table T4.7: Location and Bank-full Capacity of Cross-sections in the Lower Rufiji Floodplain

Table T4.8: Coefficients and efficiency of Linear Perturbation Model (LPM) in Linear Transfer Function Form (LTF) when estimating flows for filling missing flow data at various stations in Rufiji River Basin

No.	Name of Catchment		Order of Moving Average	Pure Lag	Order of Autoregressive Procedure	Coefficients for LPM (LTF)	Model Efficiency R^2 (%)
	Output	Input(s)					
1	1kb8	-Areal rainfall	2	0	1	0.867086 0.0726932, 0.349300	63.61
2	1kb10	-Areal rainfall	2	0	1	0.921371 0.455692, 0.830200	68.57
3	1kb15a	-Areal rainfall	2	0	1	0.841391 0.0868478, 0.172030	57.39
4	1kb14	-Areal rainfall	2	0	1	0.87728 0.0464519, 0.0907861	24.94
5	1kb4	-1kb10 -1kb8	2 2	0 0	1	0.965731 0.0715711, -0.044823 0.103817, -0.0247441	73.03
6	1kb17	-1kb4 -1kb15 -1kb14	2 2 2	0 0 0	1	0.983965 0.102110, -0.0743150 0.165712, 0.355225 0.232438, 0.194783	72.26
7	1ka3	-1ka61 -1ka38	2 2	0 0	1	0.682795 0.471415, -0.207265 1.89408, -0.215176	80.59
8	1k3	-1kb17 -1ka3 -Intervening catchment areal rainfall	2 2 2	0 0 0	1	0.924056 0.562898, -0.403568 0.611862, -0.585037 1.98381, 3.55187	82.54
9	1ka61	-1ka5	2	0	1	0.602175 0.603355, -0.242455	

No.	Name of Catchment		Order of Moving Average	Pure Lag	Order of Autoregressive Procedure	Coefficients for LPM (LTF)	Model Efficiency R^2 (%)
	Output	Input(s)					
		-1ka37a	2	0		0.451026, 0.0113134	92.91
10	1ka5	-1ka31 -1ka42 -1ka59	2 2 2	0 0 0	1	0.705652 0.0706766, -0.0376614 0.162179, 0.237228 0.0653559, 0.129142	81.96
11	1ka37a	-Areal rainfall	2	0	1	0.923359 0.0527584, 0.349770	26.50
12	1ka38	-Areal rainfall	2	0	1	0.807509 0.0735023, 0.0943657	34.36
13	1ka42	-1ka41	2	0	1	0.888487 0.712161, -0.602433	37.55
14	1ka31	-1ka2a	2	0	1	0.952794 0.390702, -0.167378	40.04
15	1k4	-1k3	2	0	1	0.733301 0.218864, 0.134704	73.25
16	1ka59	Was reconstructed and filled in a previous study (SMUWC Project) by the consultant (WREP)					

Table T4.8 Continued: Coefficients and efficiency of Linear Perturbation Model (LPM) in Linear Transfer Function Form (LTF) when estimating flows for filling missing flow data at various stations in Rufiji River Basin

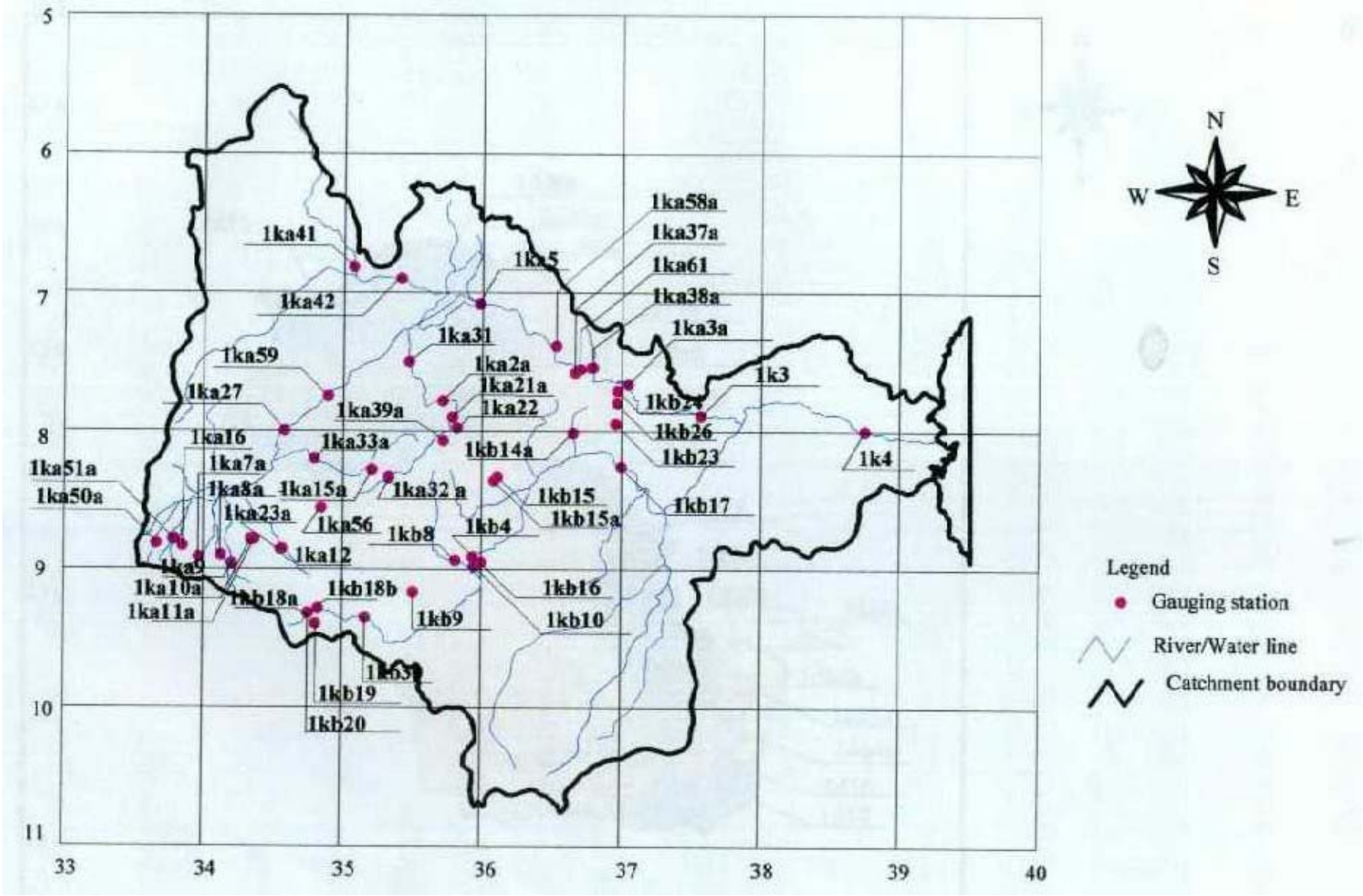

Figure F4.1: Map showing the location of the flow gauging stations in the Rufiji River Basin

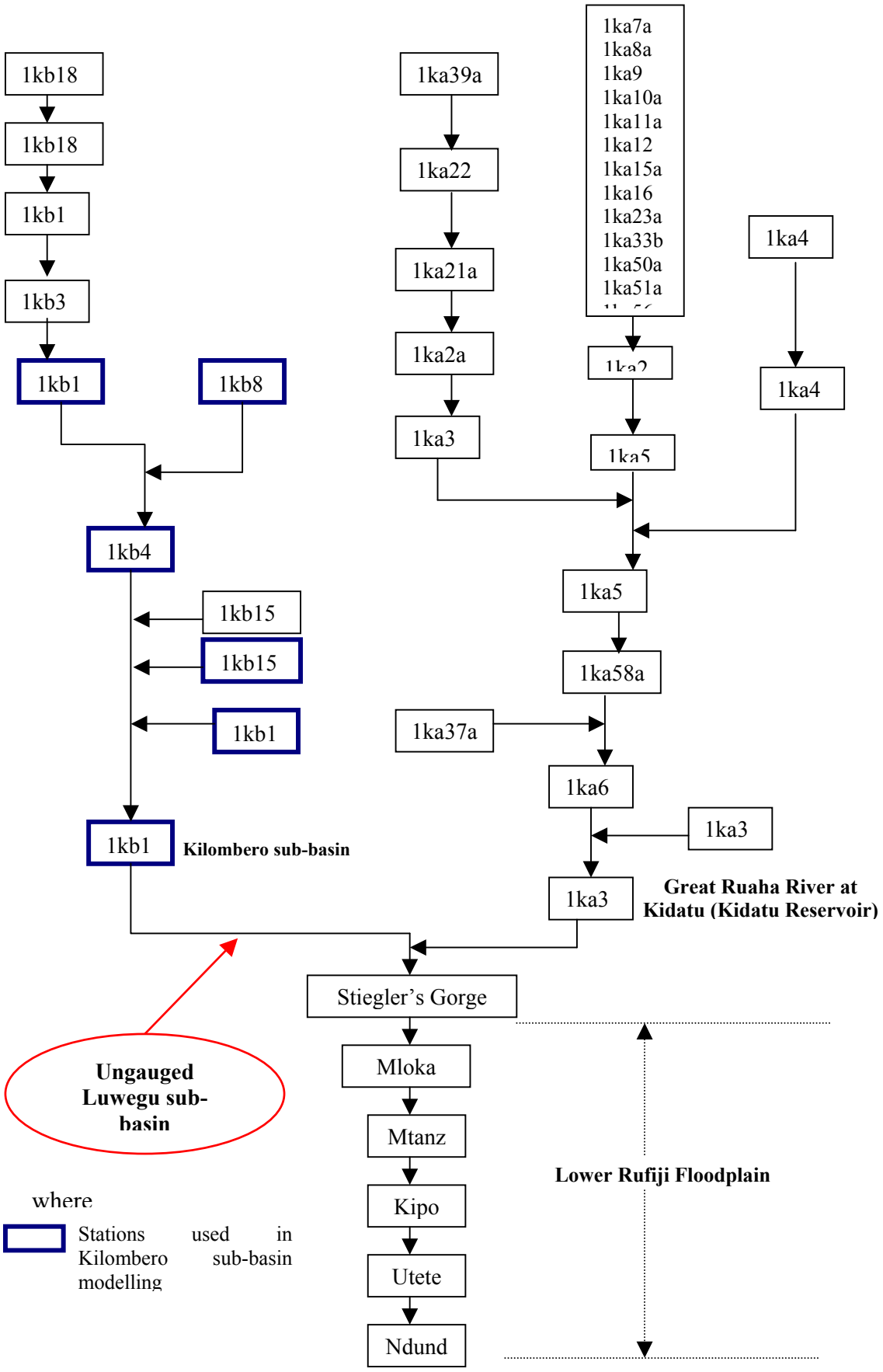

Figure F4.2: Schematic Diagram showing the Layout of Key Stations in the Rufiji River Basin

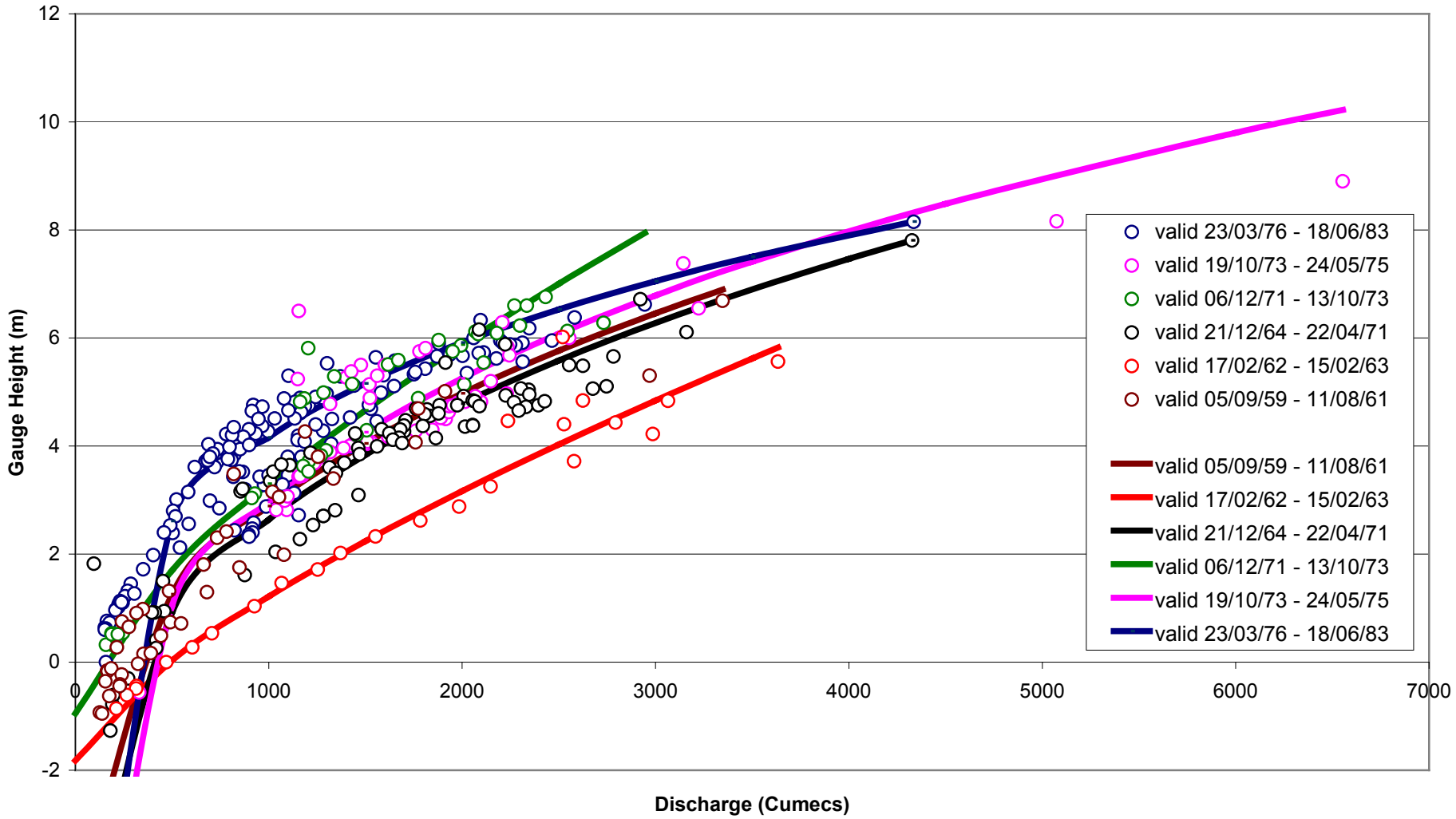

Figure F4.3: Six Rating Curves at Stiegler's Gorge (1k3) at Different Time Periods

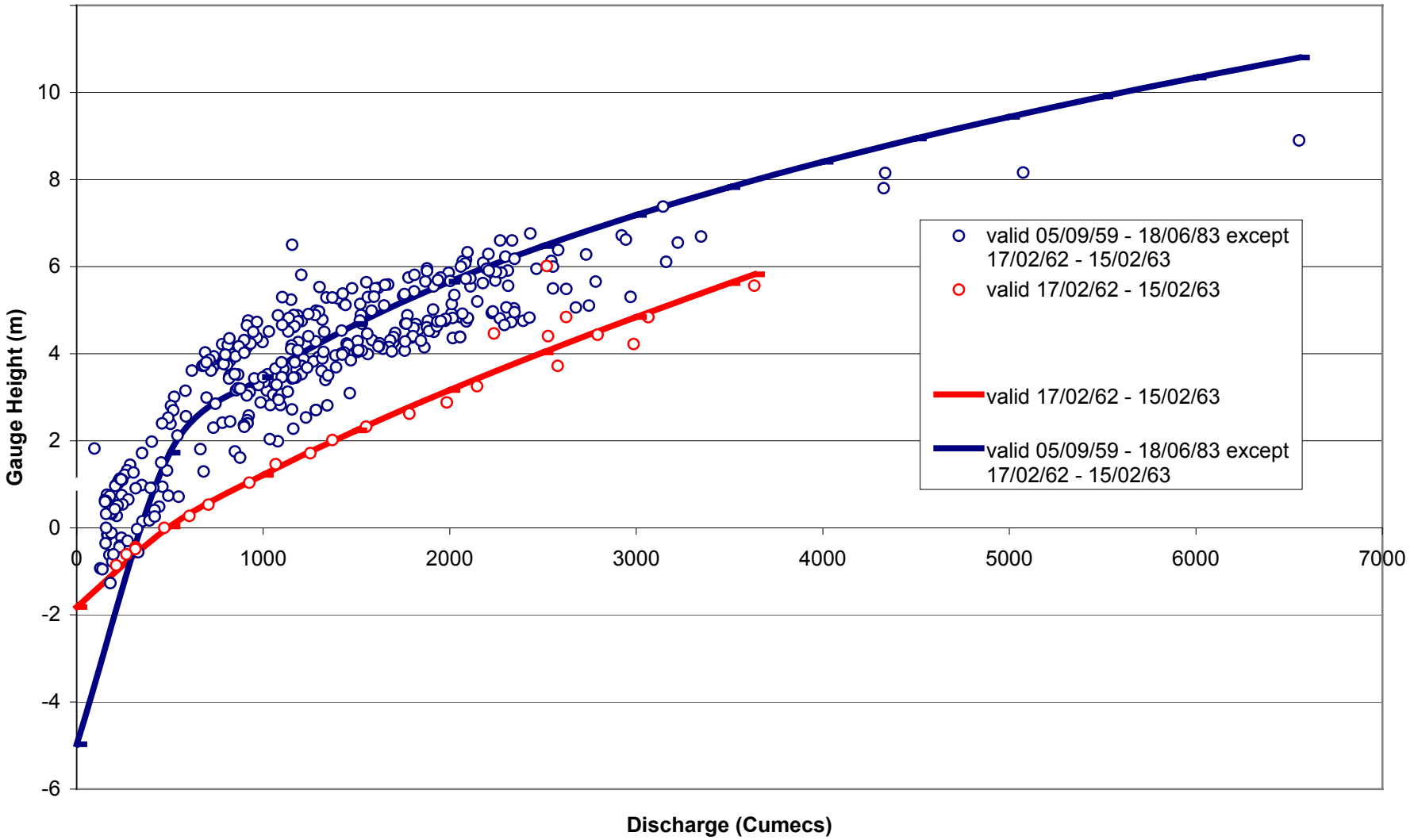

Figure F4.4: Two Rating Curves at Stiegler's Gorge (1k3)

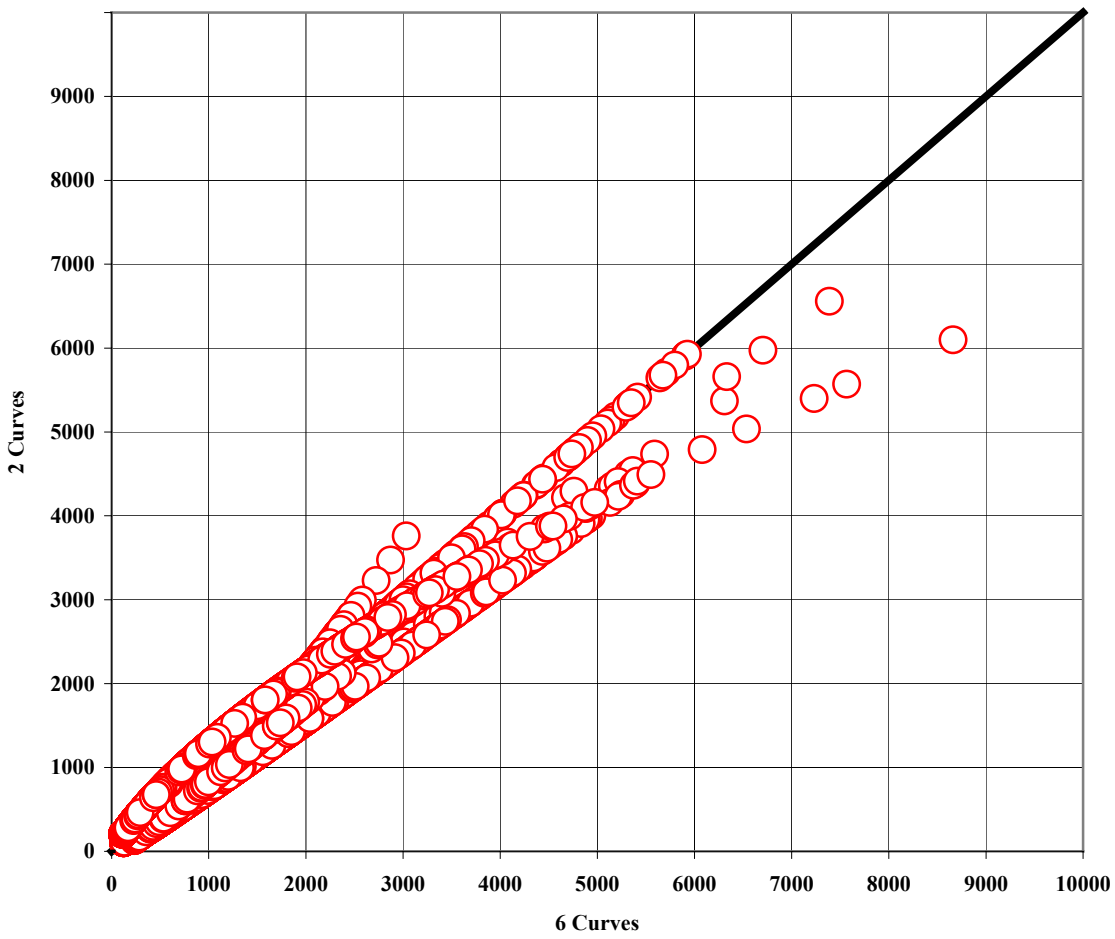

Figure F4.5: Comparison of the Two Sets of Rating Curves at Stiegler's Gorge (1k3)

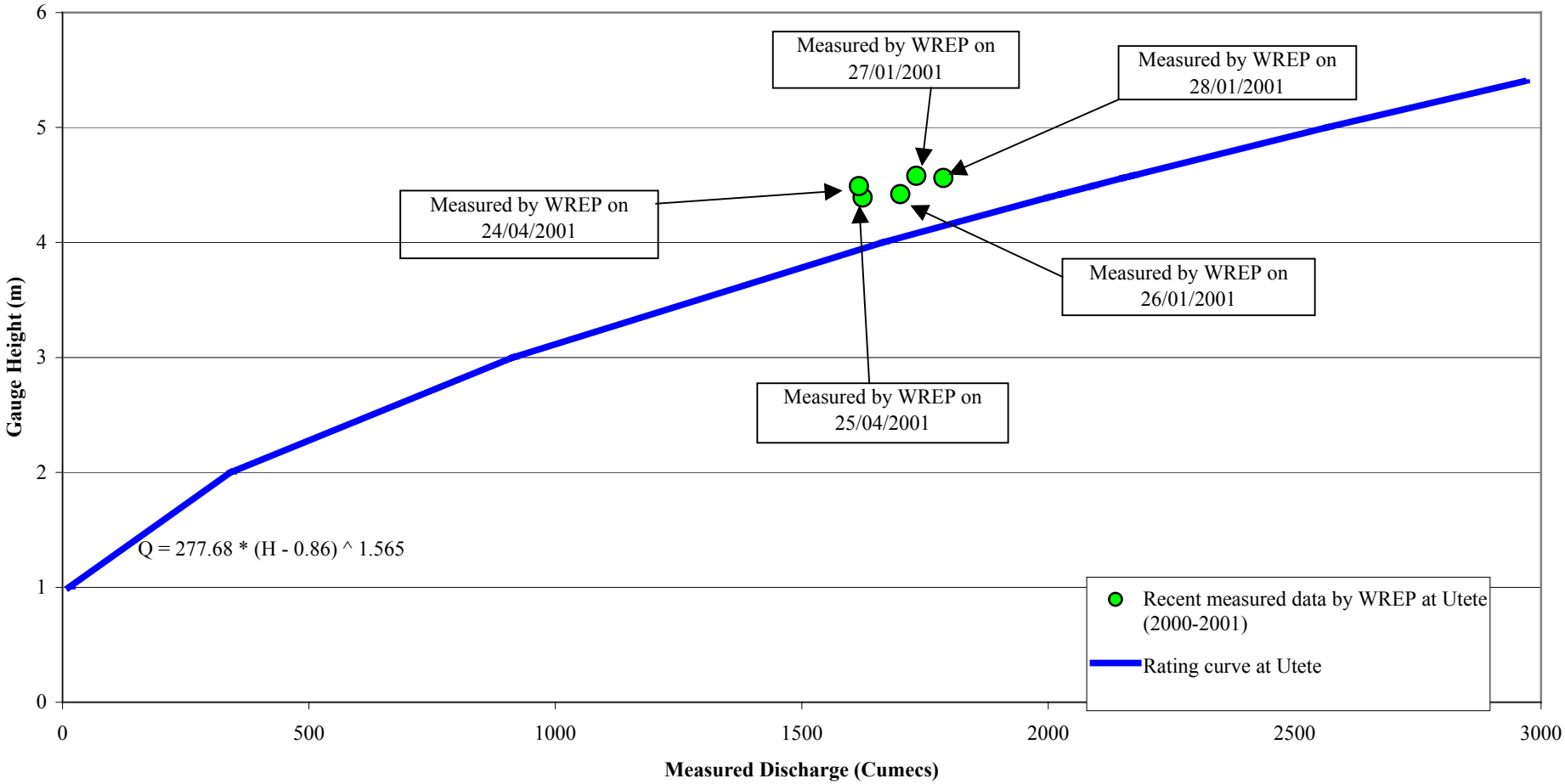

Figure F4.6: Rating curve at Utete with the Recent Spot Measurement

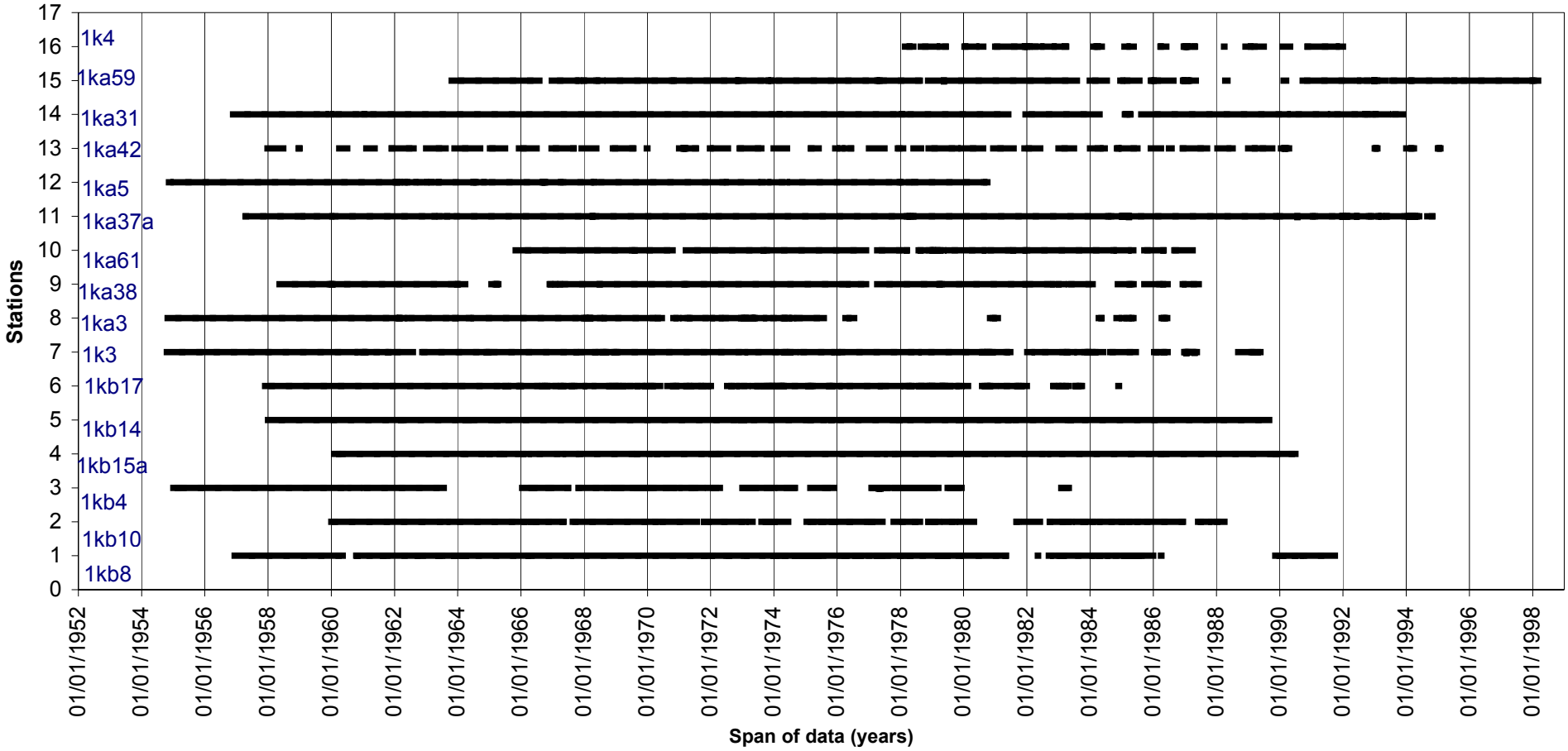

Figure F4.7: A bar diagram showing the span and availabilty of flow data in the 16 stations used in the study

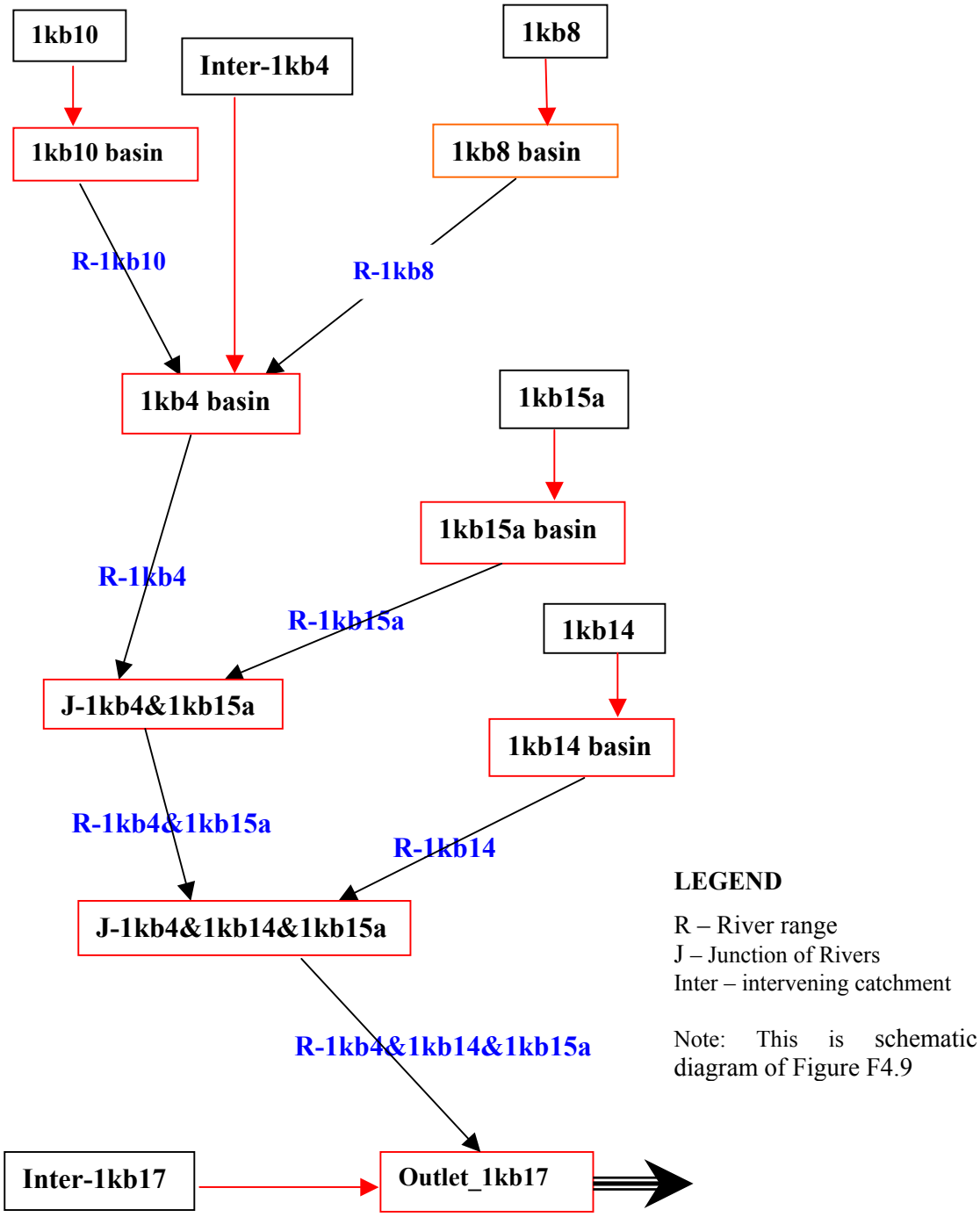

Figure F4.8: Schematic Layout of the HEC-HMS Modelling Setup of Kilombero Sub-Basin

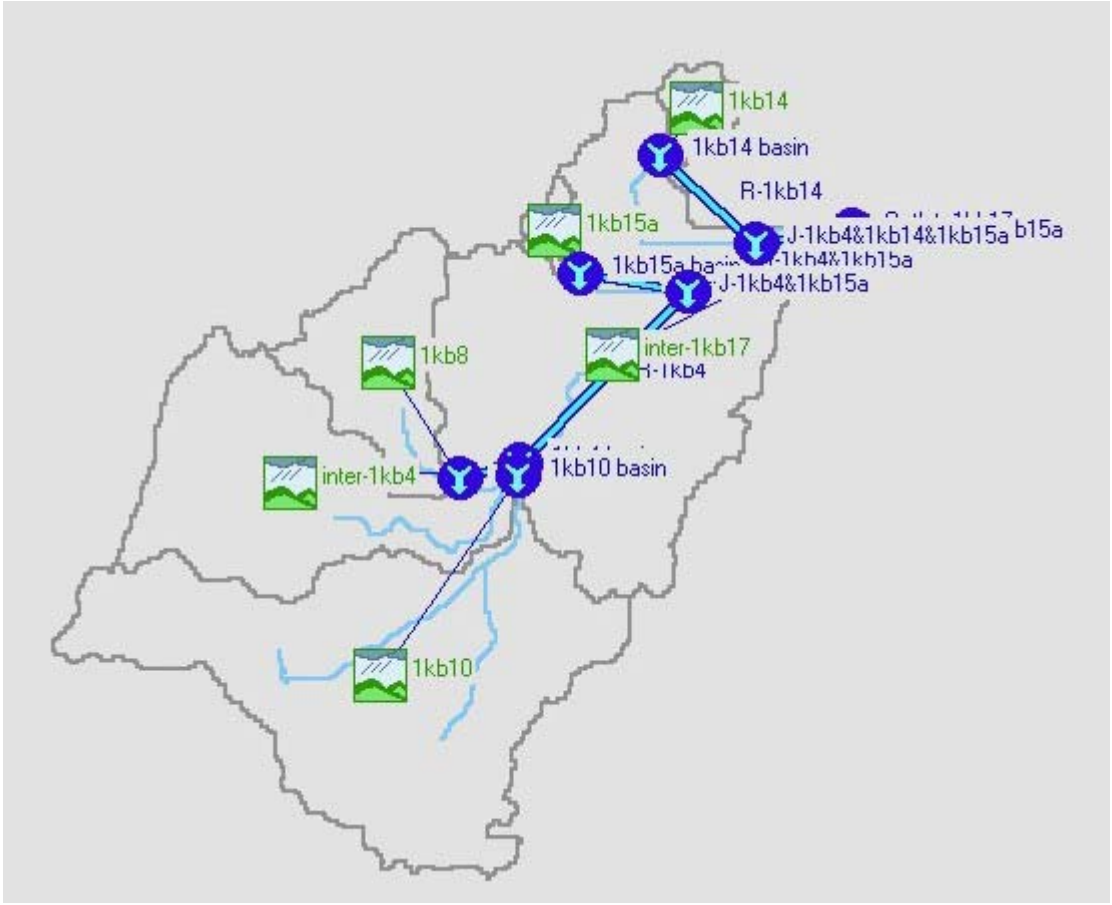

Figure F4.9: The HEC-HMS Basin Model Setup for the Kilombero Sub Basin (1kb17)

Chapter 5

5 The Sediment Data

5.1 Suspended load data at Stiegler's Gorge

Available data on sediment transport in the Lower Rufiji River Basin is very limited. The report produced by VHL (1978) on the Hydraulic Studies in the basin have indicated that some sediment measurements were taken at Steigler's Gorge in the past (from 1954 to 1970). Table T5.1 shows suspended sediment data records at Stiegler's Gorge for the period between 1954/55 and 1969/70 as compiled by Temple and Sundborg (1972). These are the same data as indicated in the VHL, 1978 report. Based on these data, the mean annual sediment transport at Stiegler's Gorge was estimated to be 16.6 million tons.

5.2 Sediment rating curve at the Stiegler's Gorge

The data on suspended sediment load obtained from various sources were plotted on a graph for comparison purposes. The plots are presented in Figure F5.1. The data plotted comprised data compiled by Temple and Sundborg in 1972, measurements done by VHL in 1978, samples collected by the Ministry of Water and samples collected by WREP in the years 2000 and 2001.

From this figure, it can be observed that the measurements made by the VHL in 1978 and the recent measurements made by WREP in 2000 and 2001 fall within the range of the rating curves compiled by Temple and Sundborg (1972). This indicates that, the two data sets are comparable and therefore the estimated mean annual suspended sediment load estimated by Temple and Sundborg in 1972 at Stiegler's Gorge might be realistic. The data obtained from the Ministry of Water appeared in two separate clusters; one consisting of data set ranging from 1973 to 1974 and the other consisting of data points from 1975 to 1980. Both cluster plots appeared far below the estimated level of sediment rating curves compiled for the flood and recession periods by VHL. The reason for the difference between the data obtained from the Ministry of Water and the rest of the data is not known. It is clear from Figure F5.1 that the sediment rating curve for the Steigler's Gorge is of a very poor quality. Naturally, one cannot rely greatly on the prediction based on the use of this curve.

5.3 Estimation of bed load at the Stiegler's Gorge

Estimation of sediment bed load at Stiegler's Gorge was based on an empirical formula, which related suspended load to the bed load. The formula could not be traced as it was not documented in the VHL, 1978 report, but it was referred to an American Society of Civil Engineers (ASCE) manual, number 54 of 1975 on Sedimentation Engineering. This manual was written by Laursen and it is presumed that Laursen's formula must have been used.

This formula is based on comparison between the shear velocity and the settling velocity of sediment grains from which a proportional relationship between the bed load and the suspended load for various sediment grain sizes can be estimated.

Other approaches were also used in estimating bed load at Stiegler's Gorge based on determining the total sediment load in the river, from which the bed load could be estimated. These used methods were by Engelund-Hansen and Colby.

Unfortunately, two of these three methods were not documented in the VHL, 1978 report but were just mentioned. The two assumptions in the Engelund-Hansen method are that the fall diameter of the sediment grains must be bigger than 0.15 mm and the sieve curve has to be steep. From the VHL, 1978 report, the Engelund-Hansen method was recommended for river Rufiji due to the fact that, the conditions on which the method is based are applicable on river Rufiji.

The Eugelund-Hansen's formula has the following form:

$$q_s = 0.05 * \gamma_s * V^2 \sqrt{\frac{d_{50}}{g\left(\gamma_s / \gamma_f\right)}} * \left(\frac{\tau_o}{(\gamma_s - \gamma_f) d_{50}} \right)^{3/2} \qquad (5.1)$$

where

q_s = transport rate by weight per unit width,
γ_s = weight density of solids,
γ_f = weight density of fluid,
g = acceleration of gravity,
V = velocity,
d_{50} = mean grain size (fall diameter),
τ_o = bed shear stress (= γ_w.R.S),
γ_w = weight density of water,
R = hydraulic radius ≅ depth, and
S = slope.

A plot of the total sediment load from the three methods versus discharge is as shown in Figure F5.2. It can be seen that the total load transport rate is not linearly related with the discharge. The total annual load depends on both the total annual flow together with its distribution over the seasons.

5.4 Recent sediment data measurements

In the years 2000 and 2001, a team of WREP technicians took some spot measurement of suspended sediment load on the Lower Rufiji River. The measurements were taken at Utete, Mloka and Ndundu.

These measurements were taken by use of depth-integrating sampler, which is designed to accumulate a sample in a bottle as the sampler is lowered to the streambed before being raised to the surface. For a given cross-section, three samples were collected at equally spaced verticals along the river cross-section and at the same time, the river discharge was recorded. The samples were then analysed at the laboratory to determine their sediment concentration. The average value for the three samples in each cross-section was taken as the average suspended sediment concentration for a given flow rate. The average suspended sediment transport load per day at each cross section was estimated as being 66,200 tons/day at Utete, 112,000 tons/day at Mloka and 85,000 tons/day at Ndundu. These estimates are for flow below 2,500 Cumecs. The detail is given in Table T5.2.

Table T5.1: Estimated load of monthly-suspended sediment transported at Stiegler's Gorge (in thousand tons)

Month / Years	Nov.	Dec.	Jan.	Feb.	Mar.	Apr.	May	June	July	Aug.	Sept.	Oct.	Total l
1954/55	54	56	272	1,995	2,447	3,881	974	483	255	167	119	96	13,899
1955/56	75	441	2,971	4,556	3,672	7,021	2,288	341	144	84	48	32	21,673
1956/57	20	181	635	1,344	1,352	3,206	2,740	315	123	75	45	28	10,064
1957/58	16	177	501	938	2,347	3,884	1,739	218	85	46	27	15	9,993
1958/59	8	444	603	1,075	2,198	1,937	632	119	71	45	27	17	7,236
1959/60	6	215	557	956	2,989	6,961	1,729	223	110	63	40	28	13,877
1960/61	20	13	172	694	1,114	1,641	2,057	183	58	38	23	25	6,038
1961/62	387	2,983	11,47	7,355	8,420	5,278	1,279	274	146	98	65	43	37,800
1962/63	34	138	2,649	3,883	6,030	10,212	3,241	257	150	71	45	34	26,744
1963/64	467	1,126	4,225	3,627	7,250	7,429	1,064	227	120	88	56	38	25,717
1964/65	27	46	966	677	1,969	4,396	1,163	119	55	42	29	26	9,515
1965/66	22	625	848	1,364	2,015	4,213	1,639	129	65	39	28	23	11,010
1966/67	87	343	596	590	901	2,633	2,602	281	89	52	34	25	8,233
1967/68	132	3,900	7,210	3,678	9,044	10,461	4,044	470	221	132	76	49	39,417
1968/69	35	31	261	1,343	1,630	2,317	3,077	313	84	50	33	27	9,201
1969/70	20	25	1,735	3,721	4497	3,703	422	113	58	42	32	24	14,392
Mean	88	672	2,233	2,362	3617	4,950	2,112	254	115	71	45	33	16,552

Table T5.2: Estimates of suspended sediment load downstream of Stiegler's Gorge

Station	Date of sampling	Conc. of sample 1 (mg/l)	Conc. of sample 2 (mg/l)	Conc. of sample 3 (mg/l)	Average conc. (mg/l)	Discharge (m^3/s)	Average suspended sediment transported (tons/day)
Utete	04/5/2000	242	202	252	232	1440	29,000
	05/5/2000	253	194	205	217	1360	25,000
	26/1/2001	564	632	706	634	1699	93,000
	27/1/2001	702	714	590	668	1732	100,000
	28/1/2001	674	496	454	541	1787	84,000
Mloka	08/5/2000	508	695	642	615	1600	85,000
	31/1/2001	714	820	944	826	2073	148,000
	01/1/2001	604	704	522	610	1951	103,000
Ndundu	11/5/2000	334	428	443	402	1210	42,000
	12/5/2000	365	543	695	534	1400	65,000
	04/2/2001	532	1350	514	796	1404	97,000
	05/2/2001	472	412	402	429	1365	51,000

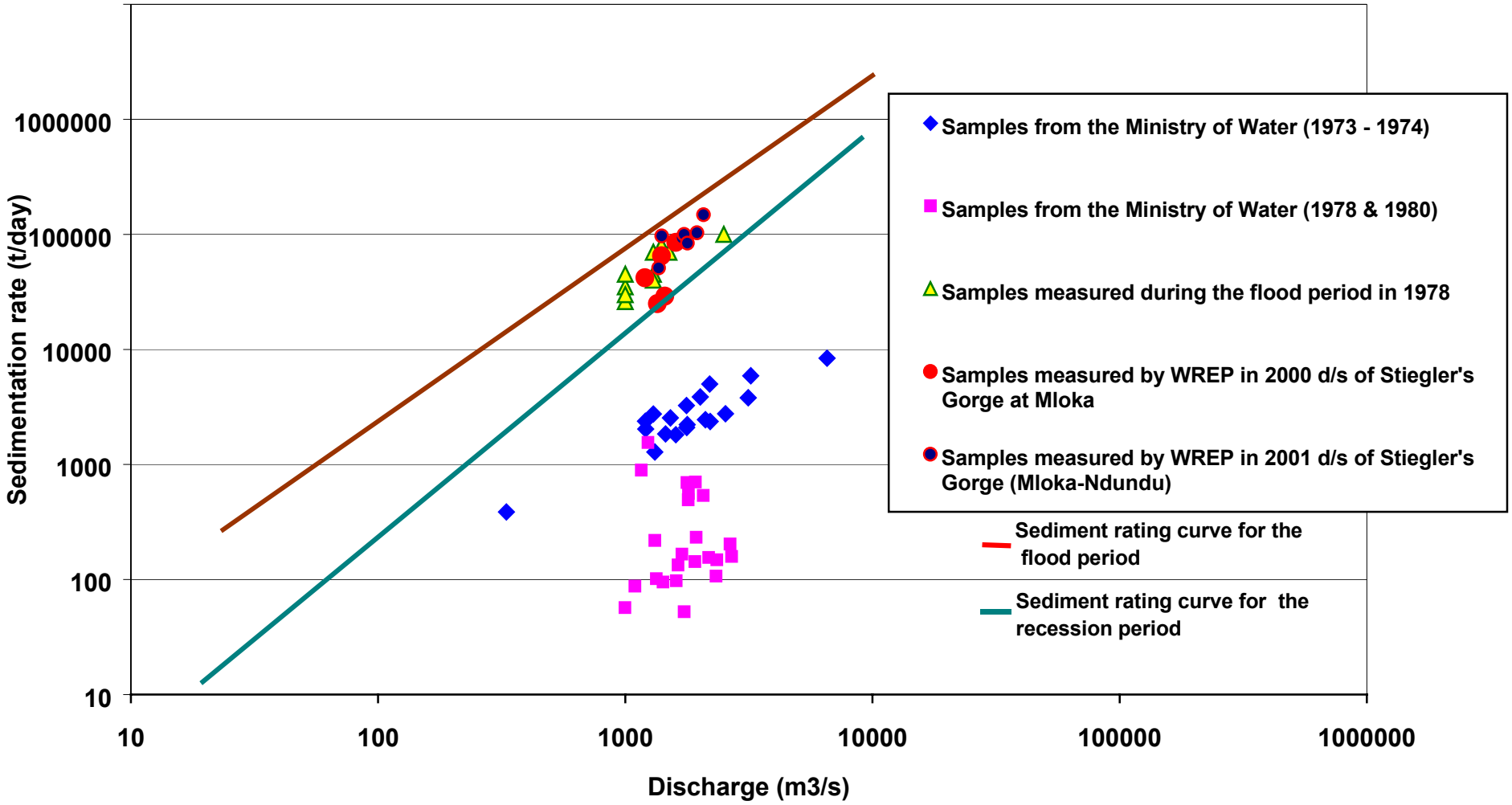

Figure F5.1: Discharge-sediment transport relationship at Stiegler's Gorge

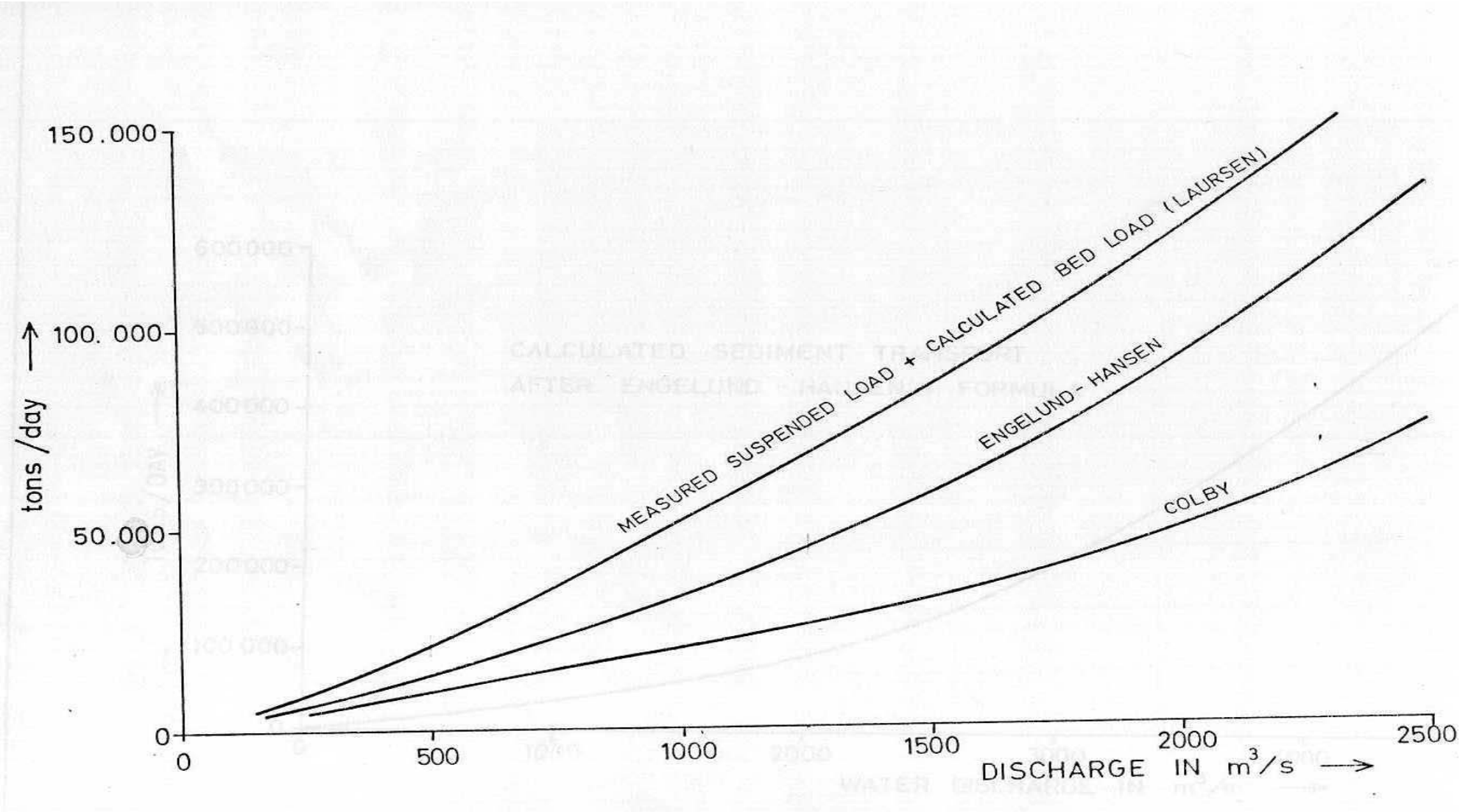

Figure F5.2: Rating curve for total Sediment transport load per day in River Rufiji

Chapter 6

6 Spatial Data

6.1 River Cross-Sections

River cross-section surveys were done, as a part of this study, at four different sites, namely; Mloka, Kipo, Utete and Ndundu in the Lower Rufiji River. The locations of these sites are shown in Figure F6.1. The cross-sections were measured for the full stretch of the floodplain as can be seen in Figures F6.2(a) through to F6.2(d). It can be observed from the plots that the topography of the floodplain from the terrace to the river channel at the measured sites is not smooth. It is irregular. The objective of measuring the cross-sections was to determine the cross-sectional area at different elevations above the river bed datum. This information is required in the development of hydraulic flood routing models.

In 1978, VHL of Norway surveyed about 36 river cross-sections in the Lower Rufiji River. Some of these cross-sections were located close to river gauging stations. Although it was the intention, in this study, to compare the recent cross-sections with those taken in 1978, but the comparison could not be made because the exact locations of the cross-sections measured in 1978 could not be identified. The benchmarks that must have been erected in 1978 could not be located at his time.

6.2 Delineation of 1 km X 1 km Grid DEM

From 1 km X 1 km grid-DEM (Digital Elevation Model) of Africa, DEM for Rufiji River Basin was delineated. The sub-basins that were delineated, in this work, are the Stiegler's Gorge sub-basin, the Kilombero sub-basin, the Luwegu sub-basin (which is an ungauged basin) and the catchment upstream of the Kidatu Reservoir. These DEMs are, respectively, shown from Figures F6.3 through to Figure F6.7. In addition to the delineation of these major sub-basins within the basin, various sub-catchments within the Kilombero sub-basin were delineated for detailed hydrological studies of this sub-basin. Figure F6.8 depicts how the areas of these delineated sub-catchments within the Kilombero sub-basin compared with their digitised boundary areas. The latter are digitised versions of the catchment maps that were drawn, as a part of an earlier study by the consultant, from 1:50,000 scale topographical maps with 10 m contours. The comparison between the DEM delineated catchments and those drawn from the topographical maps is surprisingly very close.

For ease of reference, the comparison of the areas for all the delineated catchments and sub-basins undertaken in this study is presented in tabular form in Table T6.1.

The delineation done by using ArcView GIS software was done as follows:

1. The area covering the Rufiji River Basin was windowed from the DEM of Africa that was obtained freely from USGS web-site <http://edcwww.cr.usgs.gov>. This DEM, at this stage, is in its raw form.
2. From the raw DEM (also referred to as the unfilled-DEM), the sinks within the DEM were filled to generate what is known as the filled-DEM.
3. With the filled DEM, the flow direction grid and then the flow accumulation grids were created.
4. From the flow accumulation grid, the stream definition grid as well as the stream segmentation grid were derived.
5. The flow direction grid and the stream segmentation grid were then used to delineate watershed grid. From the watershed grid, watershed polygon or shape file was created.
6. Again, from the flow direction grid and the stream segmentation grid, stream segment processing was carried out to create river network (river shape file).
7. Watershed aggregation was then performed from the two shape files (i.e. the watershed polygon and the river shape file). Watershed in this sense is defined by one outlet only, or an outlet and one or more source points which represent inflows from other drainage basins.

8. With HEC-GeoHMS package, pertinent spatial data were extracted from the delineated watershed and subsequently used to set up a hydrologic model (either lumped or distributed).

The lumped hydrologic model for the Kilombero sub-basin was developed using this package and the results are discussed in chapter 7 of this report.

6.3 Digitised Maps of the Floodplain

Two-metre interval contours maps of a scale of 1:10,000 covering the Lower Rufiji floodplain area were acquired from Rufiji River Basin Development Authority (RUBADA) and then digitised at the Institute of Resource Assessment (IRA) of the University of Dar es Salaam (UDSM). The aerial photographs of these maps were taken in July of 1976 by GEOSURVEY International, while ground control and photogrammetric mapping was done by NORPLAN in 1976/77. Table T6.2 shows the detailed information on these maps in terms of the projection, location and datum, among others.

Figure F6.9 shows the arrangement of the set of maps that constitutes the floodplain area of the Lower Rufiji River and these maps are presented in Appendix A6. In total, 106 maps covered the floodplain but 14 of them were not available. One of the 14 missing maps (the map labelled F164 in Appendix A6) was very critical because it covered an area through which the main river channel passes. The absence of the remaining 13 maps was not all that damaging as they covered very little of the flood-prone areas. They are also far from the main course of the river. The acquired digitised maps are all stored in a compact disc.

The information contained in the missing map F164 was reconstructed, manually by simple interpolation, after looking at 1:50,000 topographical map of the area for special features. This interpolation was done in the ArcView GIS environment.

The digitised maps including the reconstructed missing maps were put together into a Single Shape file. Using a 3-D Analyst of the Arc View GIS, the Triangular Irregular Network (TIN) of this shape file was created. It is presented in Figure F6.10. This TIN was subsequently used in the development of raster-based floodplain maps at different flow magnitudes with the help of HEC-RAS software. Details of these raster-based floodplain maps are discussed in chapter 9 of this report, which deals with the floodplain modelling.

6.4 Land Use and Land Cover Map of the Floodplain

Land use and land cover map of the floodplain was obtained from the Institute of Resources Assessment (IRA) in a digital format. These maps are currently being revised at IRA. In this report, previous version has been used.

This map has the features that are listed in Table T6.3. Manning's roughness coefficient was estimated for each feature within the entire Rufiji floodplain. Actually, based on the type of feature such as the land use and/or land cover, the soil types or the surface covers were classified. From this classification of the various soil types and land covers, the Manning's roughness coefficients were assigned.

These Manning's roughness coefficient estimates are needed for the floodplain modelling of the Lower Rufiji River Basin that is described in details in chapter 9 of this report. These coefficients are shown in Table T6.3 for the various land use and land cover of the entire floodplain.

Table T6.1: Comparison of Delineated Catchment Area with the Digitised Catchment Area

Catchment	Digitised Area (km^2)	Delineated Area (km^2)	Percentage Error
1kb8	2,585	2,733	5.73
1kb10	14,361	11,074	-22.89
1kb4	20,015	19,845	-0.85
1kb14	598	597	-0.17
1kb15	328	329	0.30
1kb17	33,066*	32,182	-2.67
Luwegu	-	25,983	-
Kidatu Dam (1ka3)	80,040*	81,463	1.79
Stiegler's Gorge (1k3)	177,000*	162,156	-8.39
Rufiji River Basin	-	179,260	-

*Area not digitised. Source: Analysis of Flow Regimes of Tanzania Report.

Table T6.2: Details of the Floodplain 2m Interval Contours Maps acquired from RUBADA

ITEM	DESCRIPTION
Grid	UTM Zone 37
Projection	Transverse Mercator
Spheroid	Clarke 1880 (Modified)
Latitude of Meridian	39^0 E of Greenwich
Longitude of Origin	Equator
Scale Factor of Origin	0.9996
False Coordinate of Origin	500,000 m E 10,000,000 m N
Datum	New Arc 1960
Contour Interval	2 m
Unit of Measurement	metres
Scale	1 : 10,000

Table T6.3: List of Land Use and Land Cover of the Rufiji Floodplain

Description of Land Cover	Code	Manning's Coefficient
Forest		
Natural Forest	Fn	0.060
Plantation Forest	Fp	0.100
Mangrove Forest	Fm	0.120
Woodland		
Open Woodland	Wo	0.500
Closed Woodland	Wc	0.100
Woodland with Scattered Cultivation/Cropping	WSc	0.400
Bushland		
Dense Bushland	Bd	0.085
Open Bushland	Bo	0.055
Bushland with Scattered Cultivation/Cropland	BSc	0.050
Bushland with Emergent Trees	BeT	0.050
Thicket	Th	0.100
Grassland		
Wooded Grassland	Gw	0.600
Bushed Grassland	Gb	0.035
Open Grassland	Go	0.030
Grassland with Scattered Cultivation/Cropland	GSc	0.035
Wooded Grassland Seasonally Inundated	Gws	0.055
Bushed Grassland Seasonally Inundated	Gbs	0.040
Open Grassland Seasonally Inundated	Gos	0.035
Cultivation		
Mixed Cultivation/Cropping	Mc	0.040
Cultivation with Tree Crops	Ctc	0.035
Water Features		
Inland Water	IW	0.048
Swamp/Marsh (Permanent)	S/M	0.030
Others		
Bare Soil	BSL	0.030
Settlement	S	0.014
Sand Dunes	Sd	0.016
Airstrip	Airstrip	0.014

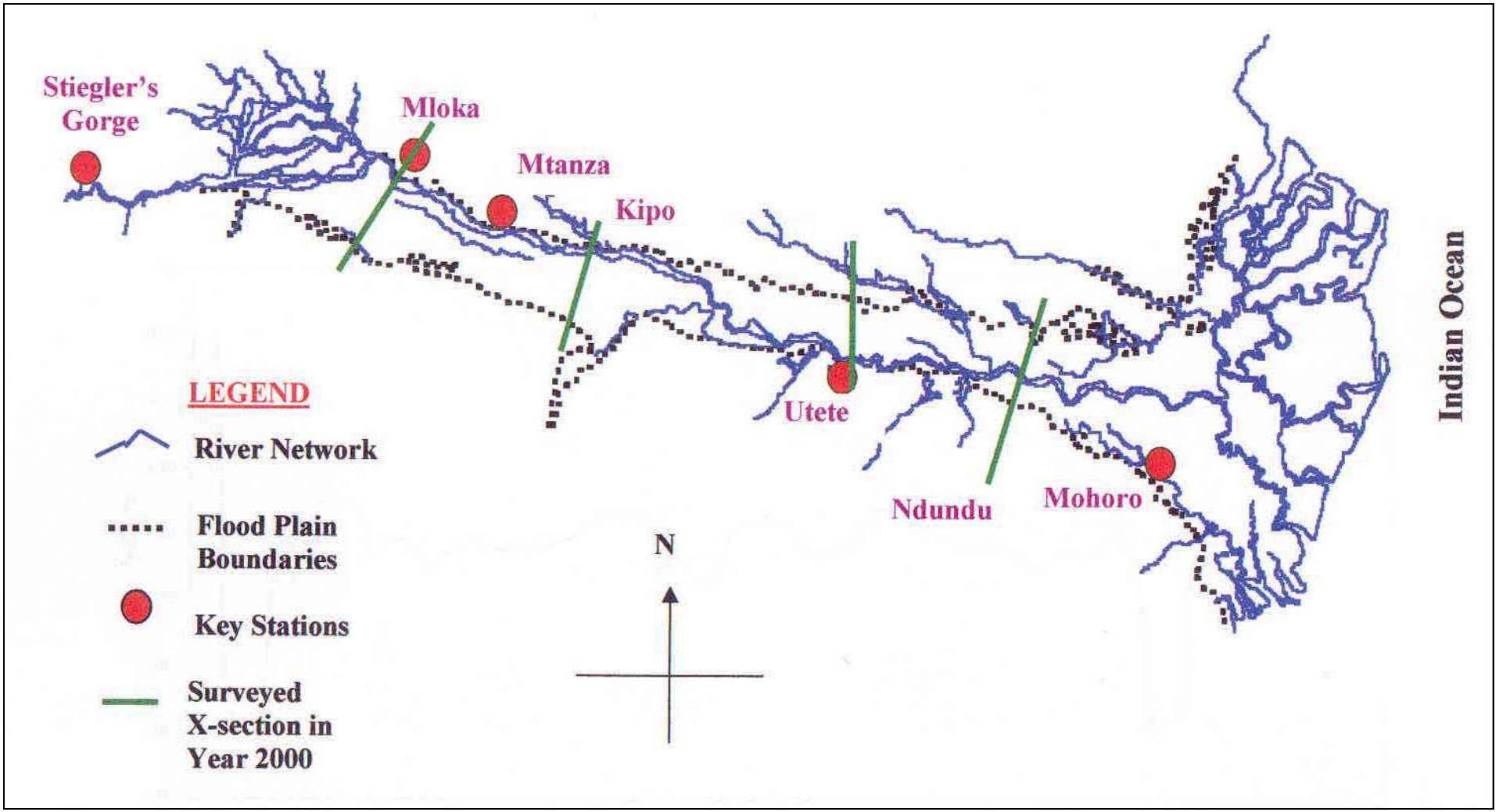

Figure F6.1: Rufiji Floodplain showing the Year 2000 Surveyed Cross-Sections and Key Stations (NOT TO THE SCALE)

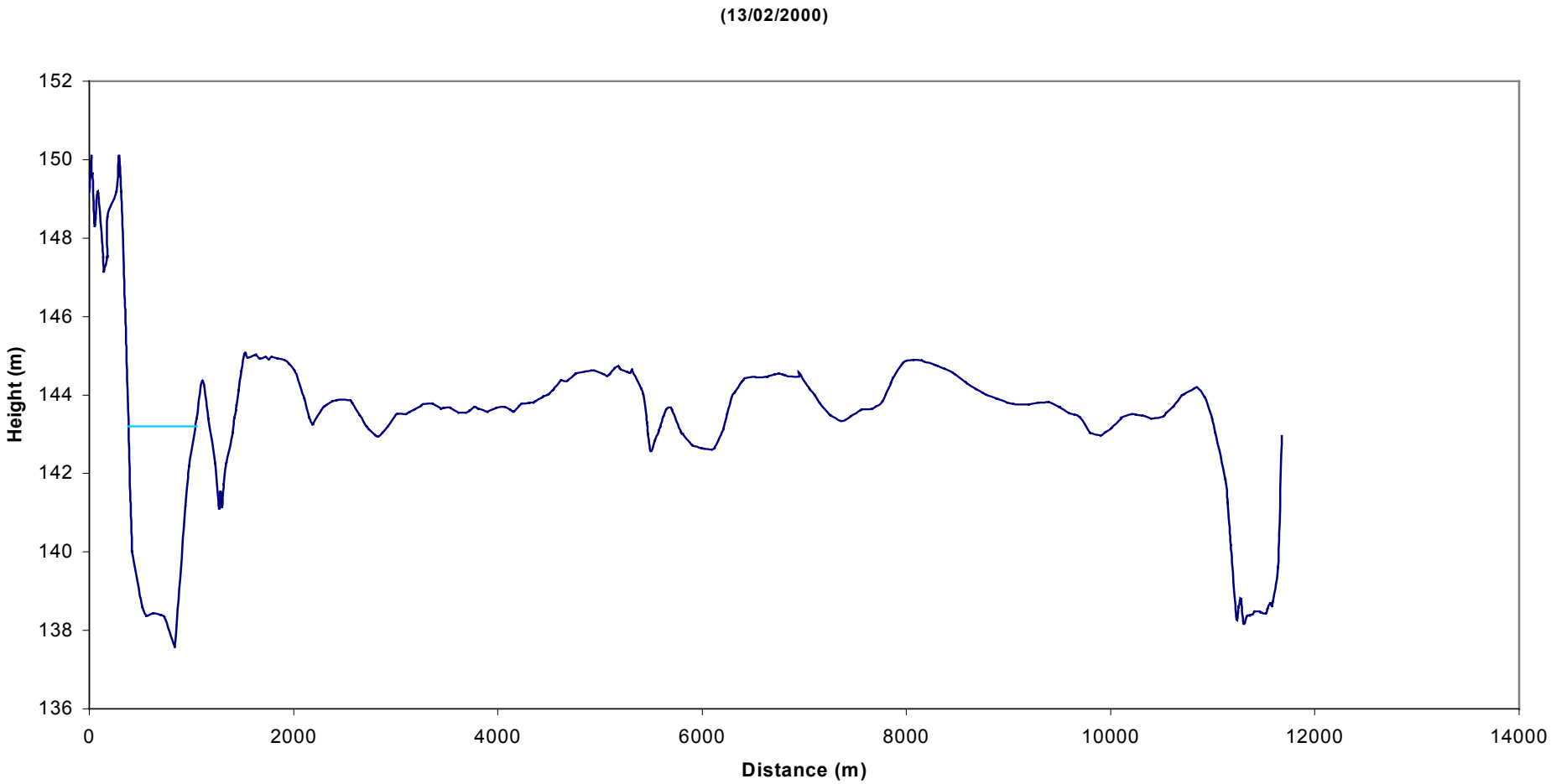

Figure F6.2 (a): Plot of cross-section across the floodplain at Mloka – Surveyed on the 13th Feb. 2000

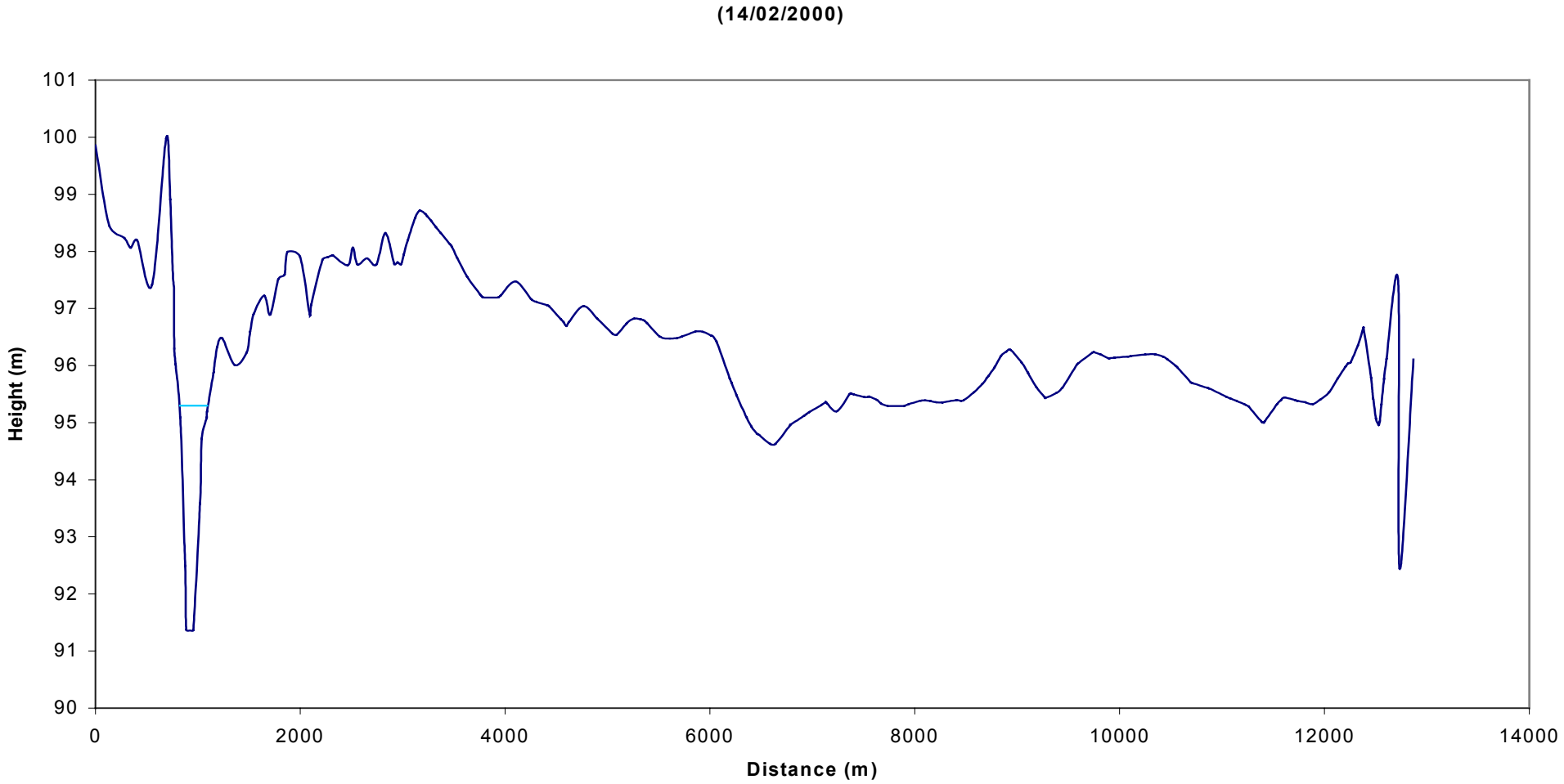

Figure F6.2 (b): Plot of cross-section across the floodplain at Kipo – Surveyed on the 14th Feb. 2000

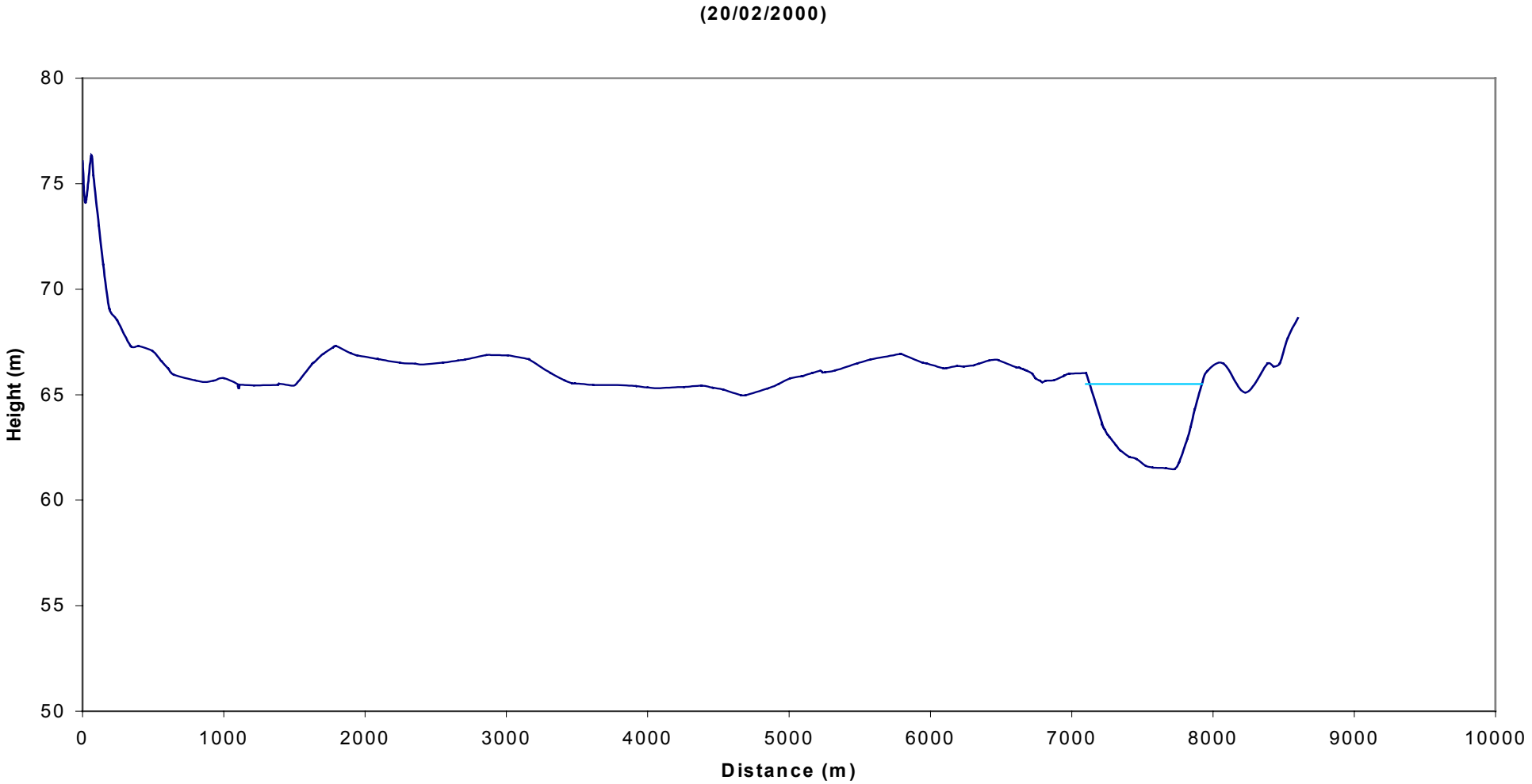

Figure F6.2 (c): Plot of cross- section across the floodplain at Utete – Surveyed on the 20th Feb. 2000

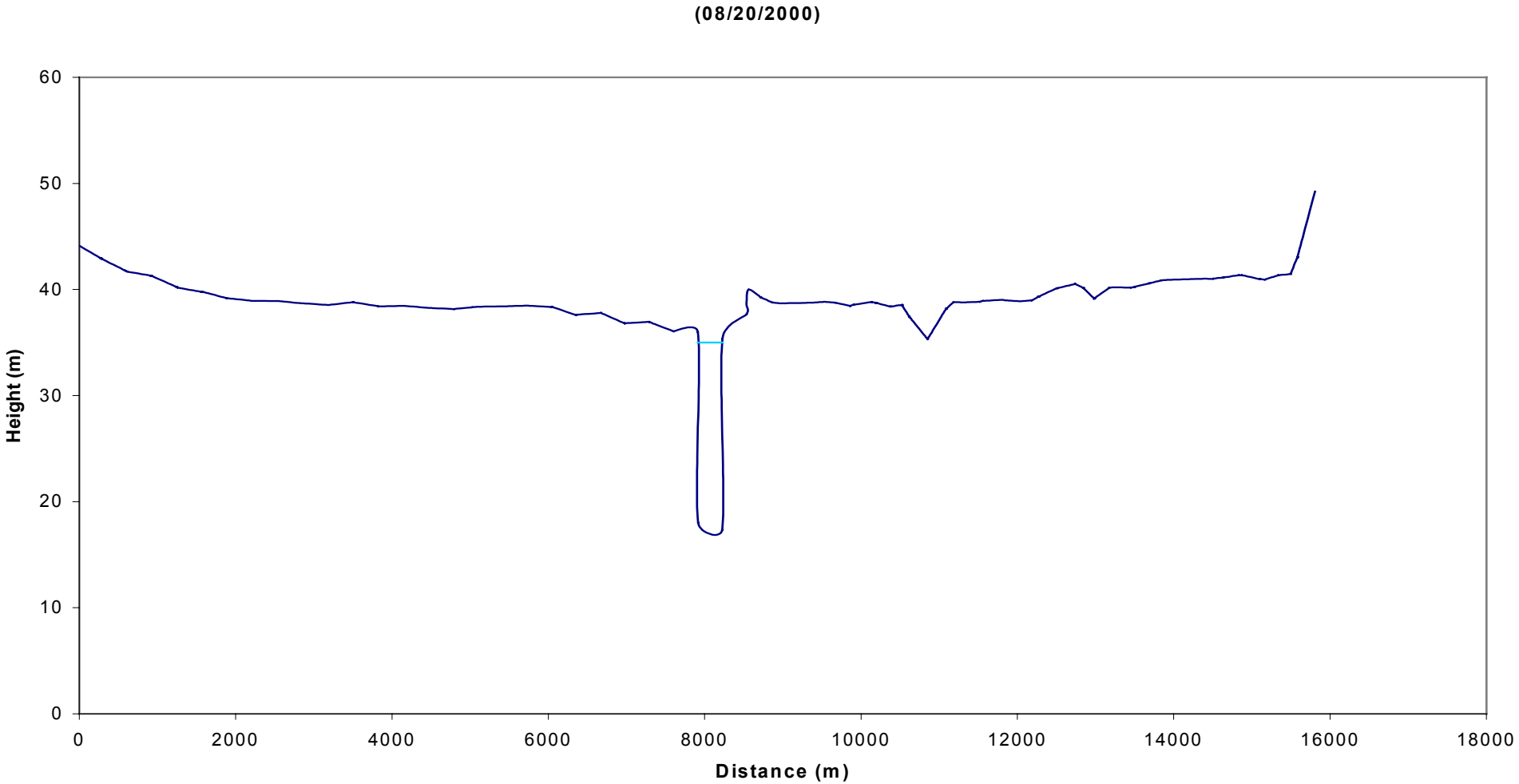

Figure F6.2 (d): Plot of cross-section across the floodplain at Ndundu – Surveyed on the 08th Feb. 2000

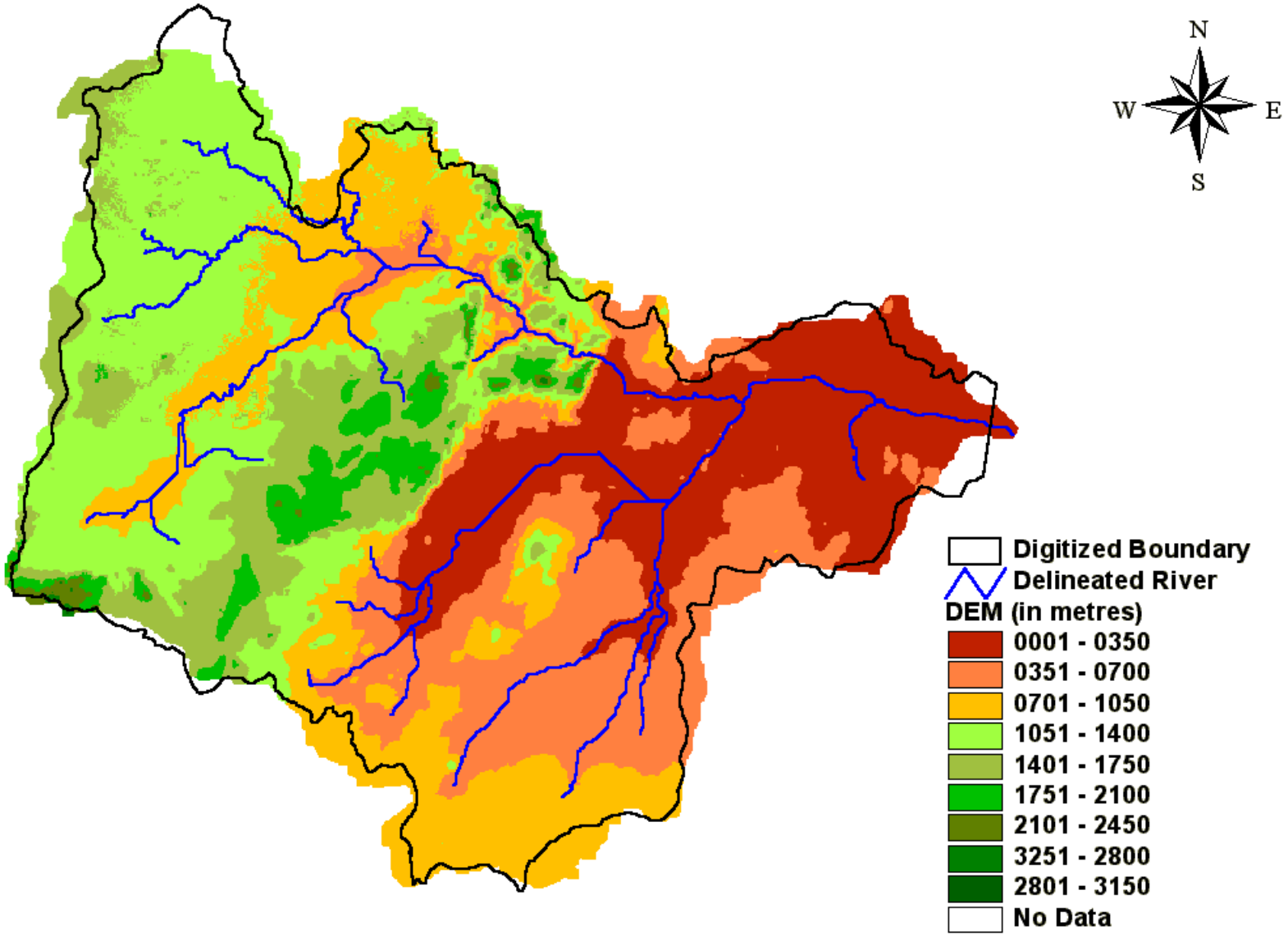

Figure F6.3: DEM of the Entire Rufiji River Basin

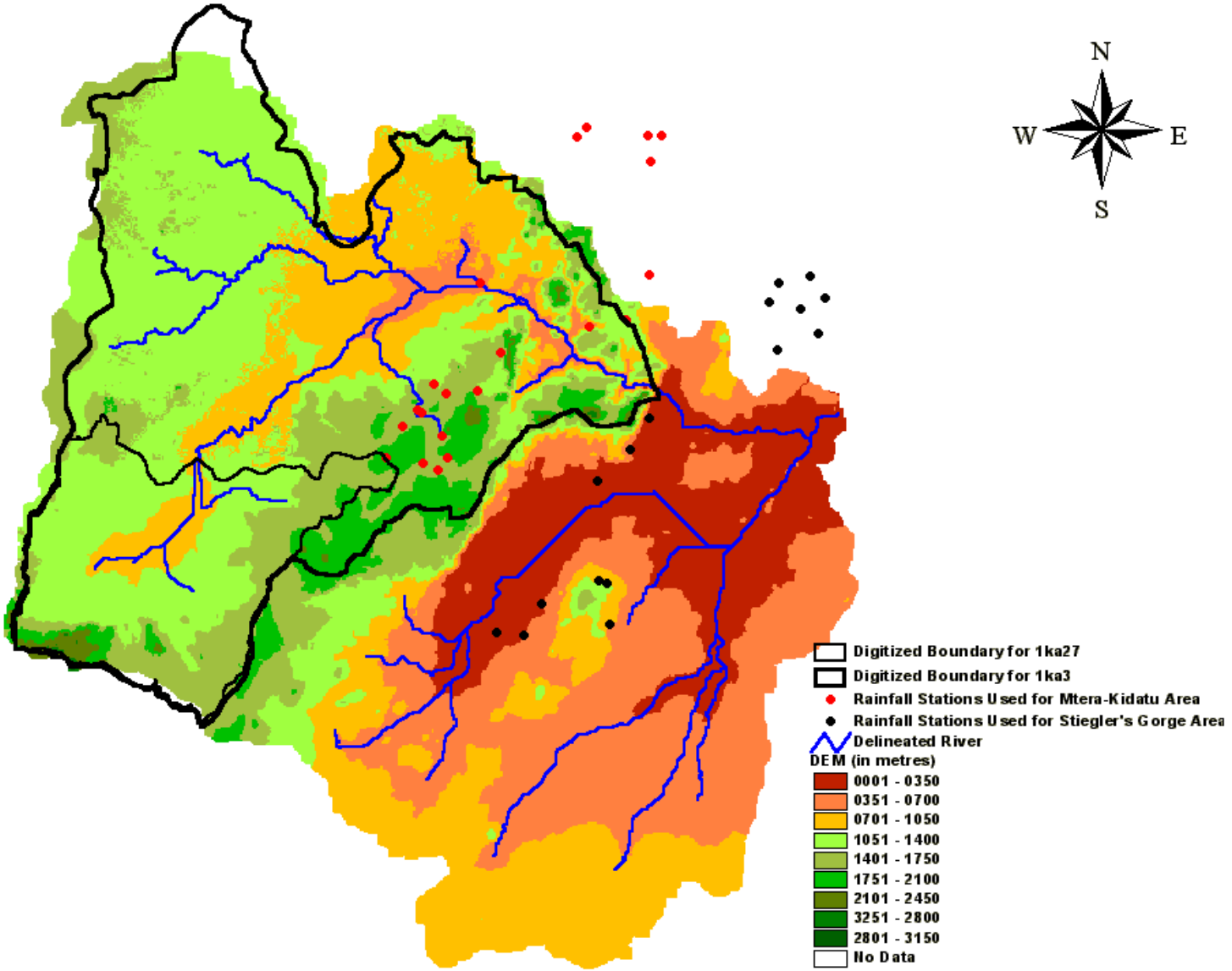

Figure F6.4: DEM for Stiegler's Gorge Sub-Basin (1k3)

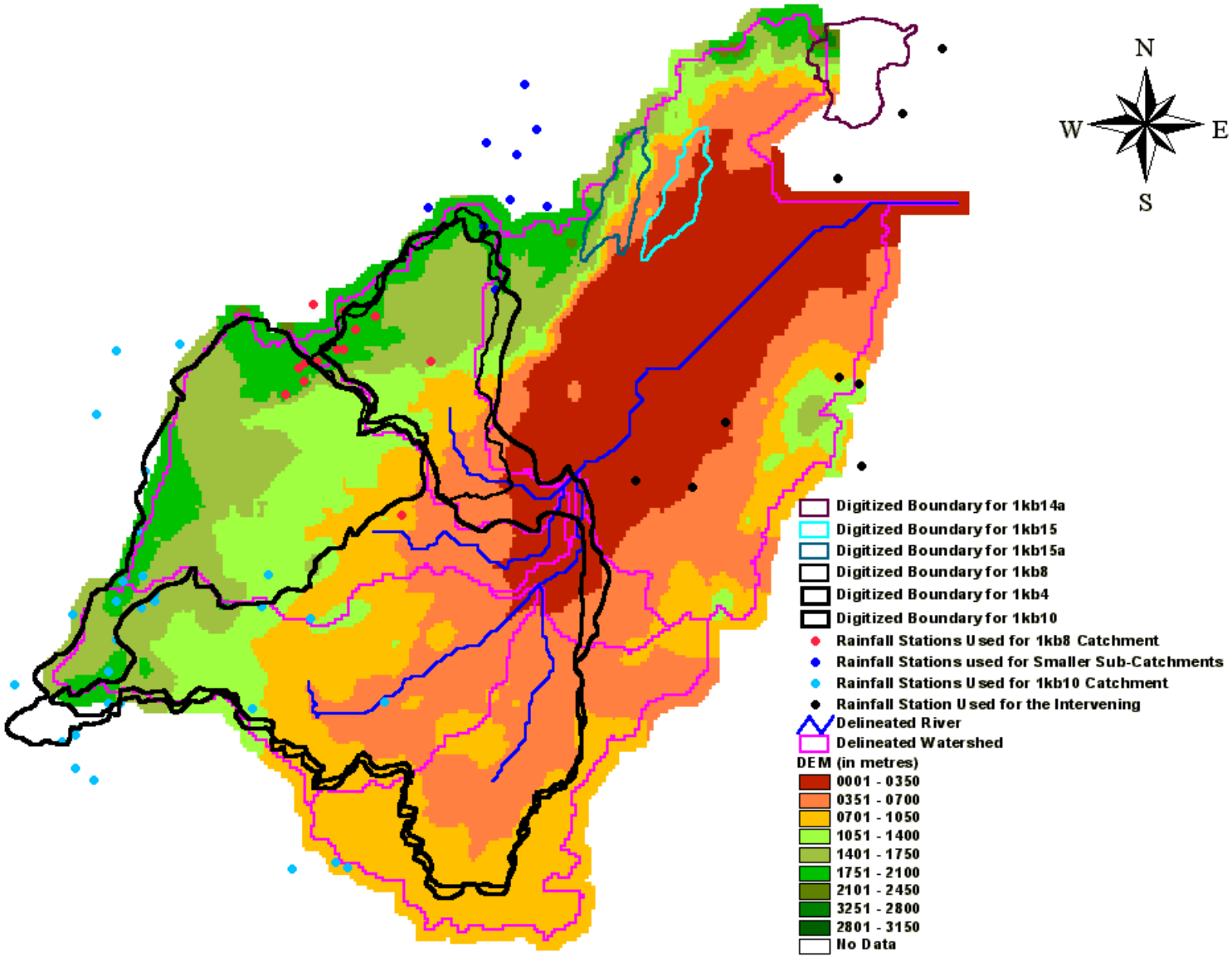

Figure F6.5: DEM for Kilombero Sub-Basin (1kb17)

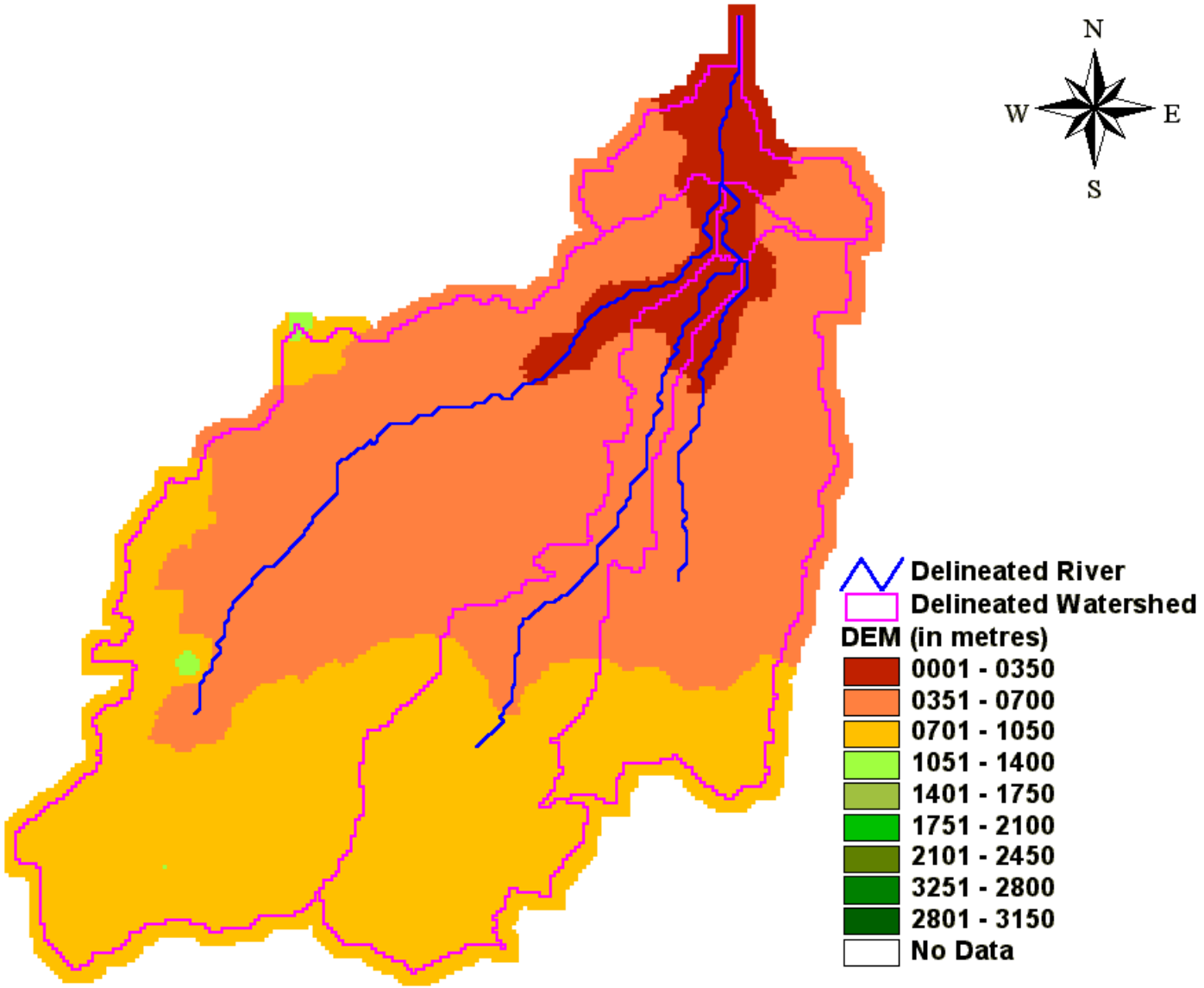

Figure F6.6: DEM for the Ungauged Luwegu Sub-Basin

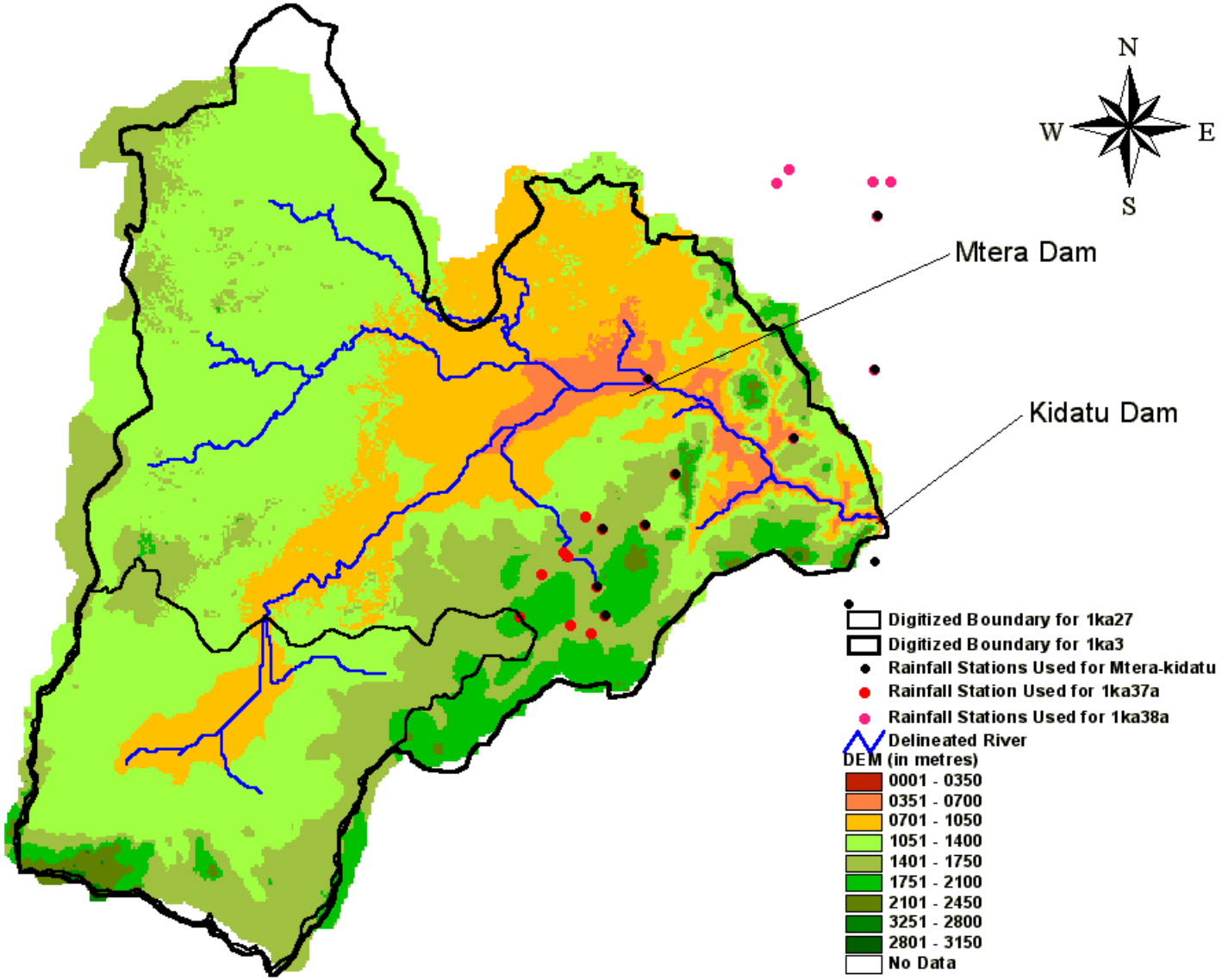

Figure F6.7: DEM for the Catchment Upstream of Kidatu Reservoir (1ka3)

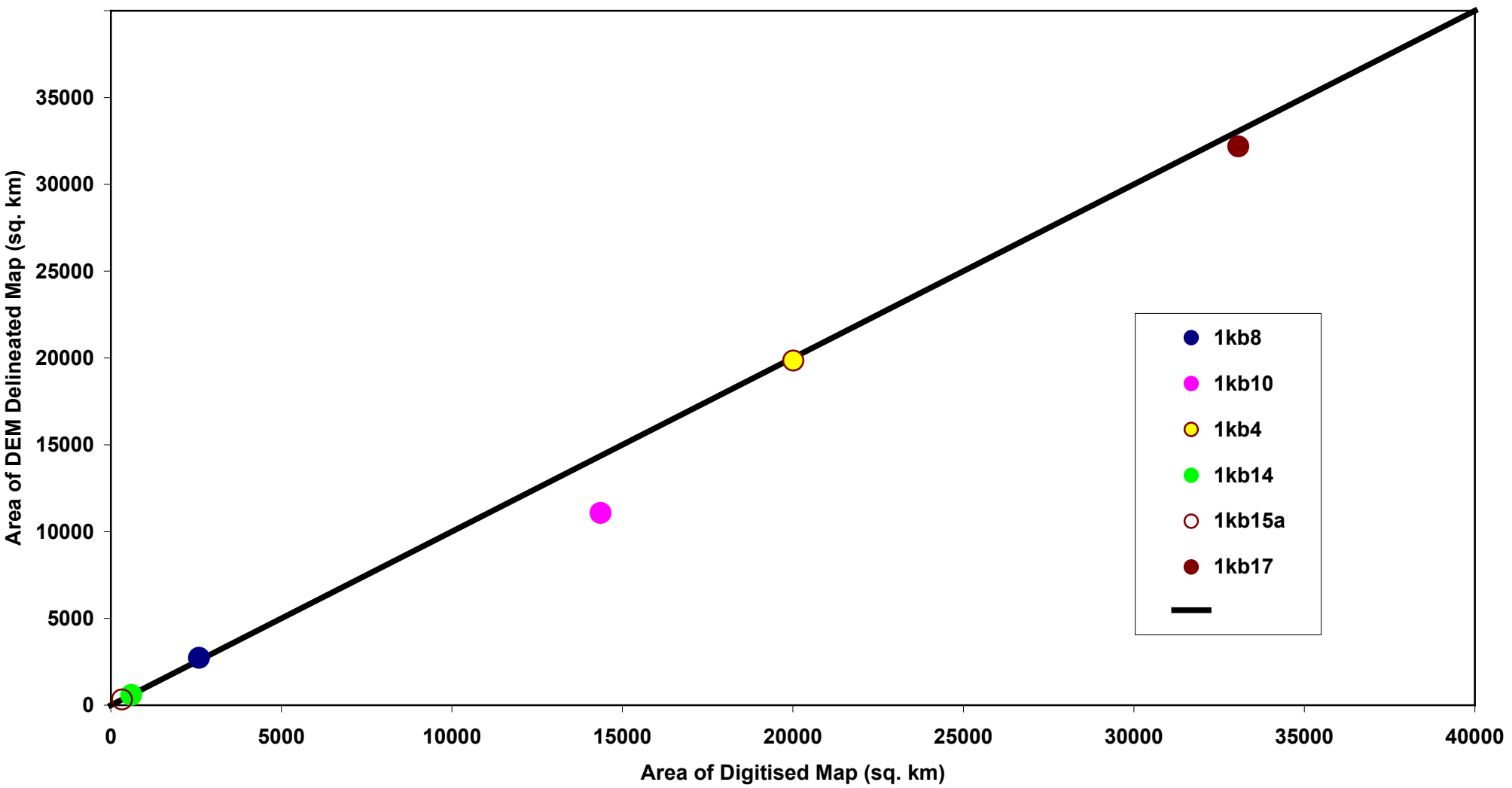

Figure F6.8: Comparison of Areas from Delineated DEMs and their Digitised Maps for Catchments within the Kilombero Sub-Basin

B061	B062	B071	B072	B081	B082	B091	B092	B101	B102	B111	B112	B121	B122	B131	B132	B141	B142	B151	B152	B161	B162	B171	B172	B181	B182	B191	B192
B063	B064	B073	B074	B083	B084	B093	B094	B103	B104	B113	B114	B123	B124	B133	B134	B143	B144	B153	B154	B163	B164	B173	B174	B183	B184	B193	B194
C061	C062	C071	C072	C081	C082	C091	C092	C101	C102	C111	C112	C121	C122	C131	C132	C141	C142	C151	C152	C161	C162	C171	C172	C181	C182	C191	C192
C063	C064	C073	C074	C083	C084	C093	C094	C103	C104	C113	C114	C123	C124	C133	C134	C143	C144	C153	C154	C163	C164	C173	C174	C183	C184	C193	C194
D061	D062	D071	D072	D081	D082	D091	D092	D101	D102	D111	D112	D121	D122	D131	D132	D141	D142	D151	D152	D161	D162	D171	D172	D181	D182	D191	D192
D063	D064	D073	D074	D083	D084	D093	D094	D103	D104		D114	D123	D124	D133	D134	D143	D144	D153	D154	D163	D164	D173	D174	D183	D184	D193	D194
E061	E062	E071	E072	E081	E082	E091	E092	E101	E102	E111		E121	E122	E131		E141	E142	E151	E152	E161	E162	E171	E172	E181	E182	E191	E192
E063	E064	E073	E074	E083	E084	E093	E094	E103	E104	E113	E114	E123	E124		E134	E143	E144	E153	E154		E164	E173	E174	E183	E184	E193	E194
F061	F062	F071	F072	F081	F082	F091	F092	F101	F102	F111	F112	F121		F131	F132		F142	F151	F152		F162	F171	F172		F182	F191	F192
F063	F064	F073	F074	F083	F084	F093	F094	F103	F104	F113	F114	F123	F124	F133	F134	F143	F144	F153	F154	F163	F164	F173	F174	F183	F184	F193	F194
G061	G062	G071	G072	G081	G082	G091	G092	G101	G102	G111	G112	G121	G122	G131	G132	G141	G142	G151	G152	G161	G162	G171	G172	G181	G182	G191	G192
G063	G064	G073	G074	G083	G084	G093	G094	G103	G104	G113	G114	G123	G124	G133	G134	G143	G144	G153	G154	G163	G164	G173	G174	G183	G184	G193	G194
H061	H062	H071	H072	H081	H082	H091	H092	H101	H102	H111	H112	H121	H122	H131	H132	H141	H142	H151	H152	H161	H162	H171	H172	H181	H182	H191	H192
H063	H064	H073	H074	H083	H084	H093	H094	H103	H104	H113	H114	H123	H124	H133	H134	H143	H144	H153	H154	H163	H164	H173	H174	H183	H184	H193	H194
J061	J062	J071	J072	J081	J082	J091	J092	J101	J102	J111	J112	J121	J122	J131	J132	J141	J142	J151	J152	J161	J162	J171	J172	J181	J182	J191	J192
J063	J064	J073	J074	J083	J084	J093	J094	J103	J104	J113	J114	J123	J124	J133	J134	J143	J144	J153	J154	J163	J164	J173	J174	J183	J184	J193	J194
K061	K062	K071	K072	K081	K082	K091	K092	K101	K102	K111	K112	K121	K122	K131	K132	K141	K142	K151	K152	K161	K162	K171	K172	K181	K182	K191	K192
K063	K064	K073	K074	K083	K084	K093	K094	K103	K104	K113	K114	K123	K124	K133	K134	K143	K144	K153	K154	K163	K164	K173	K174	K183	K184	K193	K194

Figure F6.9: REMP Network for Lower Rufiji Floodplain (2-metre Interval Contours Maps)

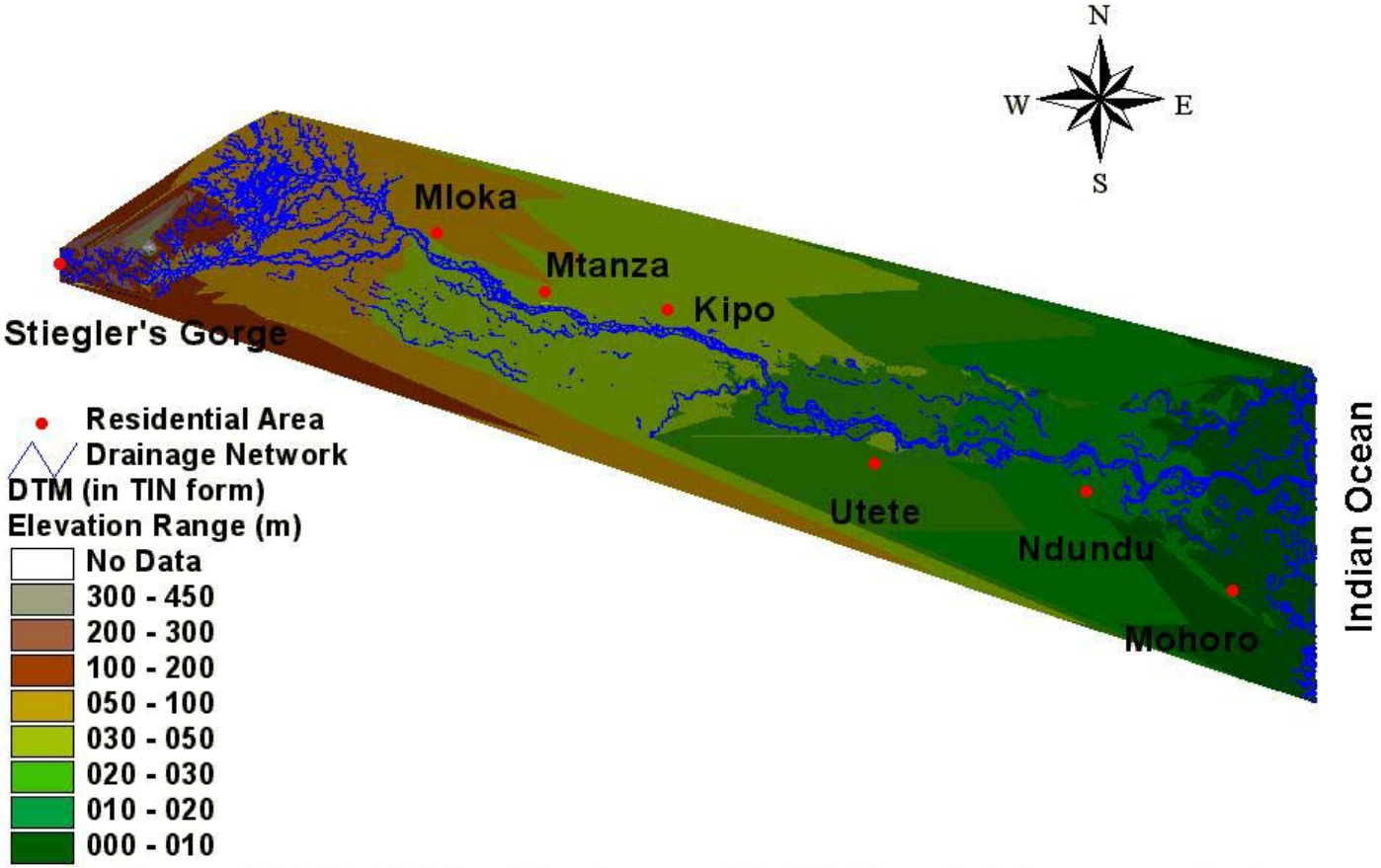

FIgure F6.10: DTM of the Lower Rufiji Floodplain generated from Digitised 2m Interval Contours Maps

Chapter 7

7 Catchment Simulation Model

7.1 Introduction

This chapter, although entitled as Catchment Simulation model, actually deals with development and application of sub-models for various sub-systems or sub-elements of the Rufiji River Basin. These sub-models when put together into a single model will, eventually, lead to the development of the Catchment Simulation model. The work presented in this chapter is a first step towards the ultimate objective of having a single simulation model for the basin, which can be used for impact analysis and for choosing various management options.

The sub-models tried in this chapter are:

(a) Inflow estimates into Mtera Reservoir.
(b) Inflow estimates into Kidatu Reservoir.
(c) Kidatu to Stiegler's Gorge Sub-Basin Model.
(d) Stiegler's Gorge to Mloka Sub-Basin Model.
(e) Kilombero Sub-Basin Model.

The models used were predominantly of the Systems type but in the Kilombero sub-basin a simple Lumped Conceptual model and a Semi-Distributed Hydrological model were also tried.

The following Systems models were applied:

(a) Simple Linear Model (SLM),
(b) Linear Perturbation Model (LPM)
(c) Linear Varying Gain Factor Model (LVGFM)

The mathematical details, of each of these models, are not discussed in this chapter because it was felt that mathematical details would, unnecessarily, burden the text of this chapter. The three models listed above are all based on multiple regression equation where the dependent variable is the daily runoff and the independent variables are daily rainfall values recorded on the day of the observation of runoff and a few days prior to that day. The Linear Perturbation Model is a modification of the Simple Linear Model where seasonal variations in rainfall and runoff are accounted for in the regression equation. The Linearly Varying Gain Factor Model is a further extension of the regression equation, where non-linearity due to high intensity of rainfall is accounted for.

All the three models were used in their parametric formulation of the Linear Transfer Function mode. The parameters were estimated by the method of Ordinary Least Squares.

For the catchment of Kilombero and for five of its sub-catchments, a lumped conceptual model was also applied. The model chosen was the Soil Moisture Accounting and Routing Model (SMAR). A two-parameter version, i.e., the basic version of this model was used in the study. This basic version of the model assumes that the runoff generated is dependent on the amount of soil moisture. If the soil is saturated the runoff generated is higher than when it is dry. The loss of water, due to evaporation, depends upon the availability of soil moisture. Water is lost at a potential rate when the soil moisture storage is full. Actual evaporation decreases as the soil moisture storage decreases. The routing is done by a series of Linear Reservoirs.

For the catchment of Kilombero, a Semi-Distributed model was applied. This was done by using the standard software of HEC-HMS. Simplest version of the HEC-HMS model was applied in this work. As a result one cannot use these models (the HEC-HMS and the SMAR models) for any impact analysis. Much more work is required to bring the application of the Lumped Conceptual and the Semi-Distributed models to fruitful levels. On the other hand, application of the Systems

type of models was conclusive. These models were used for developing real-time flood warning systems and for establishing the impact of the construction of Mtera/Kidatu Reservoir System on the annual maximum floods in the Rifiji River Basin.

Normally, one would have thought that an impoundment of the size of Mtera/Kidatu Reservoir System would reduce the annual maximum floods in the river. But it was interesting to note that since the impoundment the magnitude of the highest floods have actually increased rather than decreased due to releases from the Kidatu Reservoir. Releases from Kidatu are not based on forecasts done by a forecasting model. Instead they are based on actual measurements and the actually observed levels of water in the reservoir. If the reservoir is above a certain level then the water is released. In the event of very high floods a lot of water is released which in turn have the effect of creating an artificial flood wave.

7.2 Estimation of Inflows into Mtera Reservoir (1ka5)

Simple Linear Model (SLM), Linear Perturbation Model (LPM) and Linear Varying Gain Factor Model (LVGFM) were used to relate the flow at 1ka5 (Mtera) with inflows at 1ka31 (Mawande), 1ka42 (Kisigo) and 1ka59 (Msembe Ferry). Figure F7.1 shows a schematic diagram indicating the location of the stations in relation to the outlet.

Since Mtera Reservoir was impounded in 1980 the model was calibrated for pre-impoundment period of 1957 to 1975. The data of 19 years was used for the calibration of the model and the remaining 4 years, 1976 to 1979, was used for the verification of the model. All the three models registered an efficiency (R^2) of above 90% during calibration, with LVGFM having the highest efficiency of 94.26% and LPM the least of 90.35%. The results are presented in Table T7.1. The same order of efficiency was observed during verification with LVGFM having an efficiency of 73.53%, while LPM had an efficiency of 69.85%. Table T7.2 presents the optimised model parameters.

The SLM, LPM and LVGFM had a volumetric error of 2.49%, 1.05% and 7.11% respectively as shown in Table T7.14. LVGFM had the least error of 40.58% in estimating the highest observed peak flow at Mtera, while SLM had the greatest error of 64.75%.

SLM was used for estimating inflow at Mtera because the SLM had the best estimate of flow volume compared to LPM and LVGFM. SLM is also the simplest among the three models and the results are not vastly different from the other models.

Scatter plots showing the observed and estimated flow at Mtera for the selected model, i.e. SLM, is shown in Appendix A7.1 while model error diagram is shown in Appendix A7.2. Observed and estimated peak hydrographs at Mtera for the three models are as shown in Appendix A7.3.

7.3 Estimation of Inflows into Kidatu Reservoir (1ka3)

River flow data at Kidatu (1ka3) was consistently available from 1954 to 1975; prior to impoundment of the reservoir. Scanty discharge data after impoundment of the reservoir was also available for the period 1982 to 1985, as obtained from the Ministry of Water.

Observed flow at three flow stations; 1ka5 (Mtera), 1ka37a (Lukosi at Mtandika) and 1ka38 (Yovi) were combined with the average rainfall over the intervening catchment to estimate flow at the Kidatu station. A schematic diagram showing the location of these stations is as given in Figure F7.2.

Three systems type of models, namely; Simple Linear Model (SLM), Linear Perturbation Model (LPM) and Linear Varying Gain Factor Model (LVGFM) in Linear Transfer Function form were calibrated over a period of 18 years from 1958 to 1969. Model verification was done from 1970 to 1975 (6 years).

Good model efficiencies were obtained, with all models registering an average R^2 of above 91% during calibration and 89% during the verification period. The results are presented in Table T7.3. LPM had the least error in estimating inflows in terms of volume, with an error of 0.02%, while LVGFM had the largest error of 9.34% as shown in Table T7.14. The highest observed peak flow at Kidatu was estimated by LVGFM with an error of 27.94%. The corresponding error recorded by the SLM was 52.50%.

For simplicity, Simple Linear Model was again adopted for the estimation inflows at Kidatu. Table T7.4 presents the optimised model parameters. Scatter plots showing the observed and estimated flow at Kidatu for the selected model is shown in Appendix A7.1 while the model error diagram is shown in Appendix A7.2. Observed and estimated peak hydrographs for the three models are as shown in Appendix A7.3.

7.4 The Kidatu to Stiegler's Gorge Sub-Basin Model

The observed flows at Kidatu (1ka3) and at Kilombero (1kb17) together with the average rainfall over the intervening catchment between Kilombero, Kidatu and Luwegu sub-basins were used to estimate inflows at Stiegler's Gorge (1k3). Three set of models, namely; the Simple Linear Model (SLM), Linear Perturbation Model (LPM) and Linear Varying Gain Factor Model (LVGFM) were used. The available discharge data at Kilombero (1kb17) was from 1957 to 1984. Average rainfall data over the intervening catchment was available from 1951 to 1996. Observed discharge data at Stiegler's Gorge was available from 1957 to 1985. Figure F7.3 shows a schematic diagram indicating the layout of the above three stations.

Calibration period for the three models was chosen from 1957 to 1975 (19 years) while model verification was done from 1976 to 1984 (9 years). Fairly good model efficiencies were registered for all models during the calibration period with an average R^2 of 85% during calibration. The results are presented in Table T7.5. LPM had the best efficiency during verification with an R^2 of 71.09%, while SLM and LVGFM had an average efficiency of 62%. Table T7.6 shows the model coefficients. LPM had the least error of 0.48% in estimating observed flow volume while LVGFM had the largest error of 10.92%, as shown in Table T7.14.

The highest observed peak at Stiegler's Gorge estimated by LVGFM had the least error of 26.15% compared to LPM that had the largest error of 41.48%. SLM was chosen for use in this study. Scatter plots showing observed and estimated flows at Stiegler's Gorge for this SLM is shown in Appendix A7.1 while model error diagram for the same model is shown in Appendix A7.2. Observed and estimated peak hydrographs at Stiegler's Gorge for all the used models are shown in Appendix A7.3.

7.5 The Stiegler's Gorge to Mloka Sub-Basin Model

The only available data at Mloka (1k4) were the river stage data covering 7 years from 1978 to 1984. A rating curve was developed for Mloka as discussed in section 4.2.2 in chapter 4. With the help of this estimated rating curve the stage data were converted into flow data.

The river reach between the Stiegler's Gorge and the Mloka, i.e., the last point of the upper catchment and the starting point of the floodplain, comprises a series of lakes that are inter linked with each other. This complex stretch of the river is difficult to be modelled except for treating it as a black box. As a result this stretch was modelled by the Systems type of models. The stretch of the river beyond Mloka was modelled by using a simplified hydraulics model whose details are presented in Chapter 9.

Observed daily flows at the Stiegler's Gorge (1k3) were routed to Mloka (1k4) using the SLM, LPM and LVGFM. The models were calibrated separately for the high flows and the low flows. It has been established that, the average bank full capacity for most river sections in the Lower Rufiji River is 2,500 m^3/s. Hence a threshold value of 2,000 m^3/s was set to define high and low flows. Flows below the threshold value were considered as low flows.

SLM and LPM were calibrated and verified for high, low and all season flows, while LVGFM was calibrated and verified only for all season flows. Calibration period for all models was from 1978 to 1982 (5 years), while verification was done for 2 years from 1983 to 1984. Both SLM and LPM had average model efficiency (R^2) of 66% for high flows and 77% for low flows during calibration. The results are presented in Table T7.7. SLM performed better than LPM in modelling high flows. The results during verification had a model efficiency R^2 of 97% as compared to 95% for LPM. Model coefficients for SLM and LPM for modelling inflows at Mloka are shown in Table T7.8. LVGFM had the least error of 0.81% in estimating the flow volume at Mloka, while LPM had the greatest error of 6.67% and 5.68%, for low and high flows respectively as shown in Table T7.14. LPM had the least error of 3.56% in estimating the highest peak flow at Mloka while LVGFM had the largest error of 14.49%.

Both the low flow SLM and the high flow SLM produced seemingly excellent model results. The total volumetric error was 2.37%. The highest recorded peak was only 4.41% in error. But one must remember that this modelling exercise is based on discharge data that were estimated using a rating curve that assumed that the flow at Mloka and at the Stiegler's Gorge is the same. Naturally this, incorrect assumption, has favourably biased the results of modelling between Stiegler's Gorge and Mloka. Again, the SLM was chosen in this study.

Scatter plots showing observed and estimated flow at Mloka for the chosen model is shown in Appendix A7.1 while model error diagram for the same model is shown in Appendix A7.2. Observed and estimated peak hydrographs at Mloka for all the used models are shown in Appendix A7.3.

7.6 Kilombero Sub-Basin - Systems Models

Kilombero sub-basin has an area of about 33,000 km^2. It is the main contributor of flows at Stiegler's Gorge. The sub-basin is composed of several sub-catchments. Out of which 5 were used in this study. These are: 1kb10, 1kb8, 1kb4, 1kb14 and 1kb15. The station names and their locations are as in Table 4.1, in chapter 4 of this report.

Simple Linear Model (SLM), Linear Perturbation Model (LPM) and Linear Varying Gain factor Model (LVGFM) in their Linear Transfer Function (LTF) form were applied to the 5 component sub-catchments of the Kilombero sub-basin and the entire sub-basin. Two scenarios were created for catchment numbers 1kb4 and 1kb17. In the first case Single Input Rainfall-Runoff model was tried where with average rainfall over the respective catchments formed the single input into the model. The second option of Multiple Input Routing model included upstream inflows and the rainfall over the intervening catchments.

The calibration period for calibrating the models for catchment 1kb10 was 20 years from 1960 to 1979 and verification period from 1980 to 1987 (8 years). For catchment 1kb8 the calibration period was from 1957 to 1982 (26 years) and verification period of 8 years from 1983 to 1990. Calibration and verification periods for catchment 1kb4 are 18 years (1960-1977) and 5 years (1978-1982), respectively. For catchment 1kb14, 23 years (1958-1980) was used for calibrating the models and 8 years from 1981 to 1988 was for verification of the models. 22 years, i.e., from 1960 to 1981, of data was used to calibrate the models for 1kb15a and 8 years (1982-1989) for the verifications. Calibration period for the modelling of the entire sub-basin (1kb17) was 18 years (1960-1977) and 5 years (1978-1982) of data was used to verify the models.

Table T7.9 shows the model efficiency results obtained on application of the system models in Kilombero sub-basin and its corporate catchments, while Table T7.10 shows the coefficients for SLM and LPM for estimating flows at the respective catchments. LPM performed better than SLM and LVGFM in both the calibration the models and the verifications with efficiency (R^2) of 79% and 53%, respectively for catchment 1kb10. Similarly, LPM was good the others for catchment 1kb8 with R^2 of 67% in the calibration but the R^2 for the verification not good (47%).

All models performed poorly in estimating flows for catchment 1kb14, by persistently over estimating low flows and under estimating high flows, and hence low model efficiencies were recorded. The efficiencies (R^2) for SLM were 13% in the calibration and –122% in the verification. LPM had 26% and –29%, respectively, for calibration and verification. Similarly, LVGFM had 27% for calibration and –48% for verification.

LPM and LVGFM were good in the flow estimates for catchment 1kb15a during calibrations of the models but the verifications were not impressive. The calibration efficiencies (R^2) were 64% and 63%, respectively for LPM and LVGFM, while the verification efficiencies (R^2) were 48% and 36%, respectively.

On average, all models performed better in estimating flows at catchments 1kb4 and 1kb17, as compared to the other catchments on Rainfall-Runoff modelling, in terms of model efficiency (R^2). 1kb4 had an average of 73% in calibrating the models and an average of 69% in verifying. An average 67% was obtained in calibration and 66% in verification for the entire sub-basin 1kb17.

For all catchments, LPM had the least error in estimating observed flow volume, followed by LVGFM and then SLM, as shown in Table T7.14. This order of merit was not maintained when estimating the highest observed peak flow at the various catchments, though LPM had a better advantage over LVGFM and SLM. Scatter plots showing the observed and estimated flows for the respective models applied for sub-basin 1kb17 are shown in Appendix A7.1 while model error diagrams are shown in Appendix A7.2. The observed and estimated peak hydrographs for all the catchments are shown in Appendix A7.3.

7.7 Kilombero Sub-Basin - Lumped Conceptual Model

Soil Moisture Accounting and Routing Model (SMAR) is a simple lumped conceptual model. A two-parameter version, which is the simplest version of this model, was applied to the Kilombero sub-basin and its 5 constituent sub-catchments. For each sub-catchment, the inputs to the model were average catchment rainfall and average estimated catchment potential evaporation on daily basis. The two parameters that were optimised using the historical flow data were C and H. The parameter C controls the rate of actual evaporation given the soil moisture deficit and the potential rate of evaporation. The parameter H controls the proportion of the rainfall that goes into direct runoff and the proportion that goes into the soil moisture storage.

The calibration and verification periods previously used in modelling flows using the system models were maintained. The details are presented in Table T7.11. This table shows the optimised parameters of the SMAR model and the resulting model efficiency (R^2). It was observed that, the model performed better only in modelling flows for the whole Kilombero sub-basin where it registered an R^2 of 71.90% and 76.49% during calibration and verification respectively. Poor model efficiency was recorded at 1kb15a, where R^2 of -47.29% and -71.51% were obtained for calibration and verification respectively. In estimating flow volume, the model was comparable with the system models, with SMAR occasionally taking a good position in the order of merit as seen in Table T7.14, for catchments 1kb10, 1kb8, 1kb4 and 1kb17. The model had a volumetric error (in percentage) of 4.37, 10.11, 5.10 and 3.72 in the above catchments respectively. In estimating the highest observed peak, SMAR performed better than the system models especially at 1kb4 and 1kb17, with a model error of 10.72% and 14.87% respectively.

Plots of seasonal mean variation of discharge, rainfall and evaporation for the five catchments in Kilombero sub-basin are shown in Appendix A7.4. Scatter plots showing the observed and estimated flows using SMAR for the entire sub-basin (1kb17) is shown in Appendix A7.1 while SMAR model error diagram is shown in Appendix A7.2. The observed and estimated peak hydrographs for all the catchments are shown in Appendix A7.3.

7.8 Kilombero Sub-Basin - HEC-HMS Model

The Kilombero sub-basin was modelled using the Hydrologic Engineering Center's Hydrologic Modelling System (HEC-HMS). This software is developed by the US Army Corps of Engineers.

The first step in the application of the HEC_HMS requires the use of HEC-GeoHMS package to perform drainage analysis on the Digital Elevation Model (DEM) of the Kilombero sub-basin. The HEC-GeoHMS is an ArcView GIS extension developed specifically to create input data into HEC-HMS model. HEC-GeoHMS has been developed as a geospatial hydrology tool kit for users with limited GIS experience. It allows the user to visualise spatial information, document watershed characteristics, perform spatial analysis, delineate sub-basins and streams, and expediently construct inputs to hydrologic models that can be used directly with the HEC-HMS. Location of various flow gauging stations in the sub-basin was necessary for accurate delineation of the respective sub-catchments within the sub-basin.

The tasks undertaken at were as follows:

1. Pre-processing of the terrain model
2. Basin processing
3. Setting up a HMS model with inputs from HEC-GeoHMS.

For the first task, eight data sets were derived that collectively described the drainage pattern of the Kilombero sub-basin. The first five data sets, in grid representation form, were flow direction, flow accumulation, stream definition, stream segmentation, and watershed delineation grids. The next two data sets were the vectorized representation of the watersheds and streams, and they were the watershed polygons and the stream segments. The last data set, the aggregated watersheds, was used primarily to improve the performance in the watershed delineation. The delineation procedure is outlined in chapter 6 section 6.2 of this report.

Task 2 enabled the aggregated watersheds to be merged and/or sub-divided, and with the help of the flow gauge locations. Sub-catchments were delineated within the entire Kilombero sub-basin. Figure F7.4 shows the delineated sub-catchments within the sub-basin under discussion. The physical characteristics of the streams and sub-catchments were extracted and saved in attribute tables. These attribute tables helped in the development of HMS input files. The input files are HMS basin model (schematic) file and background-map file. The basin model could either be lumped or distributed in structure. The lumped type was used in this study.

The last task involved the importation of the HEC-GeoHMS generated HMS input files into HEC-HMS model. Both the basin model and the background-map files were imported. The sub-catchments and routing element parameters were then input via HMS editors to the HEC-HMS.

The second major step was the calibration of the HEC-HMS model. The calibration period was from 1960 to 1977 (18 years) and the verification period from 1978 to 1982 (5 years). HEC-HMS does simulate precipitation-runoff and routing processes, both natural and controlled. In this study, the Initial and Constant method was used as sub-basin loss method at the various sub-catchments within the Kilombero sub-basin. The Soil Conservation Service (SCS) Unit Hydrograph was used as sub-basin transform method throughout the entire sub-basin with a baseflow method being the Constant Monthly option. The Lag method was used for the reaches of the sub-basin. The optimal parameters attained are documented in Appendix A7.5. The model had very poor model efficiency during calibration and verification. The efficiency (R^2) for the calibration was 22% and for the verification R^2 of –49% was obtained. The results are presented in Tables T7.12 and T7.13. It was observed that, the model slightly over estimated the observed peak discharge in both calibration and verification stages.
The model registered an error of 48.60% in estimating the observed peak flow as shown in Table T7.14. In estimating the observed flow volume at Kilombero sub-basin (1kb17), the model had an error of 4.21%.

Scatter plots showing the observed and estimated flows using HEC-HMS model at Kilombero sub-basin (1kb17) is included in Appendix A7.1, while model error diagram is in Appendix A7.2. The observed and estimated peak hydrographs are shown in Appendix A7.3.

7.9 Impact of Mtera/Kidatu on Annual Floods

Mtera and Kidatu Reservoirs are built on Great Ruaha River. This is one of the main contributors of flow at Stiegler's Gorge. Any deviation of flow in this river from its natural state is expected to register an impact at Stiegler's Gorge and subsequently at the floodplain and the Delta. The outflow from the two reservoirs is controlled by TANESCO for power generation. The objective of this impact analysis exercise was to determine if the building of this reservoir system had any impact on the annual maximum flows at Kidatu and at the Steigler's Gorge.

The methodology used was to compare the observed annual maximum flows at Kidatu and at Steigler's Gorge after the construction of the reservoirs with estimates of the annual maximum flows at these two locations assuming that the two reservoirs were not built. That is the hypothetical uncontrolled flow. This later quantity can only be estimated by the use of mathematical models and naturally the estimate is subject to modelling errors.

The data of outflow at 1ka3, i.e., at the outlet of the Kidatu Reservoir, was obtained from TANESCO for 1983 to 1997. This is the post impoundment period. It was calculated by adding the machine discharges and the spills on a daily basis.

Mtera Reservoir was impounded in mid-1980, while the Kidatu reservoir was impounded in 1976. The hypothetical uncontrolled flow, i.e., flow that would have occurred had there been no impoundment at Metra and Kidatu was estimated for the period of 1980 to 1993 for the Metra Reservoir and for the Kidatu the period was between 1975 and 1993.

The hypothetical uncontrolled flow at Mtera (1ka5) was estimated by the use of Multiple Input Simple Linear Model (SLM). The inputs to the model were flow at stations of 1ka31, 1ka42 and 1ka59 as discussed in section 7.2. The model was calibrated for the period 1957 to 1975. The hypothetical uncontrolled flow at Mtera, from 1980 to 1993, was estimated by the use of the model that was calibrated for the period prior to 1980 when the reservoir was not actually built.

The model for the estimation of flow into Kidatu was calibrated for the period between 1958 and 1969. This is prior to the impoundment of water at Kidatu. This model comprised four inputs. These are the flows observed at 1ka5, 1ka37a, 1ka38 and the intervening catchment rainfall. The details are presented in section 7.3.

This model was used to estimate the hypothetical uncontrolled flow at Kidatu by using observed flows at 1ka37a, 1ka38, intervening catchment rainfall and hypothetical uncontrolled flow at 1ka5 for the period between 1980 and 1993. The hypothetical uncontrolled flow at 1ka5, for this period, was estimated earlier by using the Mtera inflow model.

The annual maximum flows observed at Kidatu between 1983 and 1993 were compared with the estimated hypothetical uncontrolled annual maximum flows at Kidatu. The comparison is shown in Figure F7.5. It is interesting to note that high floods were induced by releases from Kidatu. In 1989 an annual maximum peak flow of 1,400 Cumecs was recorded. The estimated uncontrolled maximum peak flow for that year is only about 800 Cumecs. This is an interesting observation, as one would normally expect attenuation of peak floods rather than accentuation of floods resulting from impoundments. Given that the Kidatu Reservoir is of small capacity and the TANESCO that operates the reservoir does not have a proper flow forecasting system in place. It seems that when a large flood wave enters the reservoir the operators of the reservoir let the water go at the maximum capacity. The result is equivalent to an artificially induced flood wave.

To assess the impact of Mtera/Kidatu impoundment on flow at the Stiegler's Gorge the following procedure was adopted.

(a) The sub-catchment model, relating flow at Kidatu, Kilombero and the intervening catchment rainfall, described in section 7.4, was calibrated for the period 1957 to 1975. This is for the period prior to the impoundment of water at Kidatu. For the calibration of this model it does not matter if the water observed at Kidatu was controlled or uncontrolled.

(b) The calibrated model was used to extend the flow at the Stiegler's Gorge beyond 1984 because there were are observed records at the Stiegler's Gorge beyond 1984. The inputs to this model are observed flow, i.e., the controlled outflow, at Kidatu, observed flow at Kilombero and the observed intervening rainfall. The annual maximum floods of this estimated time series are plotted as green lines on Figure F7.6.

(c) The observed annual maximum flows at Stiegler's Gorge, up to 1975, are marked as black bars in Figure F7.6.

(d) The calibrated model was used to estimate flow at the Stiegler's Gorge beyond 1975 assuming a hypothetical situation of no impoundment at Mtera and Kidatu. The inputs to this model are estimated flow, i.e., the hypothetical uncontrolled flow at Kidatu, observed flow at Kilombero and the observed intervening rainfall. The annual maximum floods of this estimated time series are plotted as blue lines on Figure F7.6.

It can be seen that the impact of impoundment is minimal at the Stiegler's Gorge location.

Table T7.1: Model efficiency results for Simple Linear Model (SLM), Linear Perturbation Model (LPM) and Linear Varying Gain Factor Model (LVGFM) when estimating flows during pre-impoundment period at Mtera (1ka5)

Name of catchment		Calibration Period	Model efficiency (R^2 in %) during calibration			Verification Period	Model efficiency (R^2 in %) during verification			Catchment Area (km^2)
Output	Inputs		SLM	LPM	LVGFM		SLM	LPM	LVGFM	
1ka5	-1ka31 -1ka59 -1ka42	1957-1975	93.87	90.35	94.26	1976-1979	72.21	69.85	73.53	67,884

Table T7.2: Coefficients for Simple Linear Model (SLM) and Linear Perturbation Model (LPM) in Linear Transfer Function Form (LTF) for estimating flows during pre-impoundment period at Mtera (1ka5)

Name of catchment		Order of moving average	Pure Lag	Order of autoregressive procedure	Coefficients for SLM (LTF)	Coefficients for LPM (LTF)
Output	Inputs					
1ka5		-	-	1	0.916082	0.920842
	-1ka31	2	0	-	0.522527, -0.493698	0.507212, -0.478912
	-1ka59	2	0	-	0.621958, -0.451605	0.619501, -0.453621
	-1ka42	2	0	-	2.4789, 3.90846	2.68126, 3.99865

Table T7.3: Model efficiency results for Simple Linear Model (SLM), Linear Perturbation Model (LPM) and Linear Varying Gain Factor Model (LVGFM) in estimating flows at Kidatu (1ka3) – Prior to Impounding

Name of Catchment		Calibration Period	Model efficiency (R^2 in %) during calibration			Verification Period	Model efficiency (R^2 in %) during verification			Catchment Area (km^2)
Output	Inputs		SLM	LPM	LVGFM		SLM	LPM	LVGFM	
1ka3	-1ka5 -1ka37a -1ka38 -Intervening catchment areal rainfall	1958-1969	91.83	92.02	91.98	1970-1975	89.18	89.48	89.68	80,040

Table T7.4: Coefficients for Simple Linear Model (SLM) and Linear Perturbation Model (LPM) in Linear Transfer Function Form (LTF) in estimating the flows at Kidatu (1ka3) – Prior to Impounding

Name of Catchment		Order of moving average	Pure Lag	Order of autoregressive procedure	Coefficients for SLM (LTF)	Coefficients for LPM (LTF)
Output	Inputs					
1ka3		-	-	1	0.891805	0.897026
	-1ka5	2	0	-	0.285723, -0.165473	0.267549, -0.150276
	-1ka37a	2	0	-	0.258375, -0.163646	0.241200, -0.110379
	-1ka38	2	0	-	0.705868, -0.956481	0.693924, -0.831974
	-Intervening catchment areal rainfall	2	0	-	0.317916, 0.358403	-0.831974, 0.402290

Table T7.5: Model efficiency results for Simple Linear Model (SLM), Linear Perturbation Model (LPM) and Linear Varying Gain Factor Model (LVGFM) in modelling flows at Stiegler's Gorge (1k3) – including Pre-Impounding Period

Name of catchment		Calibration Period	Model efficiency (R^2 %) During calibration			Verification Period	Model efficiency (R^2 %) during verification			Catchment Area (km^2)
Output	Inputs		SLM	LPM	LVGFM		SLM	LPM	LVGFM	
1k3	-1kb17 -1ka3 -Intervening catchment areal rainfall	1957-1975	85.58	85.44	86.53	1976-1984	62.26	71.09	63.43	177,000

Table T7.6: Coefficients for Simple Linear Model (SLM) and Linear Perturbation Model (LPM) in Linear Transfer Function Form (LTF) in modelling the flows at Stiegler's Gorge (1k3) – including Pre-Impounding Period

Name of Catchment		Order of moving average	Pure Lag	Order of autoregressive procedure	Coefficients for SLM (LTF)	Coefficients for LPM (LTF)
Output	Inputs					
1k3	-	-	-	1	0.916082	0.920842
	-1kb17	2	0	-	0.522527, -0.493698	0.507212, -0.478912
	-1ka3	2	0	-	0.621958, -0.451605	0.619501, -0.453621
	-Intervening catchment areal rainfall	2	0	-	2.4789, 3.90846	2.68126, 3.99865

Table T7.7: Model efficiency results for Simple Linear Model (SLM), Linear Perturbation Model (LPM) and Linear Varying Gain Factor Model (LVGFM) when modelling flows at Mloka (1k4) at different flow seasons

Name of catchment		Calibration Period	Flow Season	Model efficiency (R^2 in %) during calibration			Verification Period	Model efficiency (R^2 in %) during verification		
Output	Input			SLM	LPM	LVGFM		SLM	LPM	LVGFM
1k4	-1k3	1978-1982	All seasons	75.86	85.25	83.56	1983-1984	81.15	93.61	86.96
			High Flows	66.47	66.11	-		96.70	94.57	-
			Low Flows	79.73	77.60	-		70.46	87.70	-

Table T7.8: Coefficients for Simple Linear Model (SLM) and Linear Perturbation Model (LPM) in Linear Transfer Function Form (LTF) when modelling the flows at Mloka (1k4) at different flow seasons

Flow Season	Name of Catchment		Order of moving average	Pure Lag	Order of autoregressive procedure	Coefficients for SLM (LTF)	Coefficients for LPM (LTF)
	Output	Input					
All Seasons	1k4	-	-	-	1	0.910962	0.905855
		-1ka3	2	0	-	0.146564, -0.0327338	0.146564, 0.910962
High Flows	1k4	-	-	-	1	0.667364	0.430624
		-1ka3	2	0	-	0.240743, 0.161552	0.250981, 0.341118
Low Flows	1k4	-	-	-	1	0.867433	0.864213
		-1ka3	2	0	-	0.158085, 0.0330084	0.131985, 0.0189155

KEY:

- All Seasons implies all flows considered.
- High flows implies flows above 2,000 m^3/s.
- Low flows implies flows below 2,000 m^3/s.

Table T7.9: Model efficiency results for Simple Linear Model (SLM), Linear Perturbation Model (LPM) and Linear Varying Gain Factor Model (LVGFM) when modelling river flows in Kilombero Sub-Basin

No.	Name of catchment	Inputs	Calibration Period	Model efficiency (R^2 in %) during calibration			Verification Period	Model efficiency (R^2 in %) during verification			Catchment Area (km^2)
				SLM	LPM	LVGFM		SLM	LPM	LVGFM	
1	1kb10	-Areal rainfall	1960-1979	40.26	78.68	69.18	1980-1987	10.68	52.76	46.64	14,361
2	1kb8	-Areal rainfall	1957-1982	15.71	67.47	58.37	1983-1990	-45.93	46.61	54.10	2,585
3	1kb14	-Areal rainfall	1958-1980	13.19	26.41	27.24	1981-1988	-121.89	-29.32	-48.23	598
4	1kb15a	-Areal rainfall	1960-1981	21.96	64.94	63.15	1982-1989	-0.73	47.55	35.87	328
5	1kb4	-Areal rainfall	1960-1977	69.12	77.14	69.29	1978-1982	69.50	77.29	63.29	18,043
6	1kb4	-1kb8 -1kb10	1960-1977	67.43	76.46	79.65	1978-1982	63.77	71.16	66.74	18,043
7	1kb17	-Areal rainfall	1960-1977	50.03	77.97	63.72	1978-1982	48.29	79.99	67.96	33,066
8	1kb17	-1kb4 -1kb14 -1kb15a -Intervening catchment areal rainfall	1960-1977	61.95	74.82	75.10	1978-1982	60.83	65.74	73.36	33,066

Table T7.10: Coefficients for Simple Linear Model (SLM) and Linear Perturbation Model (LPM) in Linear Transfer Function Form (LTF) when modelling river flows in Kilombero Sub-Basin

No.	Name of catchment	Inputs	Order of moving average	Pure Lag	Order of autoregressive procedure	Coefficients for SLM (LTF)	Coefficients for LPM (LTF)
1	1kb10		-	-	1	0.972267	0.923814
		-Areal rainfall	2	0	-	0.348560, 0.885336	0.400466, 0.923814
2	1kb8		-	-	1	0.936326	0.865402
		-Areal rainfall	2	0	-	0.0808825, 0.336579	0.085786, 0.373392
3	1kb14		-	-	1	0.908363	0.896572
		-Areal rainfall	2	0	-	0.055791, 0.0965514	0.0604567, 0.103117
4	1kb15a		-	-	1	0.935164	0.833624
		-Areal rainfall	2	0	-	0.102979, 0.145366	0.0920929, 0.156880
5	1kb4		-	-	1	0.986352	0.984158
		-Areal rainfall	2	0	-	0.0842982, 0.496993	0.0411763, 0.461442
6	1kb4		-	-	1	0.964451	0.971033
		-1kb8	2	0	-	0.0650289, -0.0414384	0.0533311, -0.0336285
		-1kb10	2	0	-	0.0922848, -0.0406532	0.0887855, -0.0213153
7	1kb17		-	-	1	0.990421	0.995793
		-Areal rainfall	2	0	-	0.560414, 1.18172	0.393097, 0.976001
8	1kb17		-	-	1	0.976953	0.983356
		-1kb4	2	0	-	0.0611586, -0.0640479	0.0537248, -0.0172151
		-1kb14	2	0	-	0.129207, 0.444065	0.0599840, 0.272470
		-1kb15a	2	0	-	0.06777684, 0.259160	0.139127, 0.361590
		-Intervening catchment areal rainfall	2	0	-	0.486530, 0.556002	0.307147, 0.363969

Table T7.11: Parameters of SMAR Model for various Sub-Catchments in the Kilombero Sub-Basin

No.	Catchment Name	Parameter value			Calibration			Verification		
		C	H	T	Calibration period	R^2(%)	IVF	Verification period	R^2(%)	IVF
1	1kb10	0.201	0.175	1.00	1960-1979	50.57	0.8498	1980-1987	9.52	1.2602
2	1kb8	0.221	0.270	1.00	1957-1982	38.27	0.9967	1983-1990	-61.72	1.4264
3	1kb14	0.285	0.158	1.00	1958-1980	20.81	1.000	1981-1988	-279.04	3.6953
4	1kb15a	0.100	0.156	1.00	1960-1981	-47.29	0.2155	1982-1989	-71.51	0.2086
5	1kb4	0.778	0.254	1.00	1960-1977	48.44	1.000	1978-1982	36.21	1.2321
6	1kb17	0.376	0.12	1.00	1960-1977	71.90	0.9978	1978-1982	76.49	0.9750

Table T7.12: Model efficiency results for HEC-HMS in estimating flows at Kilombero (1kb17)

Name of Catchment		Calibration Period	Model efficiency (R^2 %)	Verification period	Model efficiency (R^2 %)
Output	Inputs				
1KB17	-1kb4 -1kb14 -1kb15a - Intervening catchment aveage rainfall	1960-1977	22.06	1978-1982	-48.72

TableT7.13: Performance of HEC-HMS model in estimating several flow features during calibration and verification at Kilombero (1kb17)

Comparative feature	Calibration		Verification	
	Observed	Estimated	Observed	Estimated
Peak discharge (m^3/s)	3,400.2	3,413.4	3,493.3	4,198
Peak time (date)	28th Apr.1963	4th May1974	25th Apr.1974	17th Apr.1979
Total discharge (mm)	9,358.1	9,573.8	2,871.6	3,167.9
Average absolute residuals (m^3/s)	-	300.8	-	432.4
Total residuals (mm)	-	216.6	-	298.1

Table T7.14: Performance of Various Models in estimating the Volume and the Highest Peak of Observed Discharge in Various Sub-Catchments considered in this Study

No.	Outlet Catchment	Inputs	Min. Obs. discharge (Cumecs)	Max. Obs. dicharge (Cumecs)	Model	% error in volume	% error in peak
1	1kb10	-Areal rainfall -(Evaporation)	49.23	712.17	SLM	18.40	60.69
					LPM	0.28	61.98
					LVGFM	1.39	62.50
					SMAR	4.37	47.97
2	1kb8	-Areal rainfall -(Evaporation)	8.710	173.73	SLM	21.31	46.88
					LPM	0.07	46.13
					LVGFM	2.77	47.32
					SMAR	10.11	41.85
3	1kb14	-Areal rainfall -(Evaporation)	0.15	157.21	SLM	45.32	83.14
					LPM	0.11	81.84
					LVGFM	18.18	85.66
					SMAR	31.28	78.42
4	1kb15a	-Areal rainfall -(Evaporation)	0.32	128.16	SLM	30.59	64.50
					LPM	0.01	54.60
					LVGFM	10.44	61.54
					SMAR	79.51	77.25
5	1kb4	-Areal rainfall -(Evaporation)	16.74	548.17	SLM	10.20	45.15
					LPM	0.36	42.45
					LVGFM	3.37	59.70
					SMAR	5.10	10.72
6	1kb4	-1kb8 -1kb10	16.74	548.17	SLM	0.75	48.47
					LPM	0.14	39.67
					LVGFM	3.40	32.77
7	1kb17	-Areal rainfall -(Evaporation)	100.36	3,493.30	SLM	38.89	49.85
					LPM	2.24	37.88
					LVGFM	2.62	55.45
					SMAR	3.72	14.87
					HEC-HMS	4.21	48.60
8	1kb17	-1kb4 -1kb14 -1kb15a -intervening catchment areal rainfall	100.36	3,493.30	SLM	14.72	49.00
					LPM	0.96	25.84
					LVGFM	2.72	47.45
9	1k3	-1ka3 -1kb17 -Intervening catchment areal rainfall	210.75	6,244.30	SLM	6.58	38.39
					LPM	0.48	41.48
					LVGFM	10.92	26.15
10	1ka3	-1ka5 -1ka37a -1ka38 -Intervening catchment areal rainfall	11.31	1,462.60	SLM	2.49	52.50
					LPM	0.02	48.50
					LVGFM	9.34	27.94

Continues Overleaf

No.	Outlet Catchment	Inputs	Min. Obs. discharge (Cumecs)	Max. Obs. dicharge (Cumecs)	Model	% error in volume	% error in peak
11	1ka5	-1ka42 -1ka31 -1ka59	0.17	1,121.90	SLM	2.49	64.75
					LPM	1.05	58.96
					LVGFM	7.11	40.58
12	1k4	-1k3	814.695	5,023.90	SLM	2.37	4.41
					LPM	5.68	3.56
					LVGFM	0.81	14.49

where **(Evaporation)** is additional input to SMAR Model.

Calibration Period = 1957 – 1975

Verification Period = 1976 – 1979

Catchment Area (km^2)

1ka31 = 6,838
1ka42 = 25,628
1ka59 = 24,320
1ka5 = 67,884

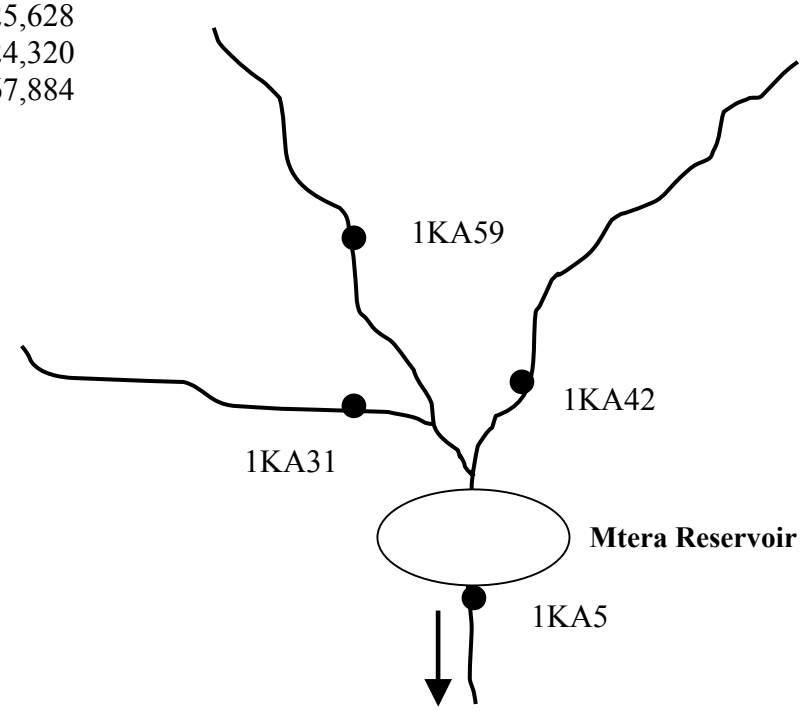

Figure F7.1: Schematic diagram showing the layout of discharge stations contributing to flows at Mtera (1ka5)

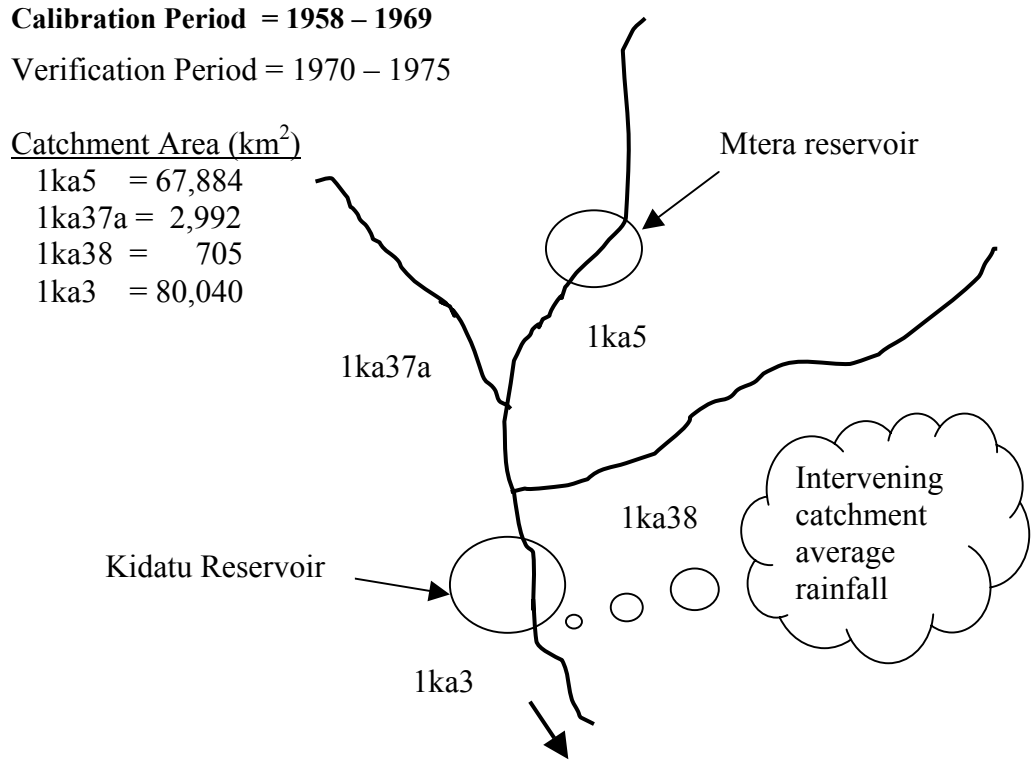

Figure F7.2: Schematic diagram showing the layout of main contributors of flows at Kidatu (1ka3)

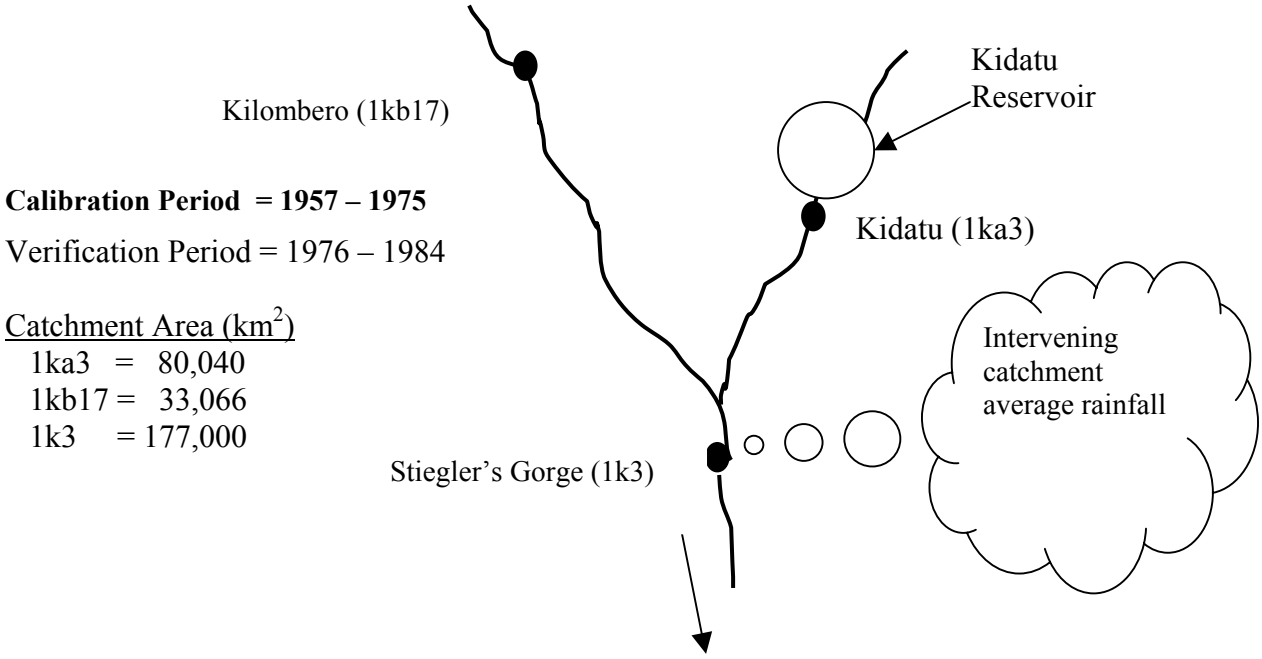

Calibration Period = 1957 – 1975

Verification Period = 1976 – 1984

Catchment Area (km^2)

1ka3 = 80,040
1kb17 = 33,066
1k3 = 177,000

Figure F7.3: Schematic diagram showing the layout of main contributors of flows at Stiegler's Gorge (1k3)

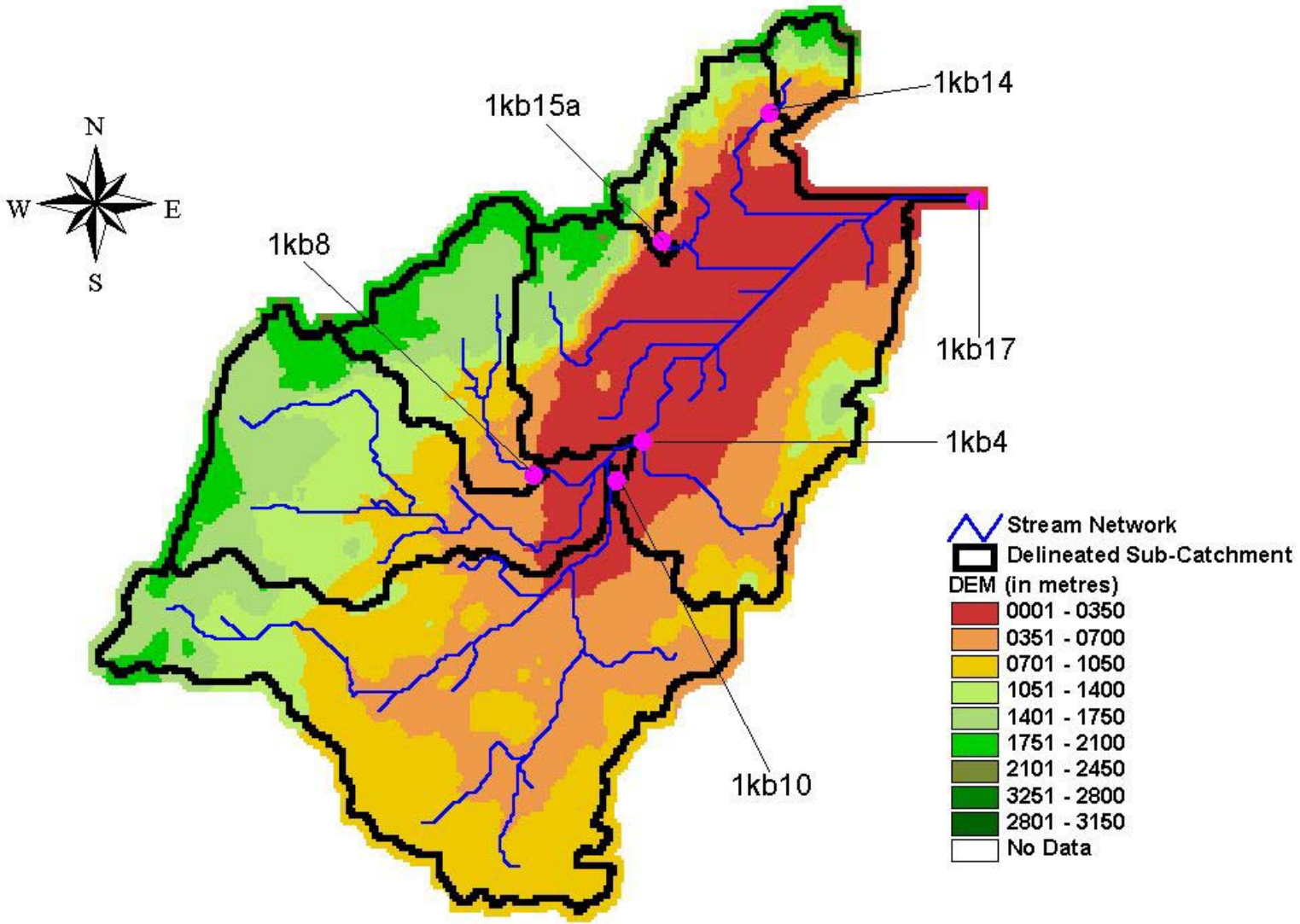

Figure F7.4: Delineation of Sub-Catchments within the Kilombero Sub-Basin as used in HEC-HMS Model

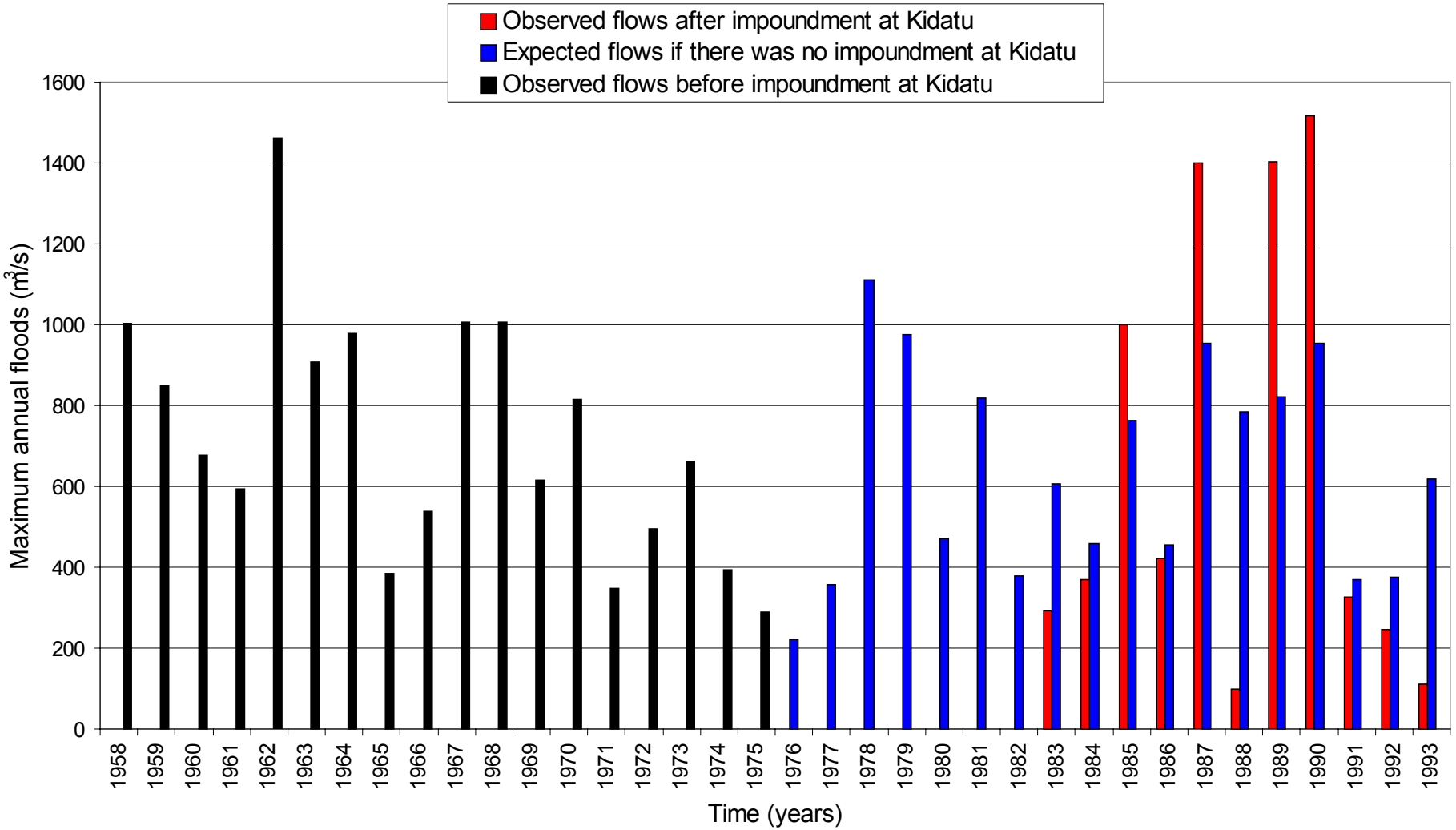

Figure F7.5: Comparison of annual maximum floods at Kidatu: With impoundment and assuming no impoundment at Kidatu

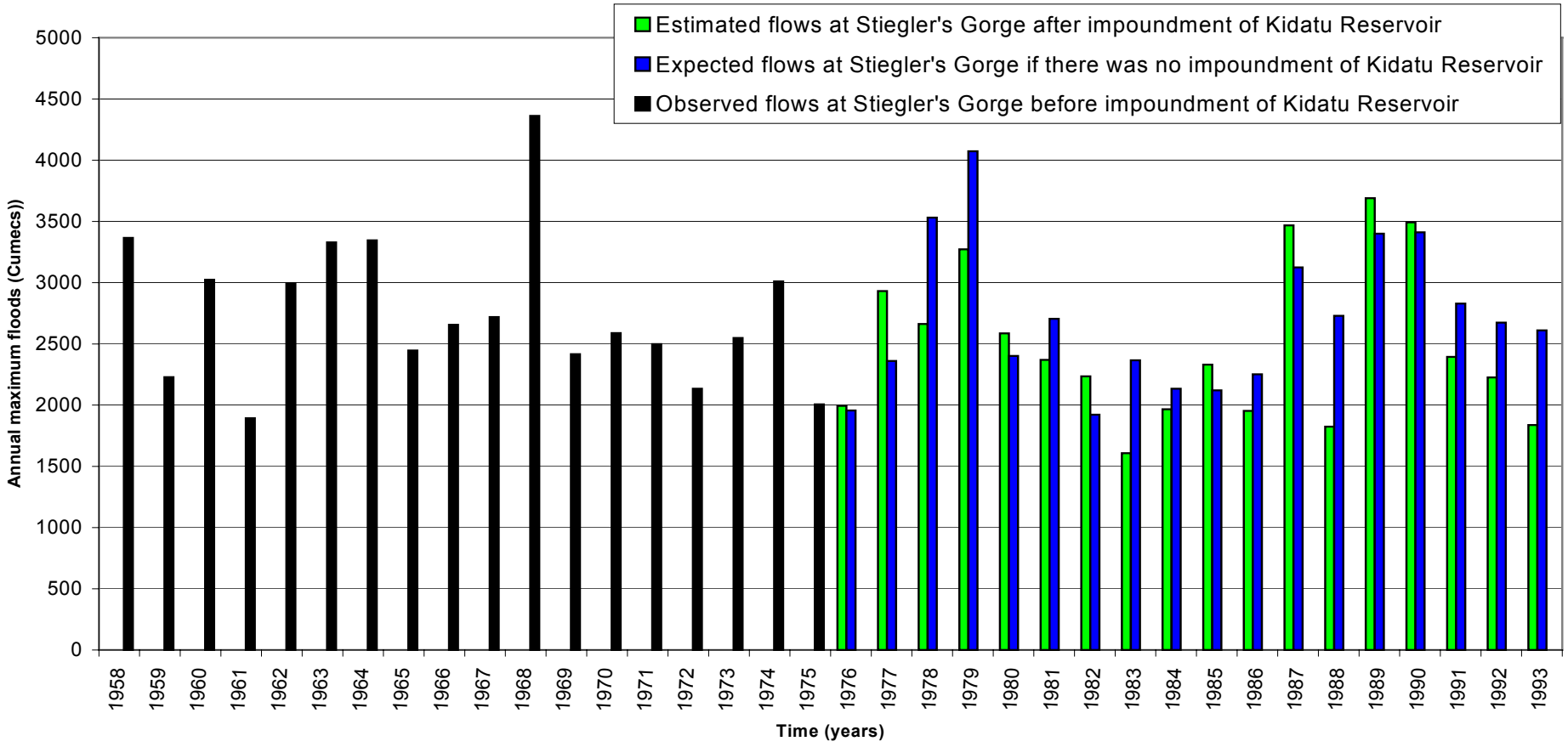

Figure F7.6: Comparison of annual maximum floods at Stiegler's Gorge: With impoundment and assuming no impoundment at Kidatu

Chapter 8

8 Real-Time Forecasting Model

8.1 Introduction

The objective of developing a flood warning system on the Lower Rufiji River is to enable the Civil Authorities in the district to evacuate people from the floodplains in the event of a large flood. Such a system requires a central mathematical model that can forecast the flood peaks at different lead times, for instance, a one day in advance or two days in advance or even ten days in advance. Of course, it would be extremely useful if the Civil Authorities can get ten days notice but unfortunately forecasts of very high lead-time are often very inaccurate. A forecast of a short lead-time, like one day forecast, is more accurate but it is less useful because it does not give much time for preparation. Therefore, the art in the development of mathematical models for flood warning is in trying to achieve greater levels of accuracy in forecasts for higher lead-time. Short lead forecasts in big river systems like the Rufiji River is a trivial matter. For instance, if 2,000 Cumecs of water are flowing at Stiegler's Gorge then it is very easy to say that there will be 2,000 Cumecs of water in Mloka and in Utete, which is within the floodplain, after a few hours. It is difficult to predict that information two or three days in advance.

River flow forecasts depend on the information available to the model for various points upstream of the point of interest. For instance, one can make use of information at Mloka to forecast flood at Utete. This will give a few hours of lead-time. If forecasts at Utete are based also on the information that is available at Stiegler's Gorge then the lead-time will increase to perhaps one day. If one goes further upstream up to Kidatu and/or up to 1kb17 in Kilombero then one may get 2 to 3 days lead-time. To increase the lead times further one has to estimate releases from Kidatu based on the outflows of Mtera and the operation policy of the reservoir system.

The magnitude of flows that are in excess of 2,500 Cumecs are known to overflow the banks in the Lower Rufiji River and cause flooding in the floodplain. It is important to know the extent of flooding in terms of depth of water that is likely to be impounded and the extent to which the floodwaters are likely to travel. This component of the forecasting model is dealt with in the following chapter.

A user-friendly computer package was developed in Visual Basic language to generate flood warnings within Lower Rufiji River. This stand-alone package is ready for installation in the basin. The description of the computer programme and its user manual is presented in volume 3 of this report.

8.2 The Model Formulation

The Real-Time Flow Forecasting Model for the Lower Rufiji floodplain comprised two sub-models:

1. The Kilombero-Kidatu-Stiegler's Gorge sub-model
2. The Stiegler's Gorge-Mloka sub-model

The purpose of the first sub-model is to forecast flows at Stiegler's Gorge (1k3) on daily basis, based on observed or forecasted flows at Kidatu (1ka3), Kilombero (1kb17) and the intervening catchment average rainfall. The second sub-model forecasts flows at Mloka (1k4) on daily basis, using observed or forecast flows at Stiegler's Gorge as input. Figure F8.1 shows the layout of the Real-Time Flow Forecasting Model described in this chapter.

The Kilombero-Kidatu-Stiegler's Gorge sub-model is described by equation 8.1.

$$Z_{t+L:t} = \alpha\left(Z_{t+L-1}\right) + \beta_1\left(X_{t+L}\right) + \beta_2\left(X_{t+L-1}\right) + \omega_1\left(Y_{t+L}\right)$$

$$+ \omega_2\left(Y_{t+L-1}\right) + \eta_1\left(R_{t+L}\right) + \eta_2\left(R_{t+L-1}\right) \quad (8.1)$$

The Stiegler's Gorge-Mloka sub-model is described by equations 8.2 and 8.3, respectively, for high and low flows.

$$Q_{t+L:t} = \psi\left(Q_{t+L-1}\right) + \tau_1\left(Z_{t+L}\right) + \tau_2\left(Z_{t+L-1}\right) \quad (8.2)$$

$$Q_{t+L:t} = \lambda\left(Q_{t+L-1}\right) + \mu_1\left(Z_{t+L}\right) + \mu_2\left(Z_{t+L-1}\right) \quad (8.3)$$

where

$\mathbf{Z_{t+L:t}}$	is the lead-**L** forecast flow value at the Stiegler's Gorge site, made from the forecast origin **t**,
$\mathbf{Q_{t+L:t}}$	is the lead-**L** forecast flow value at Mloka, made from the forecast origin **t**,
$\mathbf{X_t}$	is the flow value at time **t** at Kilombero discharge gauging site,
$\mathbf{Y_t}$	is the flow value at time **t** from Kidatu Reservoir,
$\mathbf{Z_t}$	is the flow value at time **t** at Stiegler's Gorge discharge gauging site,
$\mathbf{R_t}$	is the rainfall value at time **t**, averaged (areal) for the intervening catchment downstream of the Kidatu Reservoir and the Kilombero gauging site but upstream of the Stiegler's Gorge gauging site,
T,t	is either the time for which the data has been observed (recorded), or the time for which the forecast values are obtained from other source(s), as appropriate, for computation of the forecast flow values at the Stiegler's Gorge site and at Mloka, and
(α, β, ω, η, ψ, ι, λ and μ)	are various model coefficients. They were estimated by the method of least squares over the calibration period of the models. The calibrated coefficients are given in Table T8.1

Equations 8.1 to 8.3 are special forms of the Linear Transfer Function Model. This model form, comprising one Autoregressive and two moving average terms, was chosen simply because it corresponds to the Muskingum Routing Model. This model has been widely used for channel routing.

The Kilombero-Kidatu-Stiegler's Gorge sub-model was calibrated using historical flow data at Kilombero (1kb17), Kidatu (1ka3) and Stiegler's Gorge (1k3) together with average rainfall over the intervening catchment, which is downstream of Kidatu and Kilombero but upstream of Stiegler's Gorge. Historical data at Stiegler's Gorge (1k3) and Mloka (1k4) were used to calibrate the Stiegler's Gorge-Mloka sub-model, at low and high flows respectively. A threshold of 2,000 Cumecs was set to define high and low flows.

The results of calibration and verification of these sub-models have already been presented in chapter 7 of this report. These are quite satisfactory in both the cases except that one must keep in mind that these models were not calibrated for recent data. For many years the gauging station at the Stigler's Gorge is damaged and no records are being maintained at this location.

One-day lead forecast, i.e., tomorrow's flow at Mloka can be obtained by using equation 8.2 or 8.3 depending on the flow magnitude from Stiegler's Gorge. This forecast is based on observed flows at Stiegler's Gorge and at Mloka of today and predicted flow at Stiegler's Gorge tomorrow, which can be obtained using equation 8.1.

Two-day lead forecast, i.e., to forecast flow for day after tomorrow at Mloka, can again be done by the same equations, i.e., equation 8.2 or equation 8.3. But in this case both quantities on the right-hand-side of the equations are unknown. These are the flow at Mloka tomorrow and flow at Stiegler's Gorge for tomorrow and for the day after tomorrow. These quantities are not known. Therefore one has to estimate them. The best estimate of tomorrow's flow at Mloka is the one-day lead forecast explained above. Flow at Stiegler's Gorge for tomorrow and the day after tomorrow may be estimated by using the Kilombero-Kidatu-Stiegler's Gorge sub-model described by equation 8.1. Similarly, higher day lead forecasts can be obtained by replacing quantities in the right hand side of equations 8.1 to 8.3 by their best estimates.

To forecast one day lead time flow at Stiegler's Gorge, one must estimate tomorrow's release from Kidatu, estimate flow at Kilombero and estimate the amount of rainfall that is likely to fall in the intervening catchment in the next one day. Clearly, there is a dependence on TANESCO for forecasts of Kidatu releases and on the Meteorological office for forecasts of rainfall. The latter is very difficult not because the agency is not likely to cooperate but because it is very difficult to forecast rainfall, particularly, in tropical climatic conditions.

8.3 Results of up to Four-Day Lead Forecasts

Historical records available for the flow gauging stations involved in the formulation of the flow forecasting model were used to test the various sub-models up to four-day lead forecast. The available concurrent data length for Kilombero-Kidatu-Stiegler's Gorge sub-model was 1957-1984 (10,227 data points) and that for Stiegler's Gorge-Mloka sub-model was from 1978 to 1984 (2,557 data points).

The model efficiencies for both the sub-models are presented in Table T8.2. One-day lead forecasts are naturally better than the four-day lead forecasts for both of the sub-models. For Stiegler's Gorge, the one-day lead model efficiency was 97%. This value reduced to 90% at four-day lead. Similarly, for Mloka the one-day lead efficiency was 96%. This value decreased to 86% at the four-day level.

Figure F8.2 shows the time series plot of the observed versus the estimated values for these sub-models. The model seems to slightly underestimate the flood peaks.

The highest observed flow peak occurred on 3rd May 1974 at the Stigler's Gorge. The flood was estimated to be of 6,244 m^3/s. At Mloka, the highest observed flood occurred on the 20th April 1979. It was of 5,024 m^3/s, respectively. This highest observed flow at Mloka was produced by flow magnitude of 5,816 m^3/s at Stiegler's Gorge.

Figures F8.3 and F8.4 present the observed and the model estimated hydrographs at Stiegler's Gorge and Mloka, respectively, for the time period of 1978-1984. These figures show how the forecasting model predicted the flows up to four-day lead at the highest observed flow periods for the two sub-models.

Although, the results obtained look good but one must take into account that these results were obtained for 'perfect forecast scenario'. That means that the model assumes that knowledge of releases from Kidatu reservoir and flows estimates at 1kb17, i.e., Kilombero and intervening rainfall is known accurately. This was possible because the model was operated on historical data.

When the model will be operated in real time then one would not have any knowledge of what will be released from the Kidatu Reservoir in the next three to four days. One would not know how much rain is likely to fall in the next three to four days in the Kilombero sub-basin or in the intervening catchment. Naturally, most results will not be as attractive as they seem to be.

Table T8.1: Values of sub-models' parameters as used in the Real-Time Flow Forecasting Model develop for the Lower Rufiji River

No.	Sub-model	Parameter	Value
1	Kidatu-Kilombero-Stiegler's Gorge	α	0.916082
		β_1	0.522527
		β_2	-0.493698
		ω_1	0.621958
		ω_2	-0.451605
		η_1	2.4789
		η_2	3.90846
2	Stiegler's Gorge-Mloka (Low flow)	ψ	0.867433
		ι_1	0.158085
		ι_2	0.0330084
3	Stiegler's Gorge-Mloka (High flow)	λ	0.667364
		μ_1	0.240743
		μ_2	0.161552

Table T8.2: Real-Time Flow Forecasting Model Efficiencies obtained in forecasting flows at Stiegler's Gorge and at Mloka using Historical Data

Lead Time (in days)	Efficiency, R^2 (%)	
	At Stiegler's Gorge	At Mloka
1	97.20	96.79
2	94.51	93.18
3	92.26	89.46
4	90.21	86.21

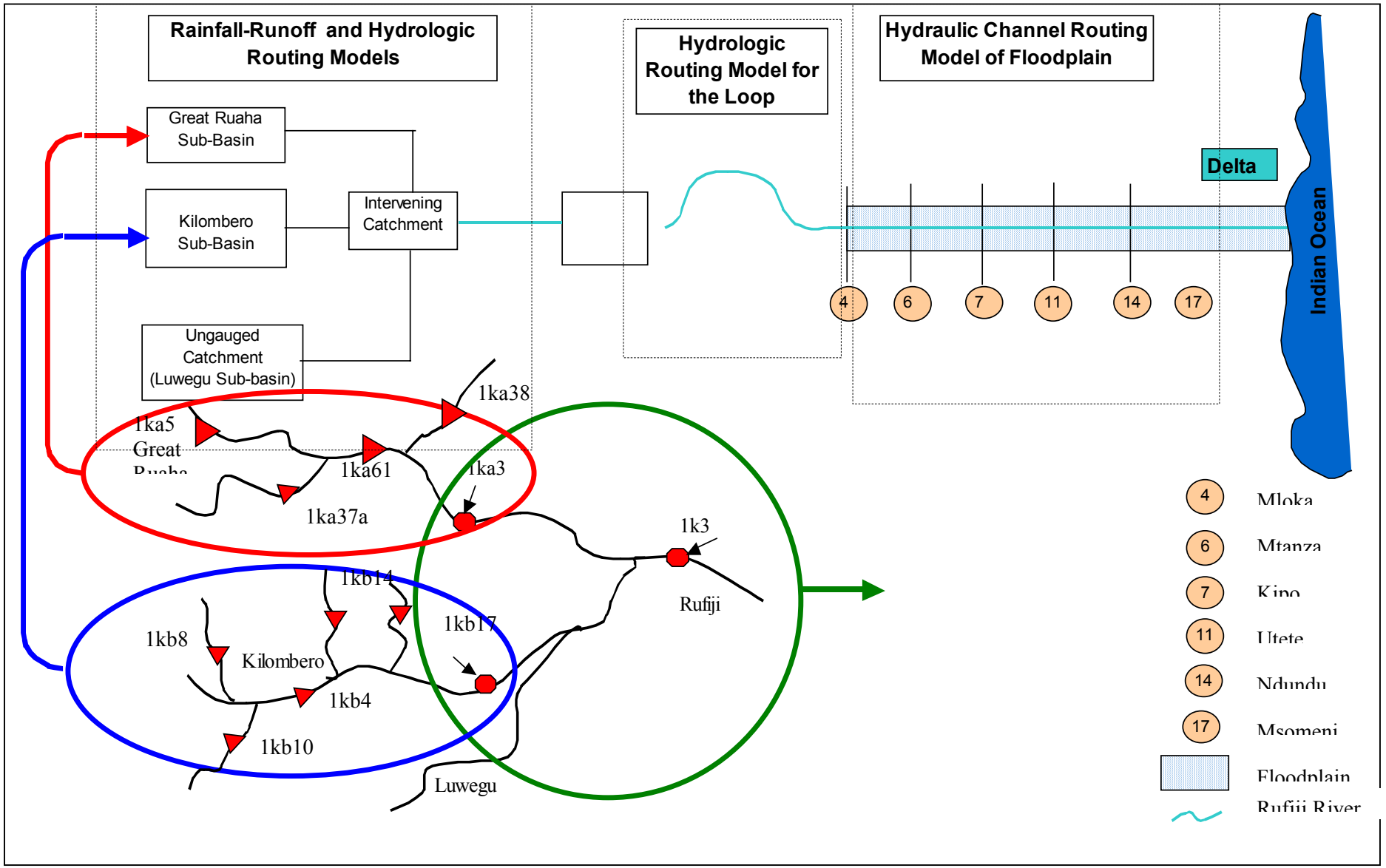

Figure F8.1: Schematic Structure of the Rufiji Floodplain Model

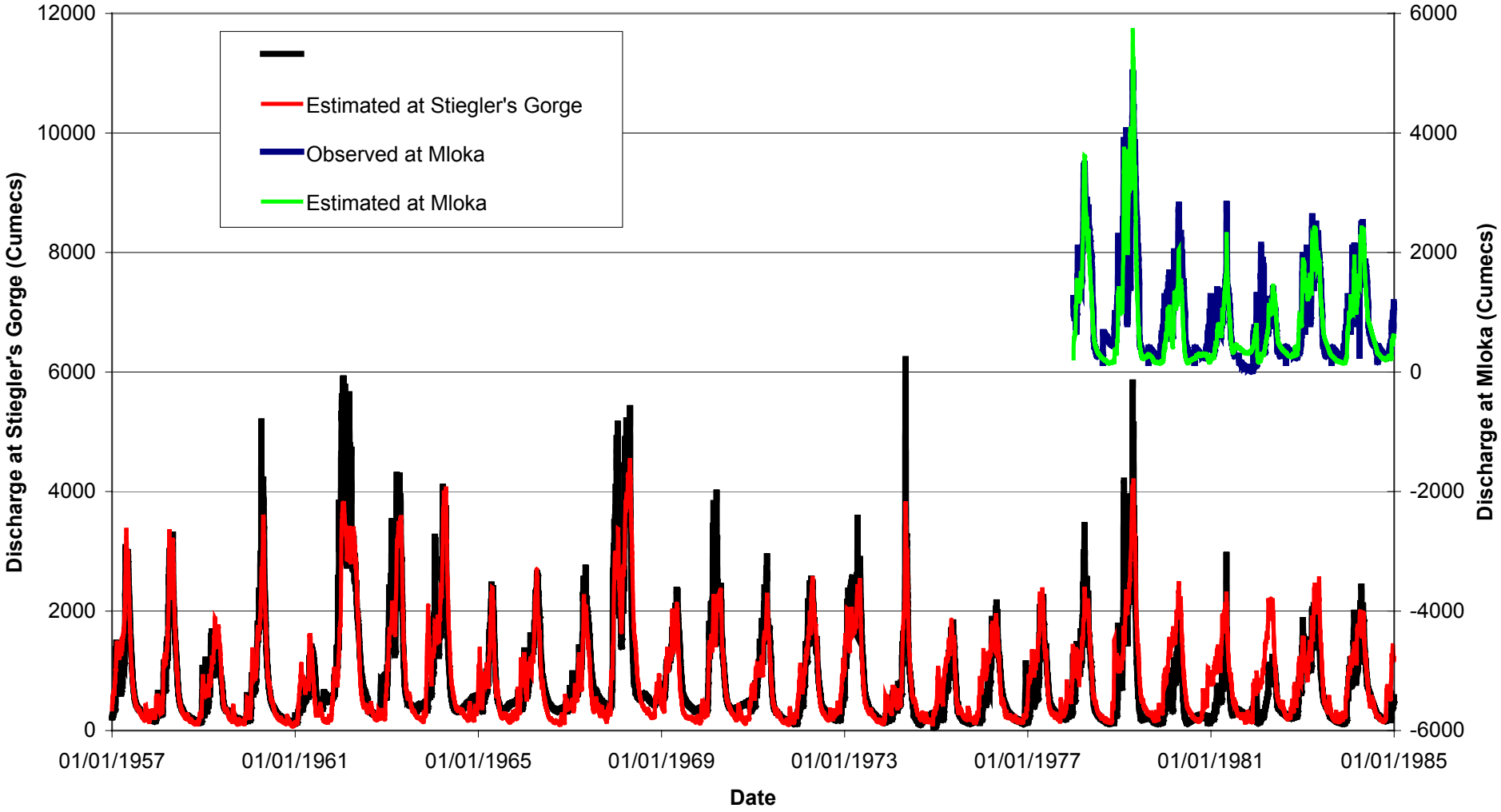

Figure F8.2: Observed and Estimated Hydrographs at Stiegler's Gorge and at Mloka

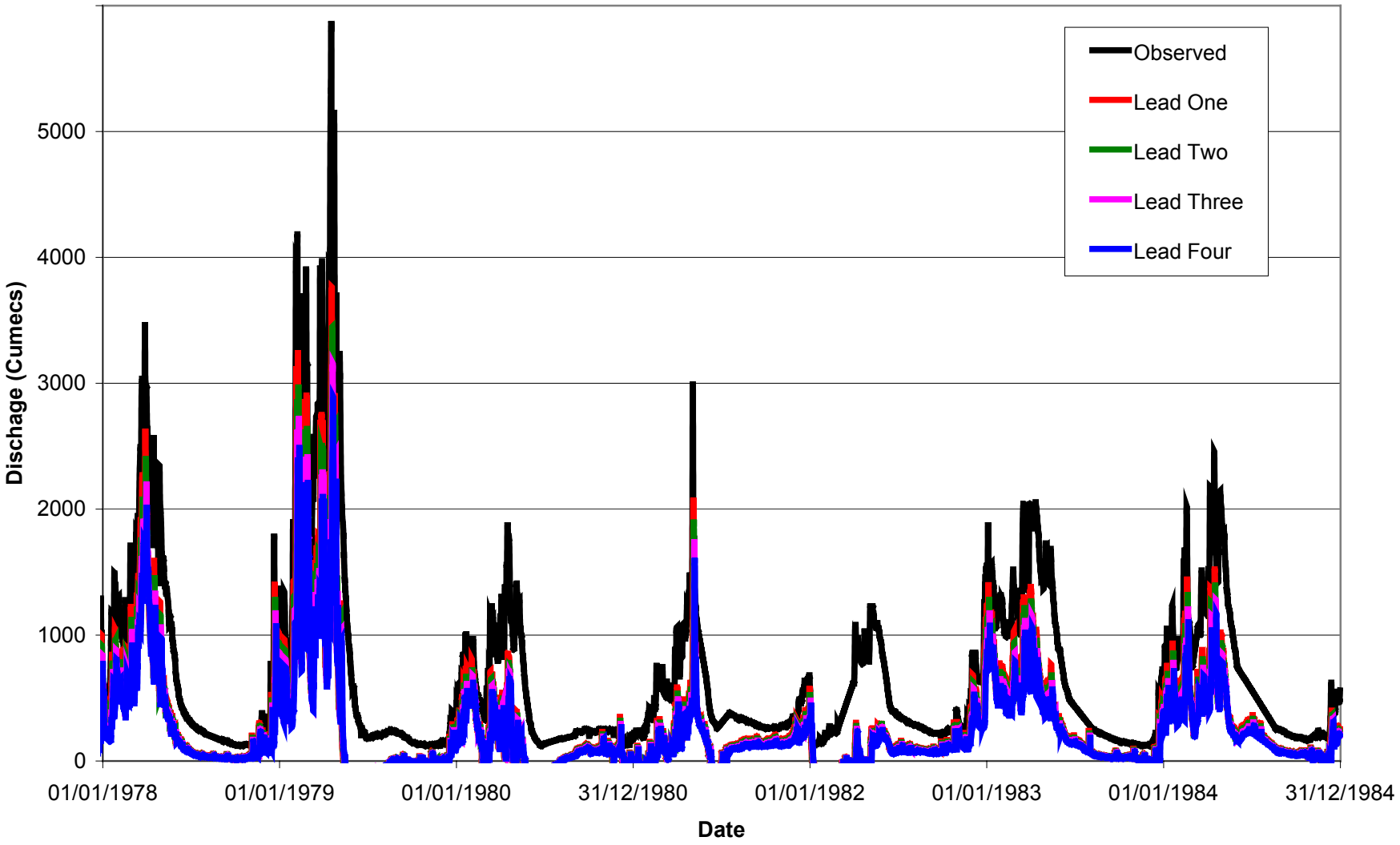

Figure F8.3: Flow Forecast at Stiegler's Gorge from 1978 to 1984

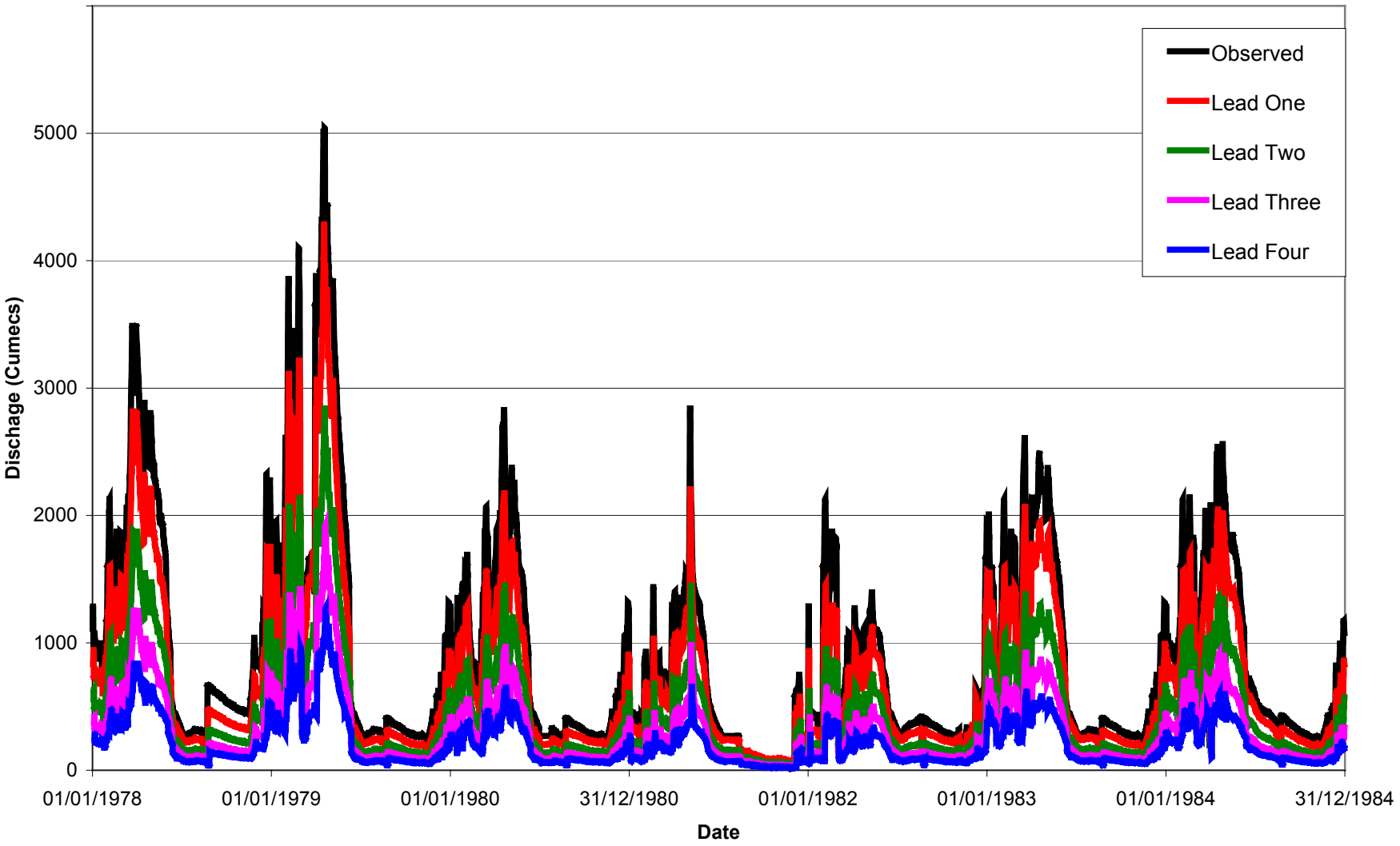

Figure F8.4: Flow Forecast at Mloka from 1978 to 1984

Chapter 9

9 Flood Plain Model

9.1 Application of HEC-RAS to the Floodplain

The Rufiji floodplain was modelled using HEC-RAS software. It is US Army Corps of Engineers' model that uses one-dimensional steady and unsteady flow hydraulics for channel flow analysis and for the determination of floodplain inundation.

HEC-GeoRAS is developed by US Army Corps of Engineers to process geo-spatial data for use with HEC-RAS. It allows users with limited GIS (ARCVIEW) knowledge to create HEC-RAS import files. The data used, in this study, for creating such import files were as follows:

(a) Historical flood records,
(b) Surveyed river cross-sections and reach data,
(c) Digital Terrain Model (DTM) in the form of Triangular Irregular Network (TIN) of the floodplain, and
(d) Land use and land cover map.

Results generated by HEC-RAS such as water surface profile and velocity data were processed with the HEC-GeoRAS. It created a file that contained river, reach and station identifiers; cross-sectional cut lines; cross-sectional surface lines; cross-sectional bank stations; downstream reach lengths for the left over bank, main channel, and right over bank; and cross-sectional roughness coefficients. This file was imported directly into ARC VIEW GIS Software.

HEC-RAS assumes that the energy head is constant across the cross-section and the velocity vector is perpendicular to the cross-section. It computes the water surface profile based on the assumption of steady gradually varied flow. It is known as the direct step method. Given the flow and water surface elevation at one cross-section, the objective of the direct step method is to compute the water surface elevation at an adjacent cross-section.

At each cross-section, the HEC-RAS requires parameters that describe the shape, elevation, and relative location of the cross-section along the stream. The following information is required:

1. River station (cross-section) number,
2. Lateral and elevation coordinates for each (dry, unflooded) terrain point,
3. Left and right river bank station locations,
4. Reach lengths between the left floodway, stream centreline, and right floodway of adjacent cross-sections,
5. Manning's roughness coefficients,
6. Channel contraction and expansion coefficients, and
7. Geometric description of structures, if any, such as bridges, culverts and weirs.

For subcrictical flow, the computations begin at the downstream boundary and proceed upstream; and for supercritical flow, the computations begin at the upstream boundary and proceed downstream. Using mixed flow analysis, the computations starts at both the upstream and downstream boundaries. At either of the boundaries, the flow and water surface elevation must be known. The computation procedure is summarized below for subcritical flow with reference to Figure F9.1.

1. Assume a water surface elevation at cross-section 1 as shown in Figure F9.1.
2. Determine the area, hydraulic radius and velocity of cross-section 1 based on the cross-section profile.
3. Compute the associated conveyance and velocity head values.
4. Calculate friction slope, friction loss and contraction/expansion loss.
5. Solve the energy equation for the water surface elevation at the adjacent cross-section.

6. Compare the computed water surface elevation with the value assumed in the step (1).
7. Repeat steps (1) to (6) until the assumed and computed water surface elevations come within a predetermined tolerance.

The mixed flow approach was used in this study and the results from the computations were processed with the ArcView GIS software. This is based on assigning map coordinates to stream and computed water surface profile data stored in HEC-RAS model coordinates. The procedure consists of four primary steps, namely; data import from HEC-RAS, stream centreline definition, cross-section geo-referencing and floodplain mapping.

The HEC-RAS output was extracted in the form of computed water surface profiles and read into ArcView GIS. The purpose of the data import step is to transform HEC-RAS output from text file format into a tabular format readable by ArcView. After this the cross-section coordinates, which were in HEC-RAS coordinates, were assigned map coordinates by associating them with geographically referenced digital representation of the stream in the form of DTM.

9.2 Results

The movement of flood flows, down stream of Mloka, was monitored by the use of HEC-RAS software. The computer program was operated to estimate the extent of inundation in the floodplain for an assumed flood peak at Mloka of 1,500 Cumecs, 2,000 Cumecs, 2,500 Cumecs and so on up to a flood magnitude of 7,000 Cumecs. The inundation maps for a peak of 3,000 Cumecs is presented in Fgure F9.2. The Figure F9.3 presents the same information for a Mloka flood peak of 6,500 Cumecs. Approximate area flooded by each flood peak, assumed in the study, is presented in Table T9.1.

This model and the flow forecasting models described in chapter 8 were put together as a flood warning package for the Lower Rufiji floodplain. The details are given in chapter 8.

The results presented in Figures F9.2 and F9.3 are not very informative because the political map of the region is not superimposed on the DEM. As a result one cannot use this information effectively.

Another major weakness of this analysis is, of course, that the results obtained have not been verified with the historically observed floods in the basin or even compared with alternative methodologies and/or software programs.

Table T9.2 shows the dates when some major floods were recorded at the Stiegler's Gorge. The extent of inundation caused by these floods is not recorded. One might be able to get some rough idea of extremes by talking to older people in the region but that was not done.

Table T9.1: Approximate Flood-Prone Areas at different Flood Magnitudes between Mloka and Delta Region

Flow Magnitude at Mloka	Approximate Flooded Area (km^2)
1,500 Cumecs	370
2,000 Cumecs	450
2,500 Cumecs	530
3,000 Cumecs	630
3,500 Cumecs	700
4,000 Cumecs	750
4,500 Cumecs	820
5,000 Cumecs	870
5,500 Cumecs	910
6,000 Cumecs	950
6,500 Cumecs	990
7,000 Cumecs	1,030

Table T9.2: Historically Observed Floods that had occurred at Stiegler's Gorge

Date of Occurrence	Flood Magnitude (Cumecs)
08th may 1955	3,417
24th April 1956	6,308
18th April 1957	3,070
01st May 1958	3,279
06th April 1960	5,214
17th December 1961	3,812
20th January 1962	5,927
22nd March 1963	4,323
24th March 1964	4,103
31st December 1967	3,783
26th April 1968	5,397
17th March 1970	4,025
14th April 1973	3,610
03rd May 1974	6,244
29th March 1978	3,483
18th April 1979	5,816
04th May 1981	2,989
20th March 1987	4,591
14th April 1989	3,329

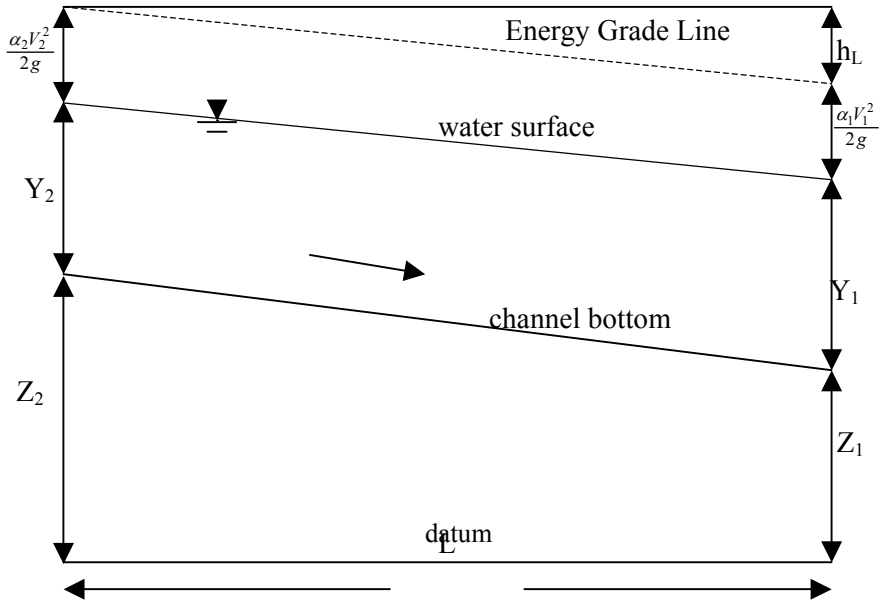

Figure F9.1: Graphical Representation of Terms in the Energy Equation

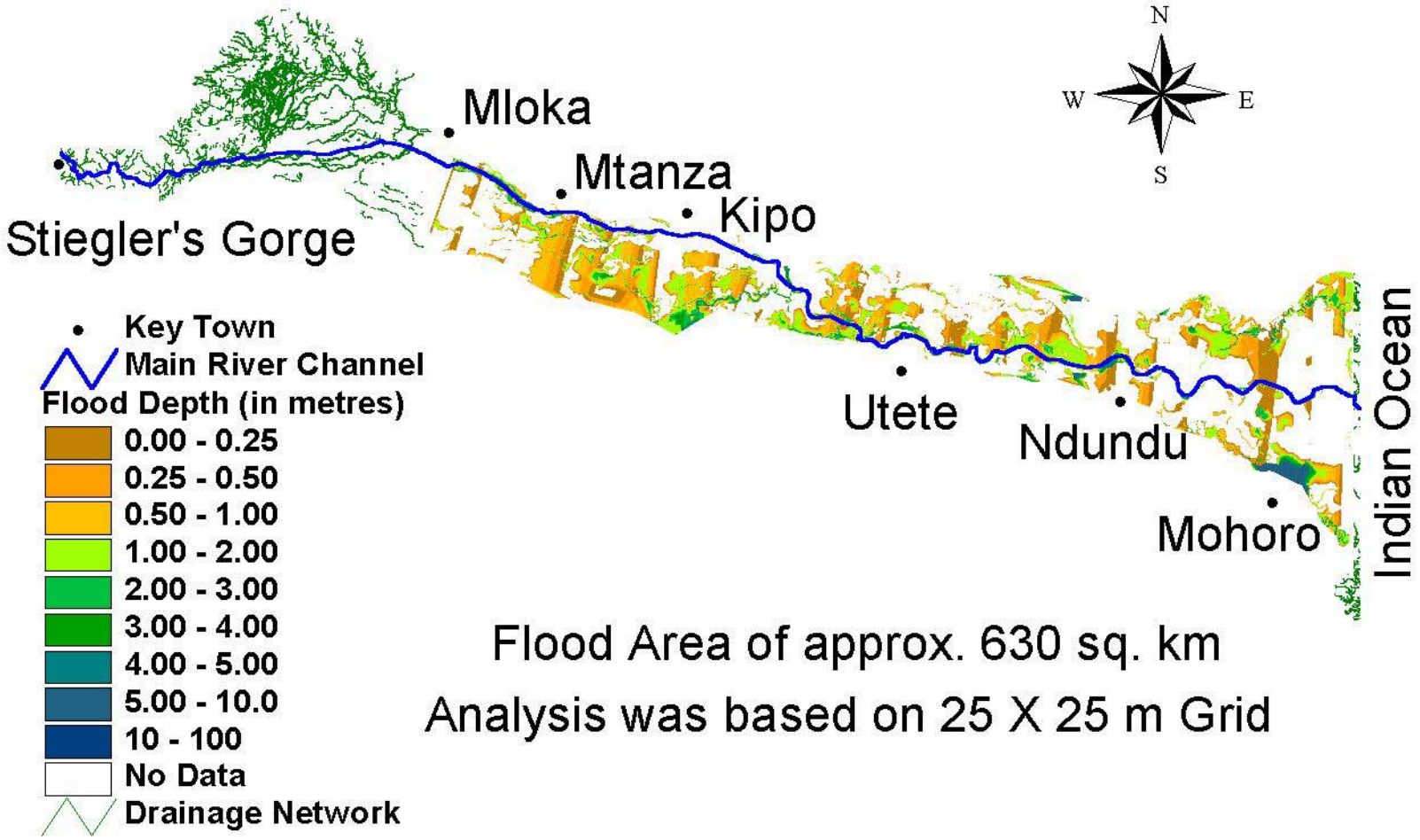

Figure F9.2: Flood-Prone Areas from Mloka to the Ocean when flow at Mloka is 3,000 Cumecs

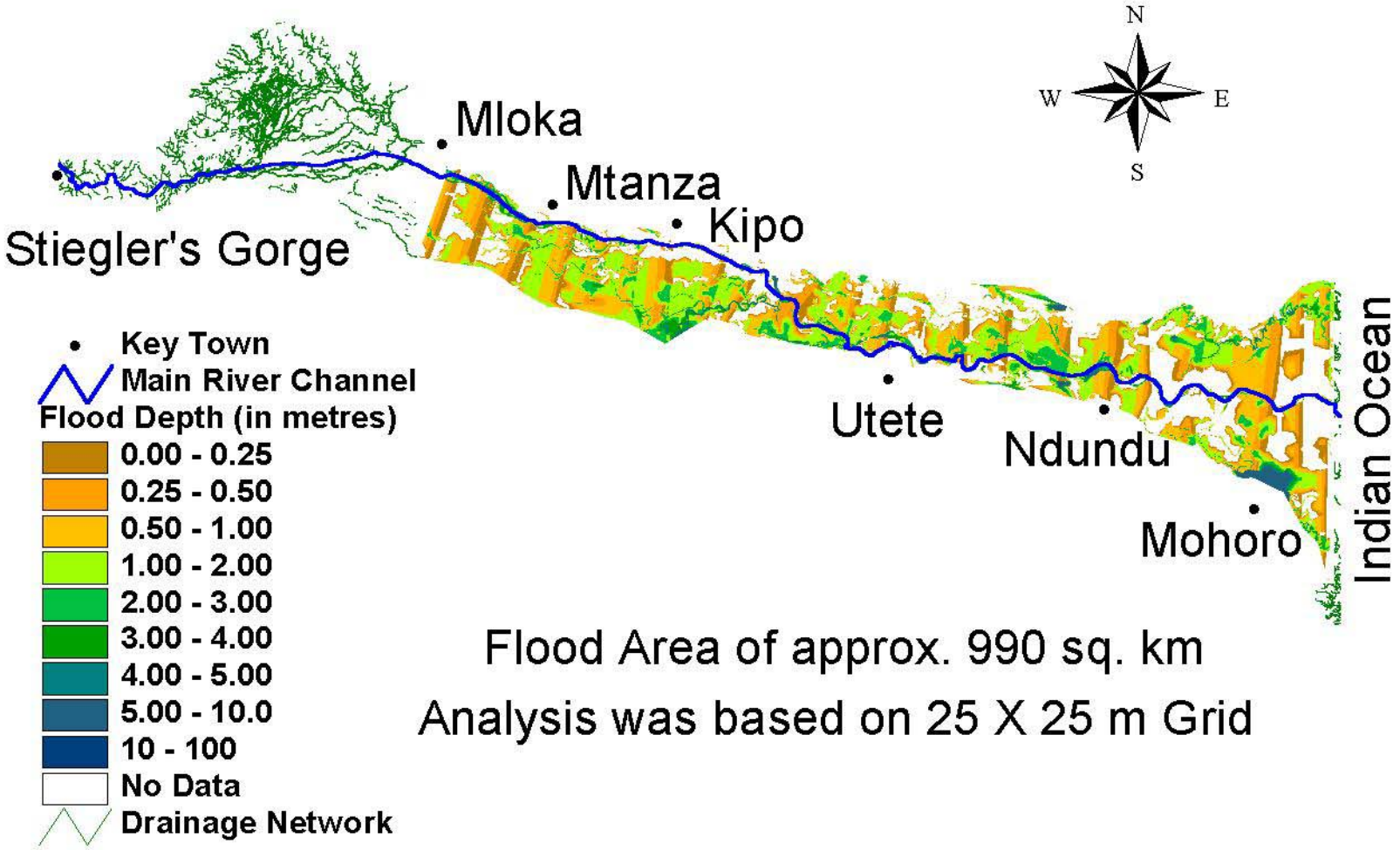

Figure F9.3: Flood-Prone Areas from Mloka to the Ocean when flow at Mloka is 6,500 Cumecs

Chapter 10

10 Future Direction

The work presented in this report, may not be conclusive, but it forms an excellent basis for future work. This project has compiled almost all the available historical hydrologic and climatological data that were available with various agencies in Tanzania and elsewhere. These data were checked, verified and processed for missing data reconstruction. And, of course, the data were properly documented.

Unfortunately, very little information and data are available on sediment transported by the river and the amount that is deposited in the floodplain and in the Delta. This information is of critical importance. But it is not readily available. Future effort must be focussed on the collection of sediment data and, if possible, estimate the amount of sediment that has been deposited over the years in the Delta. It is suggested that undisturbed vertical samples of sediment deposited in the Delta may be collected and studied for the amount of sediment deposited each year. This, exercise, is not very simple but it can be designed with the help of experts who study sediment deposits in lakes, etc.

More work is needed in data collection and in its processing in the future. Flow gauges, at some very important locations, like the Stiegler's Gorge, are missing. The rating curves at many locations are more than 20 years old. Most of them need to be updated. Climatic data are sparse and inaccurate. Information on irrigation abstractions are not accurate. The Luwegu sub-basin is totally ungauged. There are no rain gauges in the sub-basin and there is no flow gauging station. This needs to be rectified. In general, much work is needed to upgrade the level of hydrological and climatic data collection in the basin.

The hydrological modelling work presented in this report is fragmented in the sense that a number of models were tried in different sub-basins. Catchment above the Mtera Reservoir was not included for modelling work and so was the catchment of Little Ruaha. The Mtera/Kidatu Reservoir System was excluded from investigations and also the Kilombero sub-basin was not looked at in depth. Clearly, it is necessary to develop a single simulation model of the entire basin. This model must be custom built for assessing the impact of upstream Water Resources Development on the Delta. This model must also serve as a basic instrument of a management Decision Support System and provide parameters for the design of ecologically friendly water resources development in the basin.

Development of such a model requires a lot of research work in mathematical modelling and lot of spatial data like accurate DEMs. This, in turn, requires aerial surveys of the floodplain and that of the Delta. And that is an expensive affair.

A user friendly computer package was developed, in this work, as part of a flood warning system. This computer package uses Systems type of models, operational in updated mode, for real-time forecasting. It also uses the flood inundation images that were created by the use of HEC - RAS model. The choice of models, for this purpose, was satisfactory. But in the future one must recalibrate this model to make it more accurate. The architecture of this user friendly package is of interest as it might form the basis of the overall Basin Simulation model.

Information on the ecology of the Mangrove Delta is of vital importance. One has to know as to what is required in terms of Silt and Water to sustain a mangrove forest. This information must be available before any sensible model can be built for any impact analysis.